The Thesis Committee for Motaz Taha
Certifies that this is the approved version of the following Thesis

Experimental Evaluation of Foam for Mobility Control in Water Alternating Gas Enhanced Oil Recovery in a Middle Eastern Carbonate Reservoir

APPROVED BY
SUPERVISING COMMITTEE:

Quoc Nguyen, Supervisor

Wen Song

Experimental Evaluation of Foam for Mobility Control in Water Alternating Gas Enhanced Oil Recovery in a Middle Eastern Carbonate Reservoir

by

Motaz Taha

Thesis

Presented to the Faculty of the Graduate School of

The University of Texas at Austin

in Partial Fulfillment

of the Requirements

for the Degree of

Master of Science in Engineering

The University of Texas at Austin

December 2020

Dedication

To my parents, Salem and Zeinab for always believing in me, and pushing me to continue to move forward. Thank you for your support, love and patience.

Acknowledgements

I would like to thank my supervisor Dr. Nguyen for his expertise and support throughout the last two years. I would also like to acknowledge Pramod Patel (Rock Oil Consulting) for his guidance, great working relationship, and financial sponsorship of the project.

Abstract

Experimental Evaluation of Foam for Mobility Control in Water Alternating Gas Enhanced Oil Recovery in a Middle Eastern Carbonate Reservoir

Motaz Taha, MSE

The University of Texas at Austin, 2020

Supervisor: Quoc Nguyen

Various enhanced oil recovery methods (EOR) suffer from poor sweep efficiency due to viscous fingering, channeling, and gravity segregation issues. The water-alternating-gas method (WAG) used in the Al-Shaheen's Shuaiba reservoir has encountered similar problems, whereby injected gas preferentially flows into higher permeability zones and sweep efficiency is impacted. The goal of this research work was to develop an effective, and economically viable foam system that can utilize waste gas in the Al-Shaheen reservoir as a mobility control solution. This research focused on an optimized surfactant formulation that can generate foam with methane gas at the reservoir conditions in the presence of oil and an oil wet/mixed wet rock.

The formulation was tested in water wet and oil wet core flood experiments. Enhancements to the formulation were tested and their improvement to the foam strength was quantified. An anionic surfactant group alkyl-polyglycoside (APG) was first chosen

through screening experiments. The bulk foam stability was then evaluated with and without oil presence and showed APG-5 as the best among the APGs. Its adsorption to carbonate Estaillades limestone was estimated around 2.5 mg/g of rock at 55 °C and the reservoir brine salinity of 144,000 ppm.

Core flood experiments revealed that a concentration of 3500 ppm is required to achieve strong foam. The foam rheology of APG-5 and methane gas was found to be shear thinning. The ideal foam quality resulting in the strongest foam was found to be between 30 and 50 %.

The impact of oil on the APG-5 foam was studied, and found to produce effective foam in presence of residual oil in water wet cores and oil wet cores, with mobility reduction factor (MRF) values of 28 for the former and 24 for the latter. It was also shown through mobile oil experiments that foam can develop even in presence of mobile oil. Oil wet environments were shown to have weaker foams. The use of a wettability altering agent TGT-1 improved the foam propagation and steady state strength. MRF values of ~ 47 were achieved, an increase of 150%. A foam booster (Lauryl Betaine) was tested and found to enhance the propagation and steady state strength of the foam with MRF values of 52. Combining the wettability alteration, and foam boosting in a final formulation achieved and MRF of 85.

Table of Contents

List of Tables

List of Figures

1 INTRODUCTION

This chapter outlines the background and motivation behind the research project, a list of research objectives, a brief description of the research methodology used, and finally a summary of the organizational structure.

1.1 Background and Motivation

The Al Shaheen field is part of Block 5, off the cost of Qatar, as shown in Figure 1. Development started in 1992, with details provided in paper by (Finlay et al. 2014). The field currently produces 350,000 STB/D from two thin separate cretaceous carbonate formations and an overlaying sandstone formation.

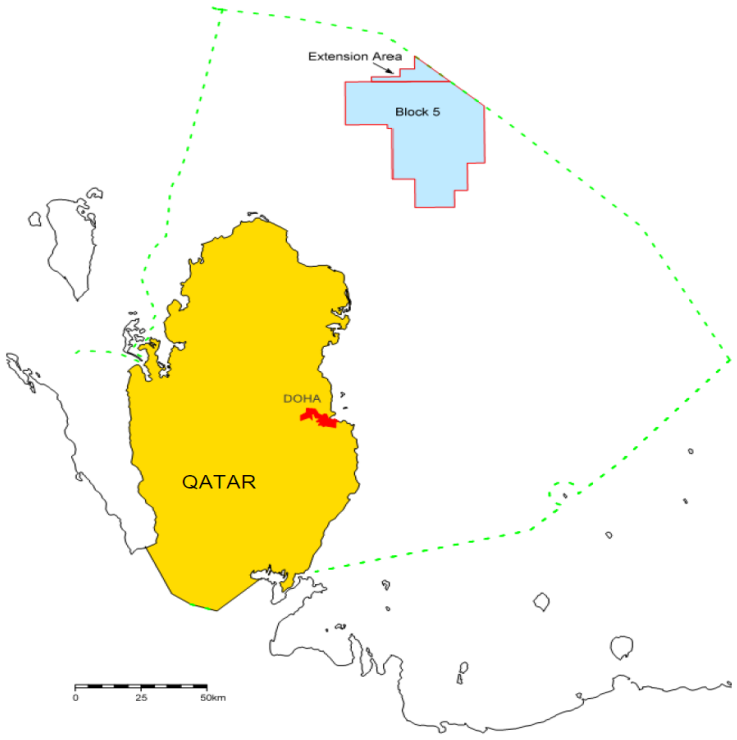

Figure 1: Al Shaheen Field Location, Block-5, offshore Qatar.

The carbonate reservoirs have thin oil columns with a large areal extent (25 km by 45 km) and rock with typical permeabilities in the 1-10 mD range. The crude oil shows great lateral variation with API gravities ranging from 16-38 within the same reservoir. The reservoir contains several gas caps with large variations in solution GOR and saturation pressures in different locations. This field has been evaluated and put on water-alternating-gas (WAG) injection using hydrocarbon gas as injection gas (Lindeloff et al. 2008).

Enhanced oil recovery (EOR) techniques can significantly extend global oil reserves if the oil prices are high enough to make these techniques economic (Muggeridge et al. 2014). EOR methods (solvent, thermal and chemical) are based on injection of materials normally not present in the reservoir (Ashour, 2011). Solvent EOR involving gas injection (carbon dioxide, hydrocarbons, and nitrogen) is the most commonly applied EOR technique for light oil (Teletzke et al. 2005). Miscible gas EOR is mostly applied through water-alternating-gas (WAG) injection to mitigate the technical and economic disadvantages of gas injection (Christensen et al. 1998; Awan et al. 2005). This technique was implemented in the Shuaiba reservoir. Re-injection of the hydrocarbon gas presents an environmentally preferable option to flaring. Alternating between injecting water and gas, reduces the volume of gas required to maintain reservoir pressure.

WAG presents an improvement in gas mobility over gas injection by itself. It reduces the tendency for the gas to finger or channel through the oil. The presence of mobile water in the pore space reduces the gas mobility through relative permeability effects (Stalkup 1983). Vertical sweep efficiency is also improved as the heavier water, tends to slump towards the bottom of the reservoir while the gas, being lighter, rises to the top (Blackwell et al. 1959).

Although the majority of WAG applications in the field have been successful, the incremental recovery achieved is generally less than predicted (Christensen et al. 1998; Awan et al. 2005). Solvent gas is lighter than oil, and less viscous, which causes it to finger through the oil by viscous fingering (Homsy 1987; Blackwell et al. 1959), heterogeneity (Waggoner et al. 1992; Araktingi et al. 1993) and gravity override issues (Claridge 1972; Fayers and Muggeridge 1990).The aforementioned variation in oil density and GOR along different layers of the reservoir can help explain the potential mobility control issues during WAG implementation.

Thus, the motivation for this research work is to develop an effective, and economically viable foam system that can utilize the waste gas in the Al-Shaheen reservoir. The foam system needs to provide mobility control at the reservoir conditions. The detailed research goals are listed in the following section.

1.2 Research Objectives

The main research objective is to design and develop a foam system that can provide effective mobility control for Al-Shaheen Field's Shuaiba reservoir conditions [144,000 ppm formation brine, 55 °C temperature, oil wet/mixed wet conditions, and in the presence of oil]. The above goal is subdivided into the following research goals:

1. Develop a surfactant formulation that can generate a stable foam at the above reservoir conditions.
    a. Evaluate foam rheology by studying the impact of shear rate and foam quality (FQ) on the resulting foam strength.
    b. Optimize surfactant concentration to find required concentration that is still economically viable.

2. Evaluate impact of oil on foam performance in natural carbonate rocks.
    a. Find the foam strength and MRF values for foam at residual oil saturation in water wet and oil wet conditions.
    b. Evaluate impact of mobile oil on foam propagation.
3. Evaluate the impact of wettability on foam propagation natural carbonate rocks.
4. Develop foam enhancement solutions that maximize the base case's foam strength and MRF achieved.
    a. Study foam enhancement by improving foam resistance to oil.
    b. Study foam enhancement by changing rock wettability towards more water wet conditions.
    c. Recommend a final foam system formulation and injection strategy.

Section 1.3 outlines, the research methods employed in this work. Detailed experimental procedures are listed in Appendix B: Experimental .

1.3 Methodology

This research work is backed by an experimental approach, whereby the research objectives are achieved through a detailed experimental program. The main techniques used include:

1. Bulk foam testing experiments: used to test for surfactant foaming ability.
2. Surfactant/oil microemulsion tests: tests for presence of type I, II, or III microemulsions formed between a surfactant and crude oil.
3. Interfacial tension measurements: in this work the pendant drop method was employed. These measure interfacial tension between water/gas, water/oil, and oil/gas. These measurements are then used to estimate parameters such as the entering coefficient, spreading coefficient, and lamella number.

4. Contact angle measurements: using a Rame-Hart device. These experiments are used to screen surfactants for their ability to alter wettability from oil to water wet.
5. Static adsorption experiments: used to estimate how much of the surfactant adsorbs onto rock grains. The surfactant concentrations are estimated using LCMS spectroscopy techniques and are then used to estimate adsorption.
6. Core flooding experiments: core floods whereby fluids are injected in sequences mimicking the production and injection history of reservoirs. This presents the most accurate lab tests that resemble reservoir conditions.

Detailed procedures and information, about the experimental tools and setups used for the above experiments, are included in Appendix B: Experimental . Materials used in this study include:

1. **Surfactants**: Anionic surfactants (Alpha Olefin Sulfonate (AOS)), cationic (Amines (C25, T25 at 50% Active Content), Lauryl Betaine (50% Active Content), nonionic (APGs with 50-70% active content), Tergitol surfactants (100% active Content).
2. **Brines**: Synthetic brine and sea water were prepared as per Table 1. The formation brine has a considerable divalent ion concentration (12600 ppm). ACS grade salts were used to create the synthetic formation brine.
3. **Outcrop rocks**: Estaillades limestone was used to simulate the Shuaiba reservoir rock. The porosity of the block ranged from 20-25%, while the permeability to brine measured was 100-120 mD. The cores used are 1 in diameter and 1 ft long. They were cleaned then dried for a week at 80 °C.

4. **Crude oil** from the Al-Shaheen Field was used. The field samples provided included sand, and a strong emulsion of oil and water. It was heated, centrifuged, and filtered twice through 1.2 μm and then 0.65 μm filters.
5. **Methane gas** at 97.7% purity provided by PRAXAIR was used as the gas phase for the foam in core flood experiments.
6. **Calcite plates:** Iceland Spar test chips sourced from WARD's natural science**,** were used to simulate carbonate rock for contact angle measurements.

Salt	**Formation Brine Composition (g/L)**	**Salt**	**Sea Water Composition (g/L)**
NaCl	99.80	**NaCl**	31.69
KCl	3.86	**KCl**	0.86
SrCl2.6H2O	1.17	**CaCl2.2H20**	1.78
CaCl2.2H2O	33.31	**MgCl2.6H2O**	11.46
MgCl2.6H2O	29.81	**Na2SO4**	4.72
Total Salinity (g/L)	**144.144**		**49.65**

Table 1: Brine Composition

1.4 Organizational Structure

This thesis starts with an introduction section outlining the background information, and research goals and objectives, as well as the methodology of research. Chapter 3 outlines pertinent literature review done for this work.

Chapter 4 presents the foam formulation and characterization, which focusses on the first research goal. Chapter 5 focusses on the impact of oil on foam, while Chapter 6 analyzes the impact of wettability, thus answering second and third research goals listed in the previous section. Subsequently, the foam formulation enhancements are discussed in chapter 7, answering the fourth and final research objective. The thesis is capped with a list of conclusions, and a summary of suggested future work.

2 LITERATURE REVIEW

This chapter highlights relevant areas of literature pertaining to foam generation, stability and propagation, as well as foam oil interactions. A review of foam for mobility control in WAG EOR applications is then presented.

2.1 Foam Mechanics

There is extensive literature on foam generation and stability. Schramm defined foam as a dispersion of gas in a continuous liquid phase whereby gas bubbles are separated by thin aqueous films. (Shramm, 1994). The thin films join in locations described as the plateau borders, where the aqueous phase aggregates. These concepts are illustrated in Figure 2.

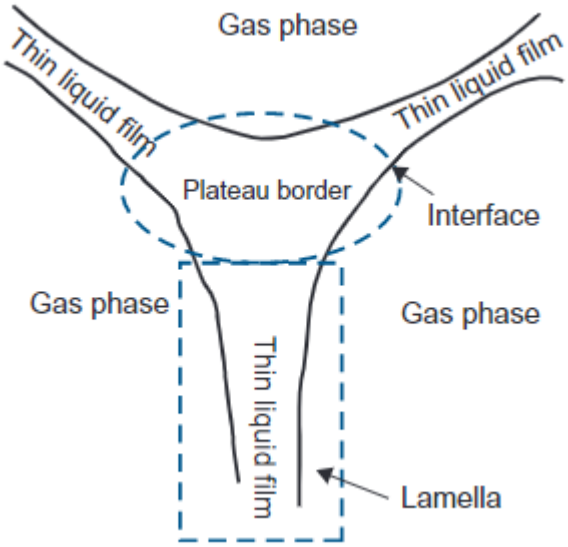

Figure 2: Schematic of a foam system (Sheng, 2013)

Foam is typically formed by mixing a liquid with a foaming agent (surfactant) with a gas. Surfactants stabilize the foam films or lamellae. A foam is typically described by the

foam quality (FQ) which represents the gas fraction in the total flow, and the texture of the foam which relates to the size of bubbles.

2.1.1 FOAM GENERATION IN POROUS MEDIA

Foam is generated in porous media by several mechanisms: leave-behind, lamella division, and snap off. Snap off is represented in Figure 3. As shown snap off occurs by gas breaking into bubbles when going through a restriction like a pore throat. This process repeats indefinitely at a snap-off site in a dynamic scenario whereby gas is injected, thus making this mechanism an important foam generation mechanism.

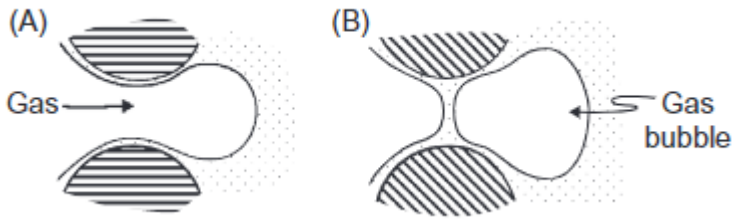

Figure 3: Snap-off mechanism. A: Gas penetrates through a pore constriction B: Gas breaks off into a new isolated bubble (Ransohoff and Radke, 1988)

Lamella division is shown in Figure 4. It refers to a pre-formed foam lamella (bubble) breaking into two when flowing through the pore structure and going around a restriction. Similar to snap-off it generates more lamella and can repeat at the division site in a dynamic scenario. Thus, it is also a predominant mechanism of foam generation.

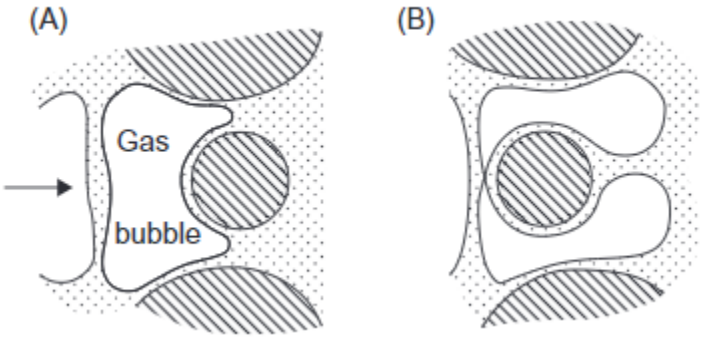

Figure 4: Lamella Division A: Gas bubble approaches obstruction B: Gas bubble divides into two bubbles (Ransohoff and Radke, 1988)

The leave behind mechanism shown in Figure 5 occurs when two gas menisci break through into two separate bubbles when moving around a restriction. This mechanism is prevalent at low shear rates (low injection velocities) and the foams generated tend to be weaker. This process does not repeat at a generation site, and it forms stationary aqueous lenses around the bubbles, thus requires a relatively high liquid saturation.

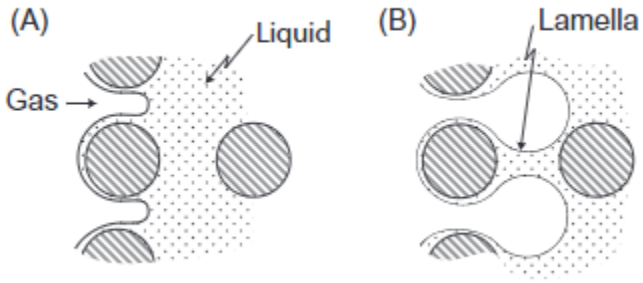

Figure 5: Leave behind mechanism. A: Gas approaches restriction B: gas lenses form through restriction leading to bubbles forming. (Ransohoff and Radke, 1988)

2.1.2 FOAM STABILITY AND COALESCENCE MECHANISMS

Foam films are thermodynamically unstable, and eventually break down with time. Thus, the term stability here describes the relative stability compared to other foams. When discussing foam stability, the following concepts are useful:

Gravity Drainage: this refers to the movement of the liquid phase draining through the foam films due to the impact of gravity. The process thins foam films and can cause their rupture.

Laplace Capillary Suction: At plateau borders the radius of curvature is larger than the flat portions of the foam lamellae. Based on the Young-Laplace equation for capillary pressure (equation 8, Appendix D: List of Equations), this creates a large pressure difference between these two locations. This leads to the suction of liquid from the flat parts of the foam lamella which thins them and can lead to rupture.

Gibbs - Marangoni Effects: when a foam film which is stabilized by the presence of a surfactant expands or thins, the local concentration of the surfactant drops. This causes a rise in the surface tension of the film, which causes a contraction of the surface/film to conserve the low energy of the film. This process causes the liquid to flow from the low surface tension region to the high surface tension region. Thus, in this case liquid moves to the thinner portions of the film, and supports the overall stability of the foam.

Disjoining Pressure: when two surfaces of a thin film are interacting, a combination of forces arise. The disjoining pressure represents the difference between orthogonal pressure at a point on the film, and the pressure in the bulk (water) phase. The pressure normal to the film surface is a function of the net forces acting there. These include electrical, dispersion, and steric forces. The thickness of the film (closeness of the two sides) determines the distribution of these forces. The composition of the fluids, and temperature also affect the forces. When the net forces are positive, we get repulsive film

forces, while negative net forces are attractive. In general, highly attractive van der walls forces destabilize films, and also highly repulsive forces between similarly charges particles can destabilize the film. These are referred to as conjoining/disjoining forces, and can both lead to film destabilization. (Manlowe and Radke, 1990).

There are two main mechanisms foam lamella coalesce by; first capillary suction, and secondly gas diffusion. (Chambers and Radke, 1991). Capillary suction discussed above is a prominent mechanism for lamella rupture. Gas diffusion is a less prevalent foam rupture mechanism.

It is important to note that a constant supply of surfactant in the liquid phase can extend the distance, and stability of the foam structure when flowing through a porous medium. As foam generation and decay is a dynamic condition, whereby foam forms and breaks constantly. A stable foam is one where the net formation exceeds the net breakage of lamellae.

The above concepts govern the foam stability at the individual film level. The presence of oil complicates these mechanisms, and requires special treatment. This is discussed in section 0.

2.2 Foam Oil Interactions

The following sections review the previous studies of the impact of oil on foam stability. First discussing the concept of a critical oil saturation for foam, then a review of classical and current theories about foam-oil destabilization mechanisms is presented.

2.2.1 Effect of Oil Saturation

The impact of oil saturation on bulk foam stability and generation was found to have conflicting results in literature. Some surfactant oil combinations can have an effective foam at higher concentrations while other combinations do not. This inconsistency in considering the effect of oil saturation on the bulk foam experiments leads us to question how oil affects foam.

Generally, oil can impact foam strength by affecting the generation mechanisms or by causing destabilization which in turn affects the stability of the foam. (Al-Majid and Kovscek, 2015) theorized that oil can affect the snap-off generation mechanism by affecting the aspect ratio required for foam bubbles to snap-off. However, it is very difficult to quantify the number of snap-off sites in an actual porous medium. Additionally, if the pores have low water saturation (high oil saturation) snap-off which requires water to be present, is limited.

Some researchers are in agreement that critical oil saturation S_o^{cr} exists above which only weak foams or even no foam can exist. However, as mentioned earlier, there is a lack of correlation between oil saturation and foam strength (in bulk tests and even core floods). This is likely due to the individual foam-film-oil physics, and the spatial distribution of the phases throughout the rock pore structure which governs the foam generation and interactions of the foam and oil, and as such affects the foam strength.

The idea of a critical oil saturation below which an effective foam can exist was found experimentally by (Friedman and Jensen, 1987) who found for a limited surfactant-oil system under study, a critical oil saturation of 15% limited any foam formation, and an effective foam only formed below 10% oil saturation. Further research by (Mannhardt and Svorstol, 1999) shows that having oil saturations higher than the critical saturation not only prevents effective foam from forming, it also creates a delayed propagation of the foam when the saturation does drop below the critical value.

A likely explanation for the variability in predicted foam strength at different oil saturation is the inherent stability of the foam-oil system at the single film level. This is subject to variation due to the type of surfactant, crude oil, concentrations of surfactant, salinity of the aqueous phase, viscosity of the phases among other factors. So, for a particular foam-oil system that shows inherently unstable foam-oil films the foam is likely to be unstable at even very low oil saturations. While an inherently stable oil-foam film is likely to result in effective foam up to certain oil saturation – critical oil saturation (or more accurately up to certain water saturation) whereby foam generation and stability of foam films is impacted.

2.2.2 CLASSICAL THEORIES BASED ON INTERFACIAL PROPERTIES

The first attempts at explaining the destabilizing effect of oil on foam is borrowed from thermodynamic theories which show that a defoamer can spread along the surface of the liquid-gas interface. The entering coefficient in terms of the interfacial properties of the oil-water (surfactant solution)-gas system:

$$E_{oil/water} = \sigma_{water/gas} + \sigma_{oil/water} - \sigma_{oil/gas}$$

Where $\boldsymbol{E_{oil/water}}$ is the entering coefficient, and $\boldsymbol{\sigma}$ is the interfacial tension between two phases.

If the entering coefficient above is positive, it is thermodynamically possible for an emulsified droplet of oil to enter the surfactant-gas interface. A negative entering coefficient indicates that the emulsified droplet would stay within the aqueous phase without entering the interface. The spreading coefficient is developed using a similar concept and is described by:

$$S_{oil/water} = \sigma_{water/gas} - \sigma_{oil/water} - \sigma_{oil/gas}$$

Where $\boldsymbol{S_{oil/water}}$ is the spreading coefficient, and $\boldsymbol{\sigma}$ is the interfacial tension between two phases.

A negative spreading coefficient indicates the emulsified oil droplet spreads along the surfactant-gas interface. An entering oil droplet $\mathrm{E_{oil/water}} < 0$, may have the oil spread along the interface only if $S_{oil/water} < 0$. This theory predicts that oil spreading along the aqueous interface with gas is a key cause of destabilization.

Lastly, the bridging coefficient describes the condition where spreading oil on either side of two foam lamellae causes a bridge to form between the two interfaces. This was developed by (Aveyard, 1994). An unstable bridge would lead to the trapped gas on either of the lamellae to coalesce into a bigger bubble, leading to foam coalescence and essentially destabilizing the foam.

The bridging coefficient is described by

$$B_{oil/water} = \sigma^2_{water/gas} + \sigma^2_{oil/water} - \sigma^2_{oil/gas}$$

Where $\boldsymbol{B_{oil/water}}$ is the bridging coefficient, and $\boldsymbol{\sigma}$ is the interfacial tension between two phases.

Negative values of the bridging coefficient result in unstable bridges. Aveyard shows that the bridging coefficient value depends on the contact angle of the surfactant

solution and oil droplet that formed after a bridging of two interfaces. Previous literature reviews show these theories resulting in good predictions on the bulk scale, but also having quite a few contradictory results.

These simple coefficients sometimes result in conflicting correlations between bulk scale and core flood scales, and while not fully explaining the process of foam destabilization, they are still attractive tools for researchers, due to the simplicity of the measurements involved, and the ability to screen for a variety of surfactant oil systems in a relatively short time.

2.2.3 LAMELLA THEORY

This theory was developed in part to support the mechanism of foam destabilization which involves the formation and movement of emulsified oil drops into the plateau borders of the foam. Foam rupture due to the congregation of these droplets in the plateau borders, which is governed by several factors such as the pseudo-emulsion film strength, and the size and number of oil droplets. (Shramm, 1994; Foam Sensitivity to Crude Oil in Porous Media). Thus, the emulsification of the oil into droplets is very important.

It is suggested that the likely cause of the oil emulsification is that oil is drawn by capillary suction into the lamella and pinched off to produce emulsified drops, this is also affected by mechanical shear effects due to the propagation of the foam through the porous medium. However, the mechanical shear effect is not described in the formulation for the lamella number developed by Shramm and Novosad:

$$L = \left(\frac{r_o}{r_p}\right)\left(\frac{\sigma_{water/gas}}{\sigma_{oil/water}}\right)$$

Where $\boldsymbol{r_o}$ is the oil droplet radius and $\boldsymbol{r_p}$ is the radius of the plateau border.

Based on this formulation, Schramm suggested the following parameters as indications of the foam stability or destabilization due to emulsified oil droplets:

Lamella #	Emulsification	Foam Type - Stability
$L < 1$	Limited oil emulsification expected	Type A Foam – Oil Resistant
$1 < L < 7$	Oil emulsifies into small droplets	Type B Foam – More instability
$L > 7$	Oil emulsifies into large number of small drops	Type C Foam – Unstable Foam

Table 2: Lamella Number Classifications

As outlined in past reviews (Farjzadeh et al, 2012), (Ma and Mateen 2018), this theory was applied in multiple studies some showing it to predict oil foam behavior

accurately (Shramm and Novosad 1990, 1992) others have shown that alone it cannot accurately predict the oil foam behavior, on either bulk or porous media scales (Dalland et al, 1994).

While the lamella number theory is used to predict the best and worst systems relatively accurately, it is still unable to account for performance observed in core flood experiments. The contradictory predictions using this model may be due to the simplified formulation of the lamella number which relies mainly on the interfacial properties of the system, and in most studies an approximate value of $(r_o/r_p)\sim 0.15$ is used which may not reflect the actual emulsified oil drop size and plateau border radius (which is affected by the pore structure, and aforementioned mechanical shear effects.

While emulsification of oil in porous media may play an important role in describing oil foam interactions, it still does not explain why some foam systems are more resistant to oil than others. This led to the consideration of the pseudo-emulsion film as the overriding factor in determining oil foam stability.

2.2.4 PSEUDO-EMULSION FILM STABILITY

As highlighted in earlier sections, both the classical theories of entering and spreading and bridging as well as the emulsification lamella theory both have considerable shortcomings in describing the effect of oil on foam. The pseudo-emulsion model was developed to understand the physics of oil destabilizing foam on a more microscopic scale.

As defined earlier the pseudo emulsion film is formed when oil contacts foam lamella, creating an interface with oil-surfactant on one side, and surfactant-gas on the other. If this film is stable, or exists in a metastable state (in a dynamic foam propagation case), then foam can propagate through a medium which contains oil and can survive

providing adequate mobility control. Several factors can influence the stability of the PS-film:

- Micellar structure of the PS-film: influenced by surfactant-oil affinity (see also the solubilized oil effect section) (Nikolov et al, 1986), (Lobo et al, 1989), (Koczo et al, 1992).
- Marangoni surface effects due to the presence of oil droplets (emulsified droplets) leading to thickness changes to foam lamellae.
- The interaction of thin film forces including electrostatic and dispersion forces (disjoining/conjoining pressure effects).
- Interfacial viscosities can also influence the PS-film stability.

Manlowe and Radke showed through micro visual studies that the breakage of the PS-film leads to film ruptures, especially for thinning films where the film forces (non-bulk attractive and repulsive intermolecular forces, steric forces) become dominant. They also showed that stable PS-films lead to stable foams. (Manlowe and Radke, 1990)

Disjoining Pressure Approach

This approach considers the measurement of the disjoining pressure in the asymmetric pseudo emulsion film at the film scale, typically using micro visual techniques. The disjoining pressure isotherm for a PS-film is more complex than that for regular foam films. In a theoretical study, Garett showed that there exist two local maxima and minima of the disjoining pressure as a function of the film thickness. (Garett, 2016). The actual disjoining pressure isotherm is a function of the foam film thickness which in turn is a function of the surfactant formulation, and the surfactant oil interaction.

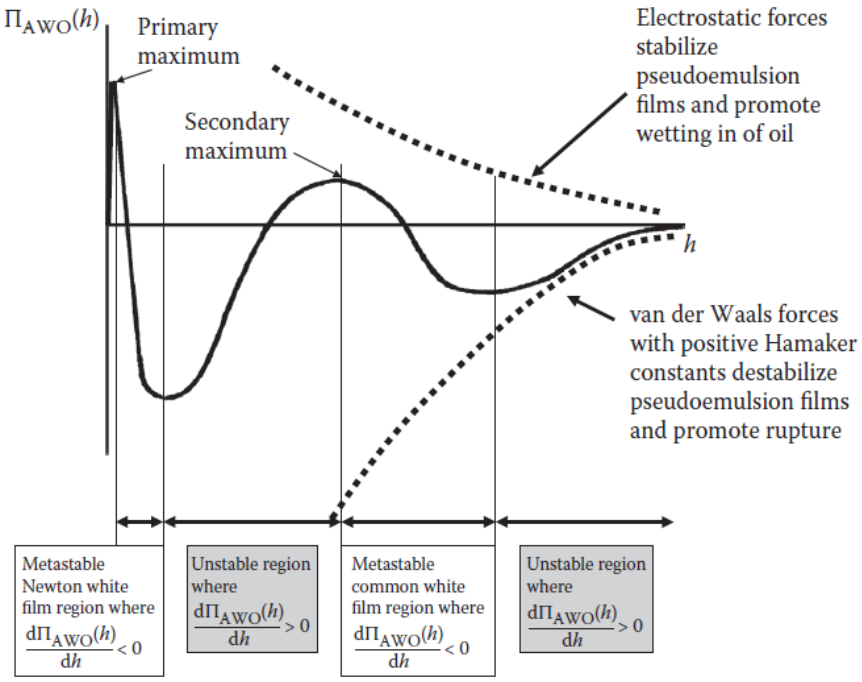

Figure 6: Disjoining pressure isotherm for metastable PS-film (Garett, 2016)

On the curve shown in Figure 6, the negative (repulsive forces) are presented above the h axis (film thickness), and positive attractive forces are presented below it, thus area under the curve for a dominant attractive forces region is positive despite being below the h axis.

$$For\ a\ PS-film:\ Net\ area\ under\ curve > 0 \rightarrow Film\ is\ unstable$$

$$For\ a\ PS-film:\ Net\ area\ under\ curve < 0 \rightarrow Film\ is\ metastable$$

$$For\ a\ PS-film\ thickness:\ h \leq 50\ nm \rightarrow Common\ white\ films\ (metastable)$$

$$For\ a\ PS-film\ thickness:\ h \leq 5\ nm \rightarrow Newton\ white\ films\ (metastable)$$

Garett shows that stable films would exist when the slope of the disjoining pressure curve is negative. At large thicknesses there is a secondary minimum caused by Van der Wals forces that dominate there, leading to the metastable common white film region.

Multiple factors can cause changes to the film thickness either thinning it or thickening it. These include ionic interactions between the surfactant and oil polar components, drainage of film due to viscoelastic properties.

At a certain point if the film thins enough, repulsive forces become dominant again, leading to a maximum in the disjoining pressure curve, which makes the slope of the curve positive and the foam in this case is unstable. If the foam thins even further, van der Wals forces dominate again, leading to a primary minimum and the secondary metastable foam region known as newton white films.

The above ranges of thickness are the general conditions suggested by Garrett for a metastable PS-film to exist. In a dynamic foam generation conditions, the foam PS-films go through thickness changes that can alter its stability.

The above applies however below a critical capillary pressure P_c^{cr} above which foam lamellae are susceptible to mechanical perturbations that cause rupture. Many researchers used the disjoining pressure concept to evaluate the PS-film stability of an oil-surfactant mixture. Bergeron borrows the disjoining pressure concept (Bergeron et al, 1993) in the formulation of the generalized entering coefficient discussed in the next section.

Generalized Entering Coefficient

Due to the lack of correlation between bulk foam predictions and porous media performance of foam oil systems using the classical spreading and entering theory, researchers tried to include the effect of the PS-film stability in a modified entering coefficient. Work done by Bergeron (Bergeron et al, 1993) relates the entering coefficient to the disjoining pressure isotherm of the asymmetric PS-film. The formulation is shown in equations 7 and 8 in Appendix D: List of Equations.

Whereby the generalized entering coefficient is:

$$E_{o/w}^{g} = -\int_{\Pi(h_\infty)=0}^{\Pi(h_0)} h \, d\Pi$$

h_∞ is film thickness that is not influenced by disjoining forces, h_0 is the film thickness at equilibrium at a particular disjoining pressure. As shown above, the generalized entering coefficient in Bergeron's definition, is the negative of the area under the disjoining pressure isotherm down to the foam film thickness at equilibrium (steady state conditions). A similar concept was also discussed by (Lobo and Wasan, 1993) where they described the use of the interaction energy per unit area to describe the PS-film stability.

Entry Barrier

The concept of entry barrier relates to the existence of a critical capillary pressure that an emulsified droplet of oil has to overcome to enter the foam film, which also relates to the strength and stability of the PS-film. Research by Denkov (Denkov et al, 2004) measured the critical capillary pressure as an indicator of the PS-film stability.

They theorize that the critical capillary pressure P_c^{cr} has physical interpretations, as the capillary pressure required to squeeze the oil droplets into the surfactant-gas interface. This is very similar to the disjoining pressure concept, and the major difference is the technique in measuring the critical capillary pressure, which is a modified film trapping technique FTT.

Denkov states that the value of P_c^{cr} can be a practical indicator of the PS-film stability, and if it's exceeded it is suggested that bridging mechanisms characterized by a high positive bridging coefficient, play the main role in foam destruction once the entry barrier has been exceeded. It is further hypothesized, that the addition of foam boosters (co-surfactants) can create a modified micellar structure in the surfactant-air interface

leading to a stronger PS-film stability, characterized by a higher oil droplet entry barrier which leads to a more oil resistant foam system.

2.2.5 SUMMARY

The literature review performed on oil foam interactions showed a general lack of consistency in terms of prediction tools used. Entering and spreading coefficients and lamella number can all sometimes lead to good correlation to the bulk foam scale but not always to the core scale. Pseudo emulsion film theory was developed to understand the microscopic phenomena that can explain oil films being stable for certain oil foam combinations. A generalized entering coefficient, was developed to incorporate the PS film stability and interfacial properties for prediction. The disjoining pressure and entry barrier approaches are also well rooted in literature in their treatment of the PS-film.

2.3 Foam and WAG Enhanced Oil Recovery

Nearly all EOR processes demand mobility control to minimize issues related to displacing phase (Chambers and Radke 1993) chief among them is WAG EOR. Creating an in-situ foam of injected gas with tailored surfactants has been reported to achieve mobility control and thus enhancing the oil recovery efficiency (Heller 1994; Srivastava and Nguyen 2010; Blaker et al. 2002). This work studies the use of a suitable surfactant, and hydrocarbon gas to create foam in situ to assist in the mobility control of the solvent gas, in order to maximize the oil recovery from WAG.

The co-injection of gas and aqueous chemical solution results in dispersed flow of two phases where the combined mobility of two phases would be less than their individual mobility, thus resulting in improved mobility control and oil displacement (Kovscek et al. 1997; Talebian et al. 2013). In addition, dispersed-gas mobility decreases with increasing rock permeability, which could not be achieved with conventional polymers for chemical EOR (Kovscek and Bertin 2002; Kapetas et al. 2015). This not only improves chemical conformance control, but also reduces the likelihood of gas plugging oil-rich low permeable rock matrix in heterogeneous reservoirs. Besides there are several other applications of aqueous foam in the oil and gas industry (Scherubel and Thorne 1981; Marquis and Kuehne 1992; Dawe et al. 1993).

Based on the 2014 worldwide EOR survey (Koottungal 2014), a comparison was made between hydrocarbon gas-EOR and CO2-EOR technologies. With 37 hydrocarbon-EOR fields worldwide in comparison to about 140 CO2-EOR fields, the hydrocarbon-EOR technology has found limited application and thus is relatively less mature than the CO2-EOR technology. Since the produced hydrocarbon gases in onshore fields can often find better economic value than re-injection in the reservoir. Regions with stranded

hydrocarbon gas such as Al-Shaheen offshore reservoir, are perfectly suited for use in foam assisted EOR.

A well-known foam trial was carried in the Snorre field on the Norwegian Continental Shelf of the North Sea from 1997 to 2000 with support from the European Commission's THERMIE Project (Svorstol et al. 1996; Blaker et al. 2002; Skauge et al. 2002; Spirov et al. 2012). The permeability of the sandstone reservoir varied in the range of 400 mD to 3500 mD. The injection in the reservoir was below the original water-oil contact. The Foam Assisted Water Alternating gas (FAWAG) was initiated in August 1998 but the concluding trial was initiated in 1999. An anionic surfactant α-olefin sulfonate, commercially known as AOS, with a carbon chain length of C14-C16 was used as the foaming agent. From design experiments, it was found that foam strength was constant down to very low surfactant concentration and foam qualities as high as 95%. Surfactant loss due to partitioning to oil, adsorption and microbial degradation was considered. Reservoir simulations were used to design the injection strategy. From foam model, minimum surfactant concentration and adsorption showed the largest impact on foam treatment efficiency. The uncertainties related to reservoir parameters were higher and showed a large impact on the oil recovery. Overall, the simulations were not conclusive regarding injection mode, rates and total surfactant volume.

Approximately 800,000 pounds of commercial grade surfactant was injected, with an overall cost of around $ 1 million and the incremental oil attributed from this implementation was approximately 1.57 million barrels which is a strong economic success even with today's low oil price.

3 SURFACTANT FORMULATION AND CHRACHTERIZATION

As outlined in section 1.2, the main goal of this research work is to find a surfactant formulation that can generate an effective foam with methane gas. An effective foam is judged based on the ability to generate strong foam in this specific reservoir with a mobility reduction factor higher than 10 at the reservoir conditions stated (144,000 ppm salinity, 55 °C temperature, and oil wet conditions). In this section the surfactant screening process is outlined, arriving at the main surfactant used in the remainder of the study.

3.1 Surfactant Screening

The initial stage of surfactant screening and selection focused on finding a surfactant that can generate a strong foam (foamability) while having sufficient aqueous stability at the reservoir conditions. This involved bulk foam tests and aqueous stability tests of 3 main families of surfactants:

1. Alkyl-Polyglycoside (APGs) – Nonionic surfactants
2. Alpha Olefin Sulfonates (AOS) – Anionic Surfactants
3. Alkyl Amines (C25, T25) – Cationic Surfactants

The key criteria of aqueous stability were evaluated by creating surfactant solutions at various salinities from 40,000 ppm up to 150,000 ppm. During this stage the highly foaming AOS surfactant was excluded, as it showed severe precipitation at salinities close to the reservoir formation brine salinity of 144,000 ppm. This is shown in Figure 7. The other surfactants tested all had sufficient solubility at the tested salinities.

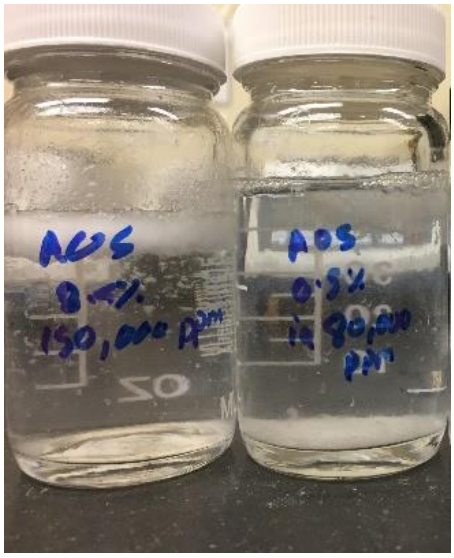

Figure 7: AOS Aqueous Stability Test

Bulk foam testing in this initial phase was carried out with a dynamic foam generation set up. This is shown in Figure 8 whereby air is injected at a constant rate into a set volume of surfactant at 0.5 %wt. concentration, the foam volume generated at steady state is then measured.

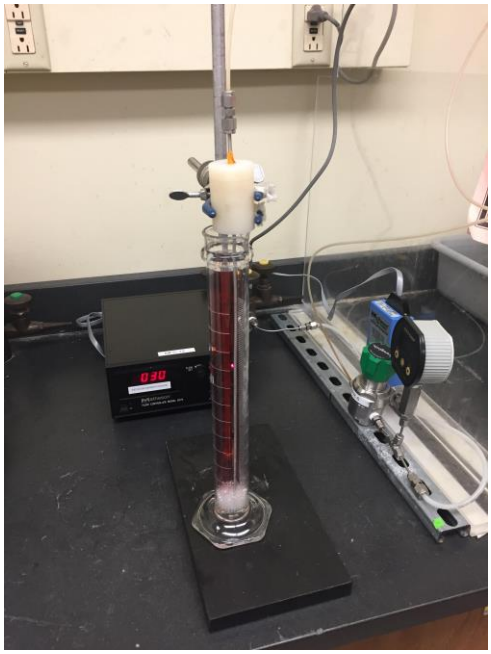
Figure 8: Dynamic bulk foam test set-up

The above test was used on four surfactants, an APG, AOS, T25 (amine) and C25 (Alkyl-amine). The results are summarized in Table 3.

SURFACTANT (0.5 %WT CONC.)	**DYNAMIC FOAM VOLUME (ML)**
APG-5 in DI solution	240
APG-5 at 150k ppm	180
T25 (150 k ppm)	23
C25 (150 k ppm)	20
AOS (0 ppm)	240 * very fine stable texture

Table 3: Dynamic bulk foam tests for screening surfactant groups

Based on the above, the nonionic APG surfactant was selected as the strongest foaming group that can handle the reservoir formation brine salinity.

3.2 APG Surfactant

In the APG group, five surfactants were available for testing, labelled APG-1 through APG-5. Bulk foam tests outlined in Appendix B: Experimental , were used on the APG surfactants, with and without the presence of oil to screen for the best foaming surfactant, and the best resistance to oil.

Table 4 lists the active content of the APG surfactants used in this project. The surfactants were generally diluted to 2.5% stock solution in deionized water, and then subsequently diluted down to the tested concentrations, at the formation brine salinity (144,000 ppm).

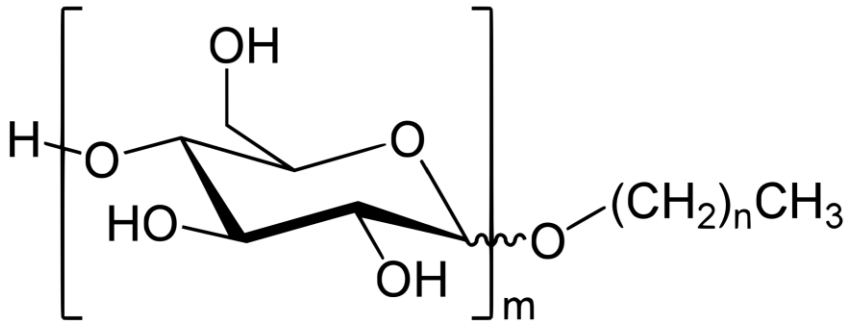

Figure 9: Alkyl Polyglycoside surfactant structure

Surfactant	Active Content
APG-1	50%
APG-2	70%
APG-3	50%
APG-4	60%
APG-5	50%

Table 4: APG surfactants.

The difference between the APG surfactants lies in the number of CH2 groups. The chemical structure of APG surfactants is shown in Figure 9 above.

Aqueous stability tests were done using 5000 ppm concentration and revealed that only APG-1 precipitates at the formation brine salinity and reservoir temperature of 55°C. This can be seen in the bulk foam tests shown in Figure 12. Following this initial screening, further testing with the best performing APG is done to evaluate its micro emulsion phase behavior with the crude oil, as well as the effect of bulk oil on the foam stability.

3.2.1 APG FOAM STABILITY WITHOUT BULK OIL

Solutions at 144,000 ppm salinity, and 1000, 2000 and 5000 ppm surfactant concentration were tested. The results of the foam stability test for (5000, 2000 ppm) solutions, is shown in Figure 10 and Figure 11.

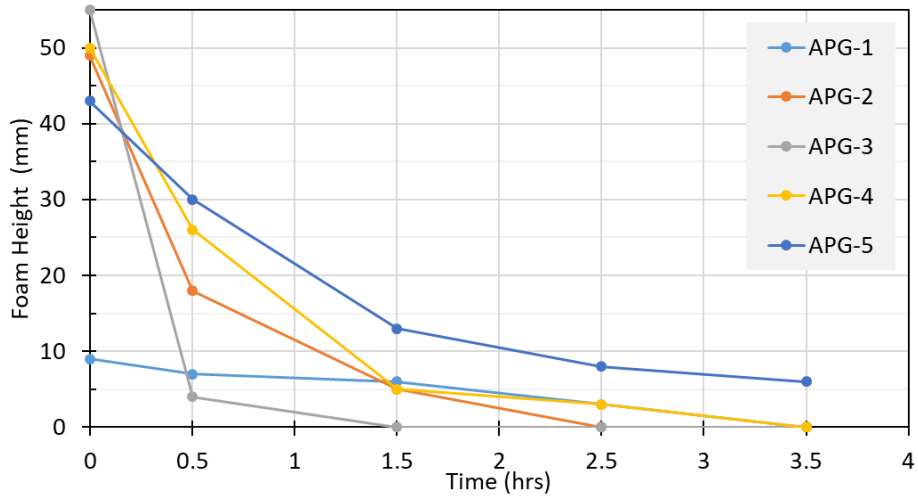

Figure 10: Bulk foam strength for APG series at 5000 ppm concentration

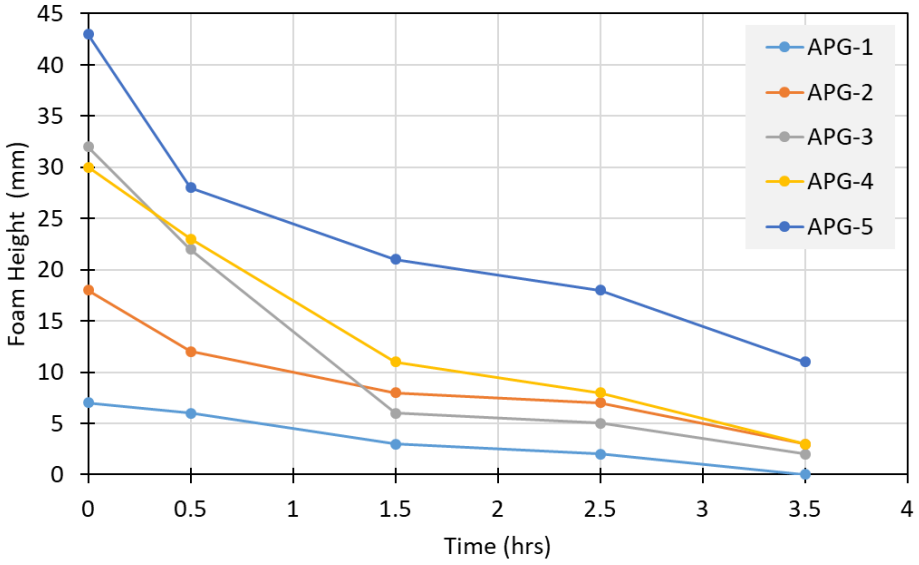

Figure 11: Bulk foam strength for APG series at 2000 ppm concentration

Figure 12 shows an example of the test at two different times. The results for the three different concentrations confirmed that APG-5 is the best foaming surfactant.

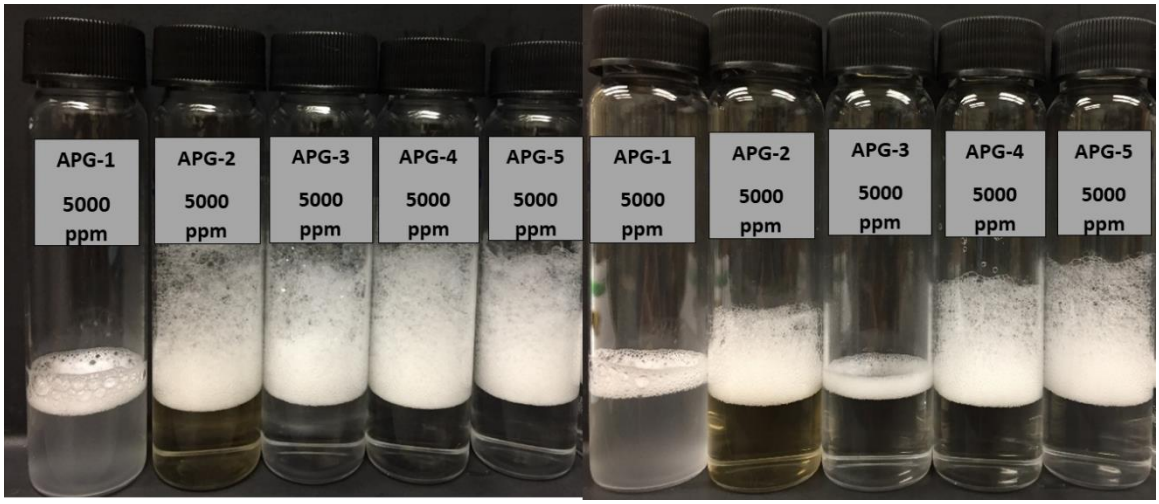

Figure 12: Foam stability test for 5000 ppm concentration at t=0, 2.5 hours

Furthermore, APG-1 showed precipitation at the formation brine salinity of 144,000 ppm and did not pass the aqueous stability requirement. The bulk foam stability for APG-5 as a function of the surfactant concentration is shown in Figure 13.

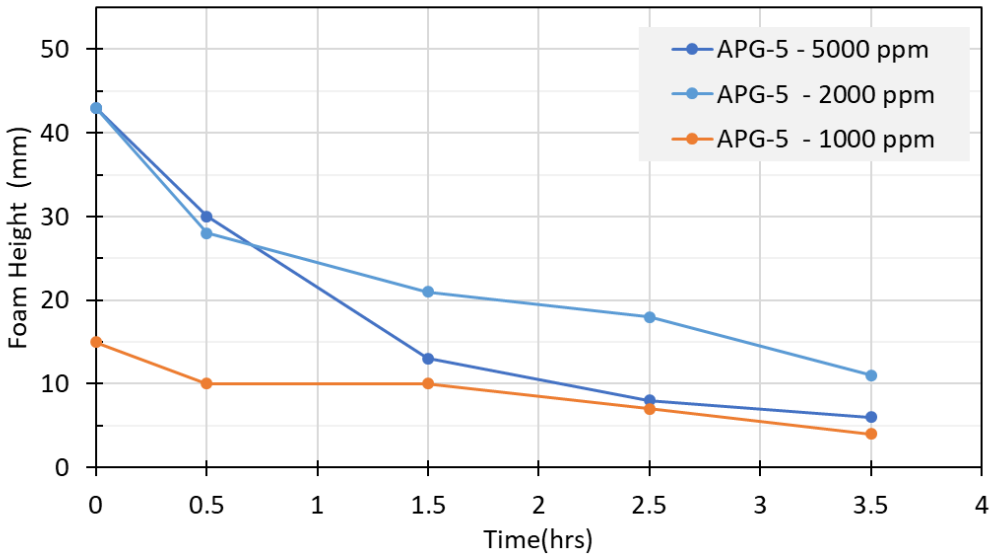

Figure 13: Foam stability for APG-5 for various concentrations

The above gives a qualitative indication of the optimal concentration for the best performer, APG-5; is between 2000 and 5000 ppm. Further testing is done in core flood experiments to further quantify the optimal concentration.

3.2.2 APG FOAM STABILITY WITH BULK OIL

The next step in screening APG surfactants was testing the foam stability in presence of oil. The same tests above were repeated but with the addition of 1 cc (10% by volume) of Al-Shaheen crude oil to the surfactant solutions.

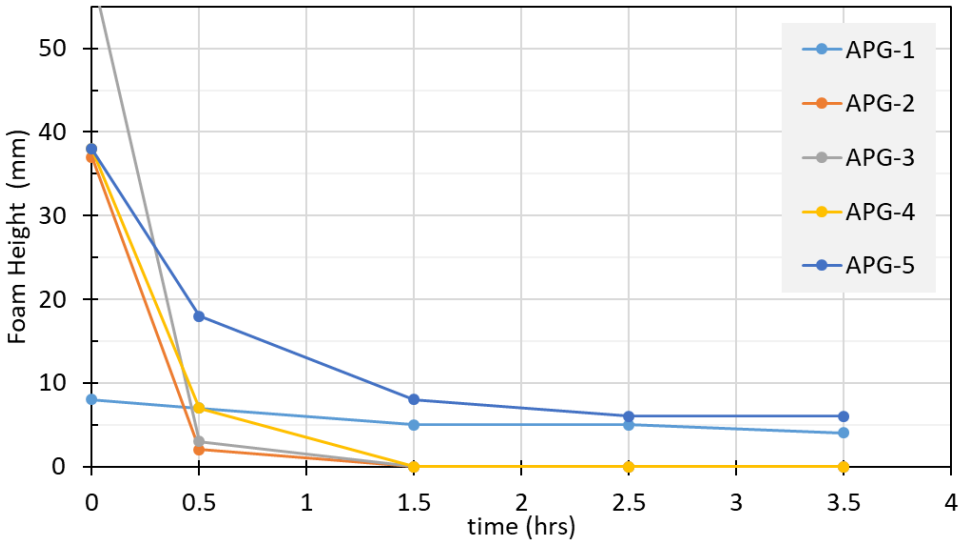

Figure 14: Foam stability in presence of oil (5000 ppm solutions, 144,000 ppm salinity)

Figure 14 shows a drop in the foam stability in the presence of oil as expected. APG-5 shows the best foam stability even in the presence of oil. A snapshot of the test at two different times is presented in Figure 15. The interaction of surfactant and oil leads to the creation of a pseudo-emulsion film (PS-film) which is inherently more unstable than a foam film of surfactant-water alone. We further consider the effect of oil on foam stability, by testing APG solutions containing only the microemulsions and no bulk oil.

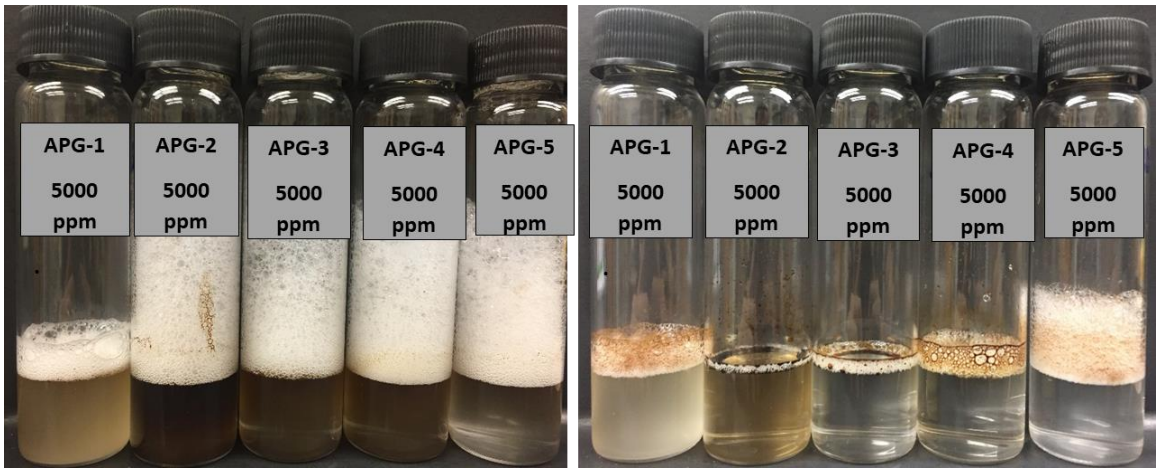

Figure 15: Foam stability test for 5000 ppm concentration, 1 ml oil, at t=0, 2.5 hours

The effect of oil emulsions in surfactant solution, as well as the effect of oil on bulk foam performance of APG-5 is presented in the next section.

3.2.3 APG-5 BULK FOAM STABILITY TESTING – EFFECT OF OIL AND OIL EMULSIONS

When oil encounters APG-5 surfactant solution it emulsifies into small droplets in the surfactant solution, a type I Windsor microemulsion phase behavior. To quantify the effect of the oil emulsions in the surfactant solution on foaming ability, a series of bulk foam tests of APG-5 solution with emulsified oil were done. First, the surfactant is mixed with oil, and then the surfactant solution containing micro-emulsified oil droplets ("solubilized oil") is separated from the bulk oil. Since the tendency to form micro-emulsions is influenced by salinity, the solutions of APG-5 were prepared at [48,000, 80,000, 110,000 and 144,000 ppm] salinities.

The different salinity solutions were tested without emulsified oil as a control case to understand the influence of salinity on foaming stability. The results are shown in Figure 16 and Figure 17. A snapshot of the test is included in Figure 18.

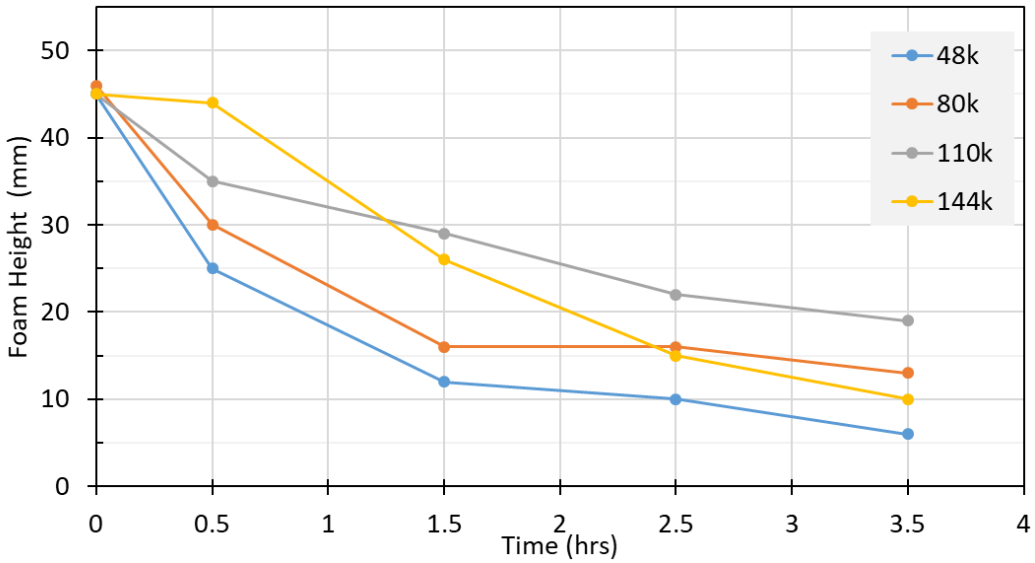

Figure 16: APG-5 bulk foam stability at various salinities

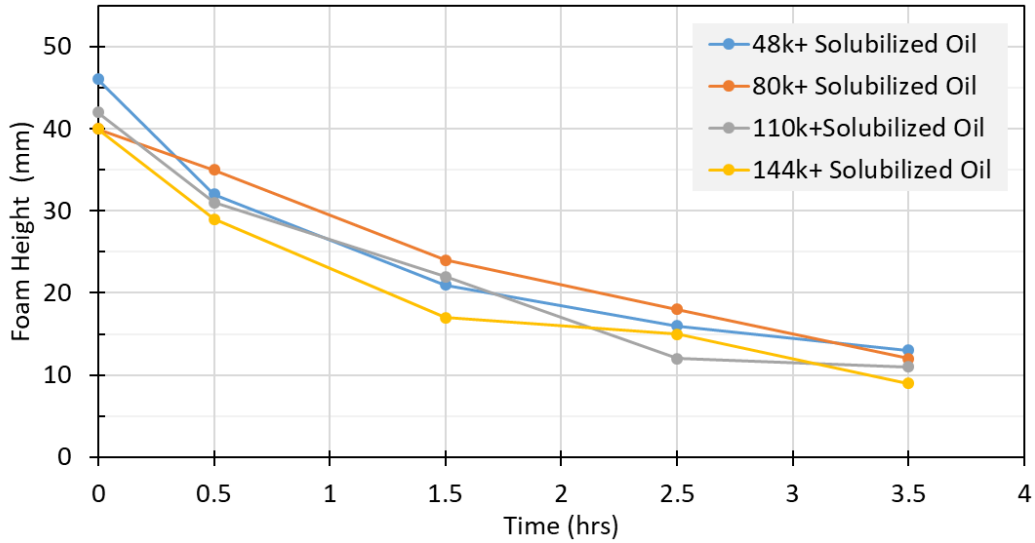

Figure 17: APG-5 bulk foam stability at various salinities with solubilized oil

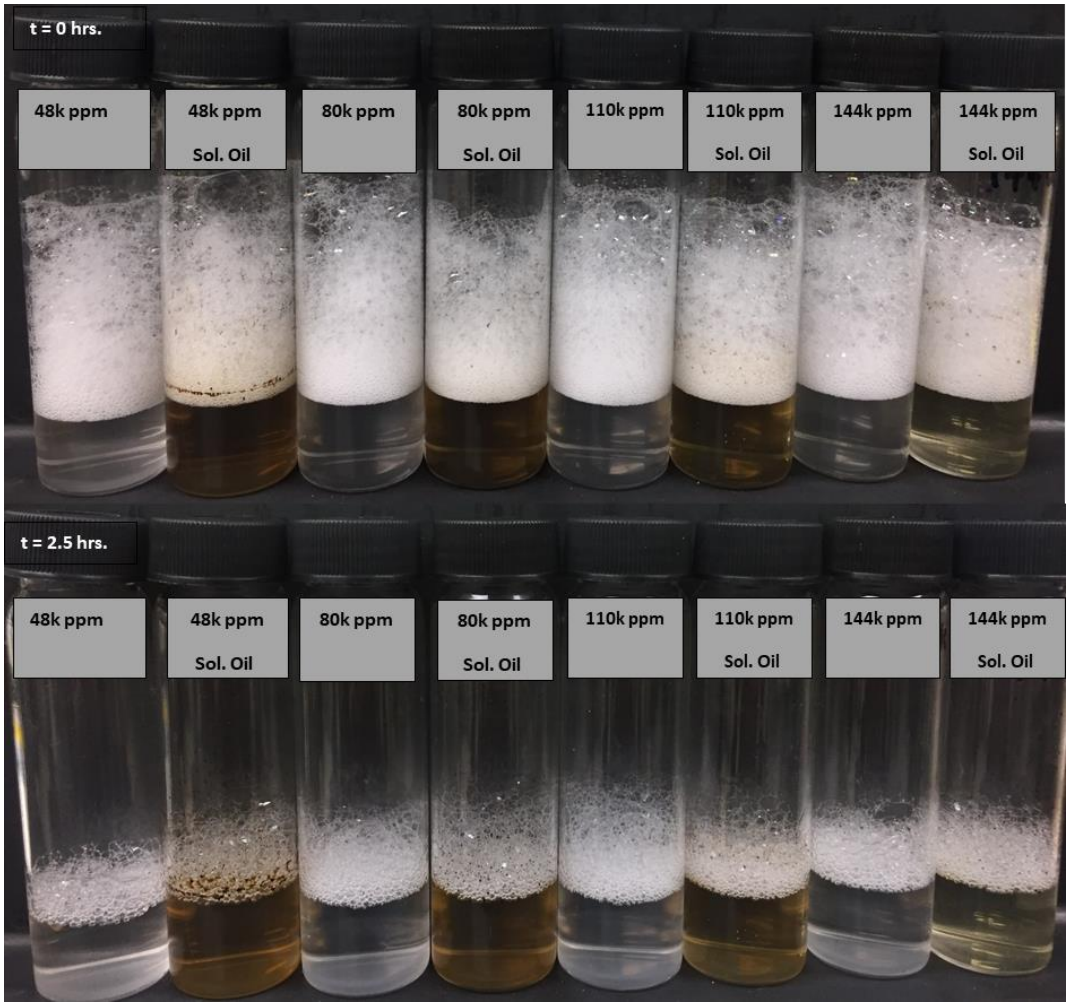

Figure 18: APG-5 bulk foam stability at various salinities with and without solubilized oil, at t=0, 2.5 hours

The results indicate that salinity has no detrimental influence on foam stability; as long as the surfactant remains soluble at the higher salinities. This is supported by work done by Liu (Liu et. al, 2005), who reported an increase in foam stability for an increase in salt concentration between 2 and 5%, then for concentrations beyond that foam stability was insensitive to the increase in salinity.

The foam strength and stability are only marginally affected by the presence of solubilized oil in the surfactant solution compared to the effect of the bulk oil. A test of

the influence of increasing bulk oil concentration was also done. Surfactant solution of 5000 ppm concentration was mixed with 3, 5, 8, and 11%wt. of crude oil. Results are summarized in Figure 19 while Figure 20 shows a snapshot of the test. As expected, bulk oil presence in the APG solution is detrimental to the foam stability.

Higher oil concentration leads to weaker foam generation and stability; however, foam still forms which indicates that in a dynamic situation whereby gas and surfactant solutions are continuously injected, a resilient foam can persist even in the presence of a relatively high oil content.

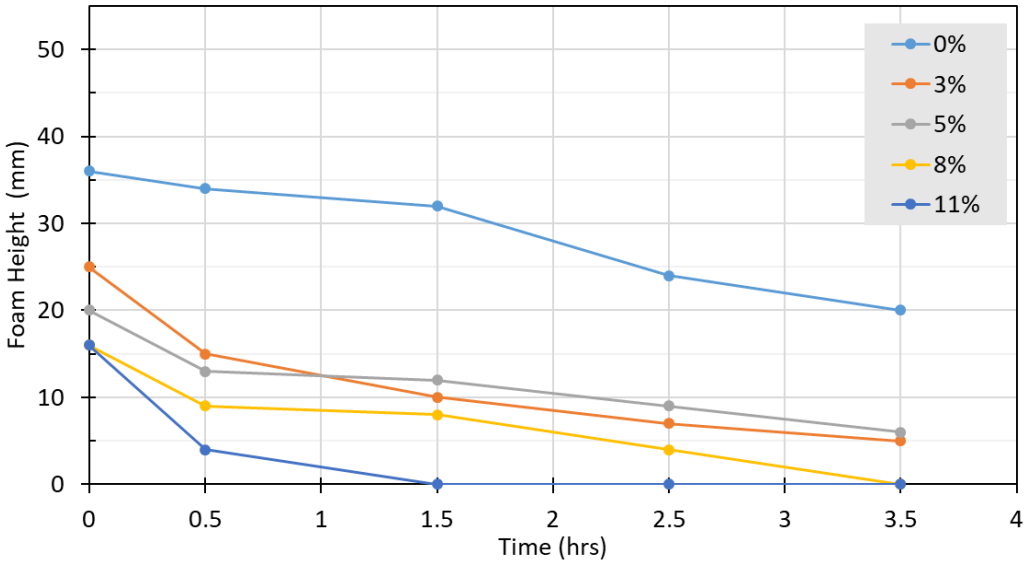

Figure 19: APG-5 bulk foam stability with varying added bulk oil %wt. and 144,000 ppm salinity

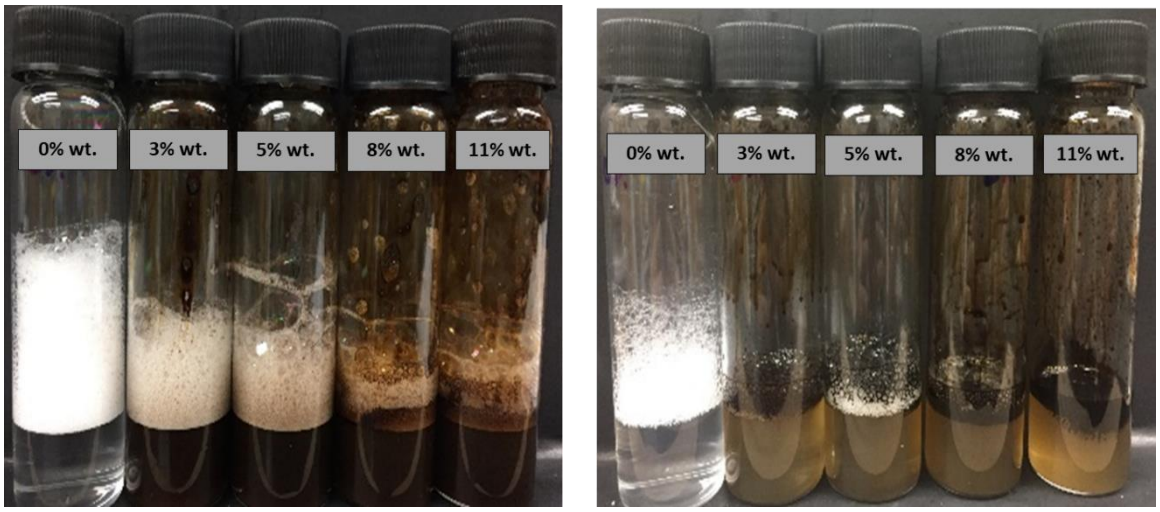

Figure 20: APG-5 bulk foam stability test with varying %wt. of oil [Left t=0, Right: 2.5 hrs.]

Based on the bulk foam stability testing, APG-5 produces strong foam even in the presence of solubilized oil in solution, at the formation brine salinity and temperature. The next stage in the characterization of APG-5 surfactant is to evaluate its microemulsion phase behavior and then its adsorption onto carbonate rock.

3.2.4 APG-5 MICROEMULSION PHASE BEHAVIOR

For this study, the main goal of the foam is to provide mobility control, and divert the gas from higher permeability zones during WAG injection. In order to verify that the APG-5 surfactant does not create strong (high viscosity) micro-emulsions, a series of phase behavior tests were carried out for various salinities from 48,000 ppm to 144,000 ppm. A snapshot of the test is shown in Figure 21 .

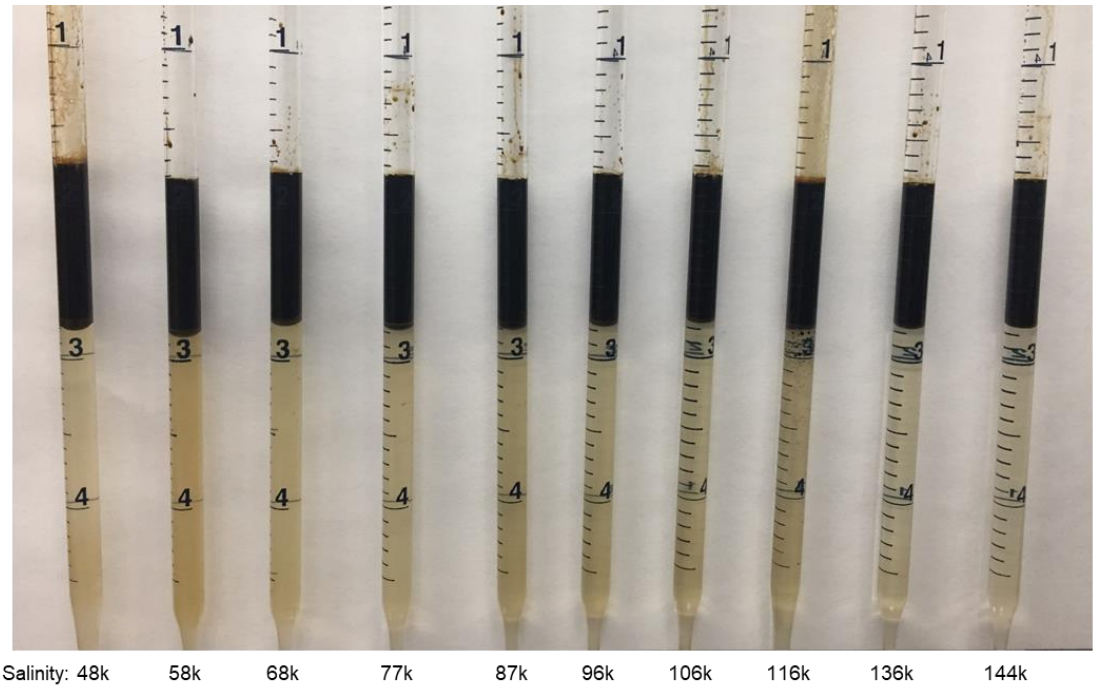

Figure 21: APG-5 microemulsion phase behavior test

As clearly seen only two distinct phases are present. An oil phase on top and an aqueous (surfactant) phase with small droplets of oil microemulsions in surfactant solution on bottom. This represents a Type-I Windsor microemulsion. There is no middle phase present and no risk of creating viscous emulsions when the APG-5 surfactant interacts with oil in the reservoir. Section 3.3 outlines static adsorption testing on APG-5 and Estaillades limestone carbonate rock.

3.3 APG-5 Surfactant Adsorption on Carbonate Rock

In order to understand the impact of surfactant adsorption in carbonate rocks, static adsorption experiments outlined in Appendix B: Experimental .

The tests done on the selected surfactant APG-5 aimed at creating the adsorption isotherm, whereby the adsorption of a series of surfactant solutions at different concentrations is estimated. The LCMS technique used is described in Appendix B: Experimental .

In summary, 10 cc of APG-5 surfactant solution was mixed with 5 grams of crushed Estaillades limestone rock (powdered and sieved through 300-600 mesh size), and mixed thoroughly over a couple of days, while at reservoir temperature of 55°C. The solution is then extracted for testing. A series of calibration samples (500, 1000, 1500, 2000, 3000, and 5000 ppm) were tested and used to estimate concentrations of the test solutions.

Figure 22 shows the adsorption results for two tests carried out at the same conditions. It can be seen that the static adsorption of APG-5 approaches 2.5 mg/g at higher concentrations.

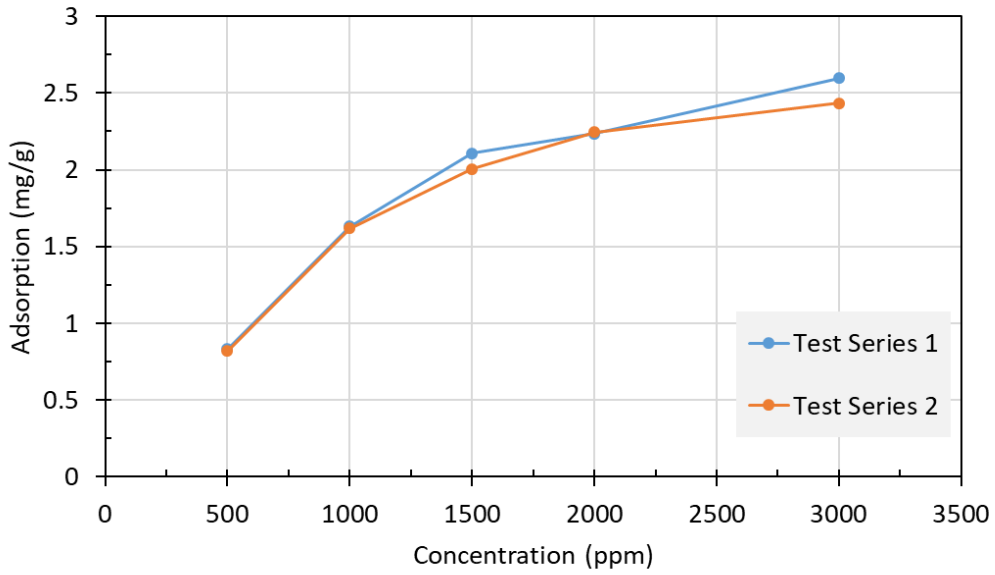

Figure 22: Adsorption in (mg of Surfactant/g of rock) for APG-5 and Estaillades Limestone

It is also important to verify the impact of oil presence and the oil wet state of the reservoir on the adsorption of the APG-5 surfactant. In order to simulate different wettability conditions, Estaillades grains were wetted in oil and aged and soaked in crude oil at 80 °C for 1 week, they were then dried at and excess oil removed. Different percentages of oil wet grains were mixed with water wet grains, and the above tests were repeated. Two test runs were carried out for 1000 ppm and 1500 ppm solutions.

The proportion of oil wet grains to water wet grains was varied from 25% to 100% of total added rock grains. For example, the 50% oil wet grains were comprised of 5 g of the oil aged grains, and 5 g of the clean Estaillades grains. The adsorption results are summarized in Figure 23.

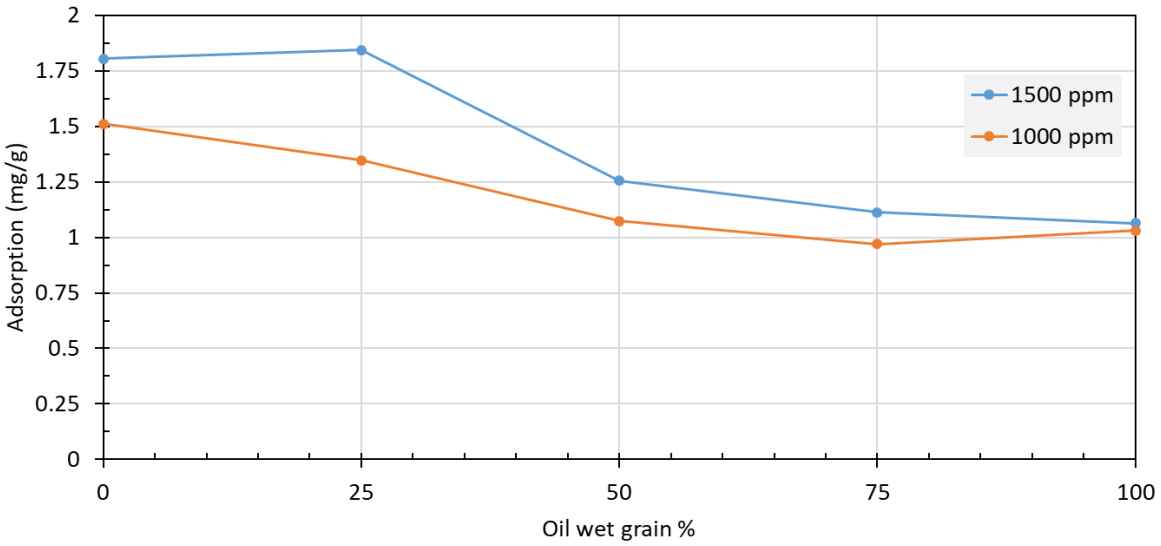

Figure 23: Effect of oil and wettability on APG-5 adsorption

It can be clearly observed that the presence of oil and oil wet grain remarkably lowers the adsorption of the surfactant onto the carbonate surface. For the 1500 ppm solution, the adsorption is lowered to 1.15 mg/g, while for the 1000 ppm solution it is lowered down to 1.05 mg/g, which represents a reduction of 40% approximately.

Additionally, Al-Shaheen field presents a mixed wet rock case, and as such evaluating the adsorption for mixed wet conditions is very important. The static adsorption results as well as the bulk foam stability tests show that the required APG-5 concentration is a range between 2000-5000 ppm. Further experiments using core floods are carried out to evaluate the ideal concentration, rates and foam qualities required.

3.4 APG Foam Characterization in Water Wet Rock Without Oil

The first step in studying the foam generated by APG-5 and methane in core floods is focused on the effect of surfactant concentration as well as foam rheology in water wet conditions and without the presence of oil. The experiments were conducted using the methodology and experimental set up outlined in Appendix B: Experimental . The experiments were conducted until a steady state pressure drop was observed across the core. Steady state results are presented in the following sections focused on the impact of concentration, and the observed foam rheology.

3.4.1 SURFACTANT CONCENTRATION

When considering the optimal APG-5 surfactant concentration for field implementation, important factors to consider include the economic limitations, adsorption rate, the effect of oil on foam stability, and finally foam strength in steady state porous media. Typical rates encountered during field implementation are above 5 pore volumes per day (PV/d) near wellbore, and 1-2 PV/d in the far field region. The injection rate used for this experiment was 5 PV/d, at 80% foam quality. The permeability to brine was measured to be 118 mD, and the porosity was determined to be 23.2%. This experiment is part of WW-A as listed in

Table 8 of *Appendix A: Summary of Experiments.*

Four different concentrations of APG-5 were tested until a steady state pressure drop was achieved. To assess foam strength, the apparent viscosity concept is employed here and is calculated as per equation 4 in Appendix D: List of Equations. A plot of the apparent viscosity of the generated foam as a function of surfactant concentration is shown in Figure 24.

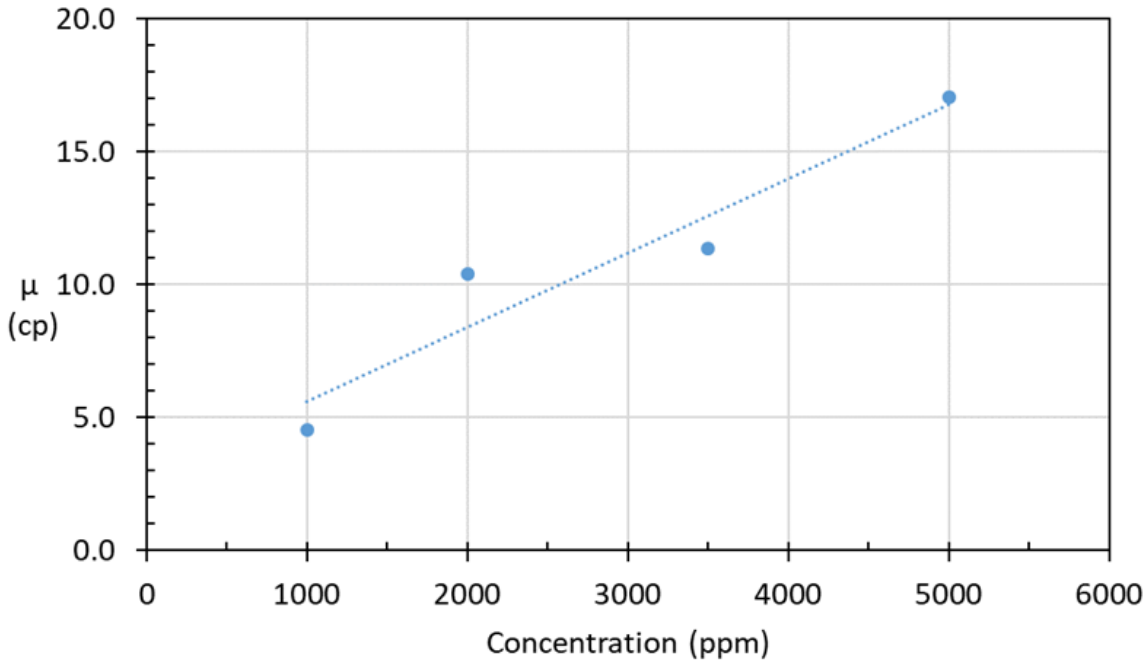

Figure 24: Effect of surfactant concentration on foam strength [5 PV/d and 50% FQ]

A linear trend can be observed between the strength of the foam generated and the concentration of surfactant solution. Based on the above results, a concentration of 3500 was considered suitable as it would be below the economic limit of 5000 ppm, as well as still providing a strong enough foam for mobility control. The next step in evaluating the required parameters for foam injection is evaluating the optimal gas fraction and understanding the foam rheology as it pertains to rates in the near wellbore, and far field regions.

3.4.2 FOAM RHEOLOGY

Following the concentration scan, the core was flooded with brine for over 20 Pore volumes, and the permeability was determined again, and was found to be around 103 mD. A slight reduction in permeability is expected due to particle immobilization during prolonged injection. Using APG-5 solution of 3500 ppm concentration, three different

injection rates were tested (2, 5, and 10 PV/d), at four different foam qualities (30,50,80, and 90). This experiment is listed as part of WW-A in Appendix A: Summary of Experiments.

While testing the 10 PV/d rate, the pressure drops at 30% FQ exceeded the system limitations (pressure limit downstream of the methane MFC is around 1600 psi) and was terminated.

The apparent viscosity at the three different rates is shown in Figure 25.

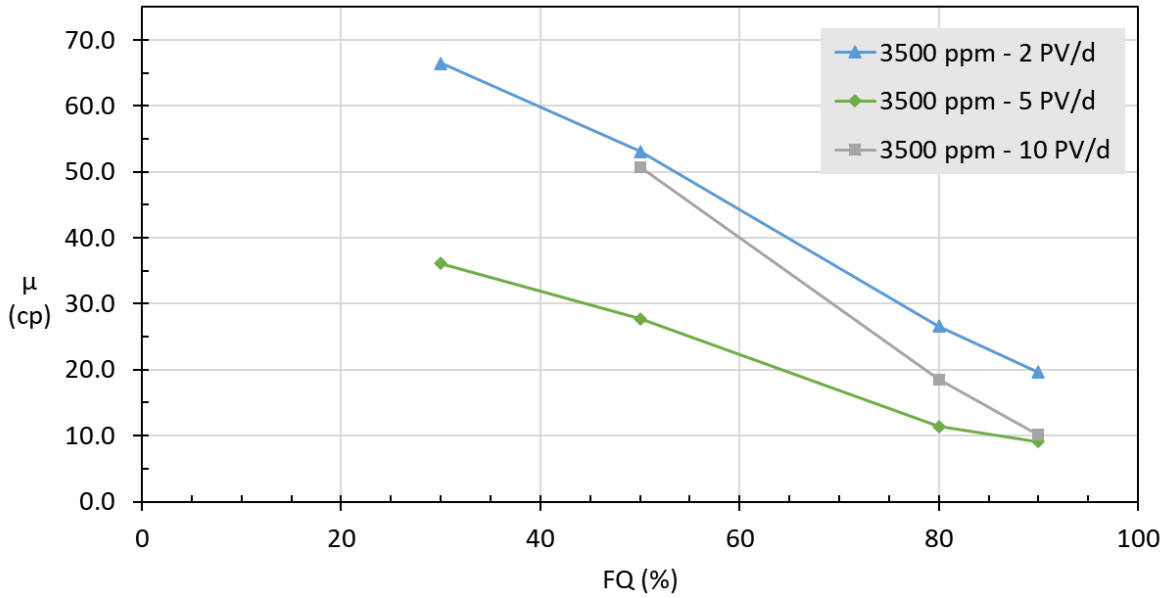

Figure 25: Effect of oil and wettability on APG-5 adsorption

Comparing the apparent viscosity results from both the 5 and 10 PV/d to the 2 PV/d shows that the foam generated by APG-5 and methane gas has shear thinning properties. This is ideal for field implementation, as the near wellbore region would have higher shear rates, and so maximizing injectivity would require lower foam strength in that region. As the shear rates slow down at the far field steady state values (in range of 1-2 PV/d), the foam viscosity rises due to this shear thinning behavior.

This is the required foam behavior for conformance control, and would indeed aid in diverting gas in the WAG injection away from thief zones. Increasing the rate from 5 PV/d to 10 PV/d shows shear thickening behavior, and this contradictory response can be attributed to the heterogeneity in the core, as well as the surfactant and foam being forced into smaller pores at the higher rates leading to a higher pressure drop and stronger foam being generated. Hysteresis and foam trapping can also explain this discrepancy, as reported by Simjoo (Simjoo et al, 2011).

We can also observe from Figure 25 that lower FQ between 30% and 50% yield the strongest foam, where a maximum foam strength peak is likely to fall in that range. For field implementation, gas availability, as well as economic considerations would both influence the decision on FQ to use. However, based on the experimental behavior of the APG-5 foam, aiming for 40% FQ would yield the optimal conformance control in the reservoir.

3.5 Summary

This chapter discussed the initial surfactant screening process that resulted first in choosing alkyl-Polyglycoside (APG) as the main surfactants for this study. Then narrowed down to APG-5 as the most effective foaming agent, with and without the presence of oil. APG-5 adsorption was studied, as well as the microemulsion phase behavior. Finally, the foam behavior in an analogue rock (Estaillades limestone) was studied in water wet conditions. The ideal concentration was found to be around 3500 ppm, and the foam rheology was seen to be mostly shear thinning. The next chapter will focus on studying the impact of oil on the APG-5 foam.

4 IMPACT OF OIL ON FOAM PERFORMANCE

In order to understand how the foam generated by APG-5 and methane gas will behave in the presence of oil in porous media a series of experiments were carried out. At the end of experiment WW-A a test of the impact of solubilized oil is presented, WW-B tested for the impact of residual oil on foam strength and WW-C tested the impact of mobile oil on foam viability.

Similar experiments were carried out in oil wet cores (cores were aged in oil for over 4 weeks). Experiment OW-A focusses on the impact of residual oil on foam in oil wet media. OW-B tests impact of mobile oil on foam in oil wet media. Results are presented in the subsequent sections.

4.1 IFT Measurements

Table 5 shows the average interfacial tension measurements done for APG-5 solution and Al-Shaheen crude oil. Equations (1, 2 and 3) listed in Appendix D: List of Equations, are used to estimate the entering and spreading coefficient as well as the lamella number.

Sample	**ST [mN/m]**
APG-5 at 0.35% - Oil	0.387
Oil-Air	45.5
APG-5 at 0.35% - Air	10.7
Entering Coefficient	-34
Spreading Coefficient	-35
Lamella Number	4.2

Table 5: APG-5-Oil-Air IFT Measurements

As shown above, the negative entering coefficient implies a highly stable foam-oil system. While the entering/spreading coefficients are not consistent predictors, literature review shows that when the entering coefficient is negative, it is reliable to assume that the foam-oil system is stable in presence of oil. The lamella number was first presented by (Schramm and Novosad, 1990) is based on the concept that foam is destabilized by the formation and movement of emulsified oil drops that move into foam plateau borders, once enough droplets accumulate and join the foam is ruptured. While (Shramm et al., 1993) showed that the lamella number was good as an indicator of foam stability to oil, (Dalland et al, 1994) showed that it cannot be used as an accurate predictor for bulk foam or porous media foam scales. In that study, negative entering coefficients for some stable oil-foam systems, resulted in very high lamellae numbers.

The lamella number of 4.2 indicates some emulsification of oil is happening, which is confirmed in phase behavior tests, and this value falls in the range of Type-B foam that can be susceptible to oil foam instability.

The highly negative entering coefficient, and the strong stability of the APG-5 foam in presence of oil in bulk foam tests indicate a stable foam-oil system, and core flood experiments were conducted accordingly. First analyzing the influence of residual oil on the foam strength, then the influence of mobile oil, and finally, the wettability of the reservoir.

4.2 Impact of Solubilized Oil on Foam Performance

Following the end of experiment WW-B, an experiment using surfactant solution with solubilized oil was done. First, surfactant solution with solubilized oil was prepared. The APG-5 surfactant solution at 144,000 ppm was mixed with crude oil, and then the surfactant solution was gravity separated leaving out the excess oil. The core flood was then repeated for the 2 ft/d rate. Steady state pressure drops at 30,50, 80, and 90% were then recorded, and the resulting apparent viscosity was computed.

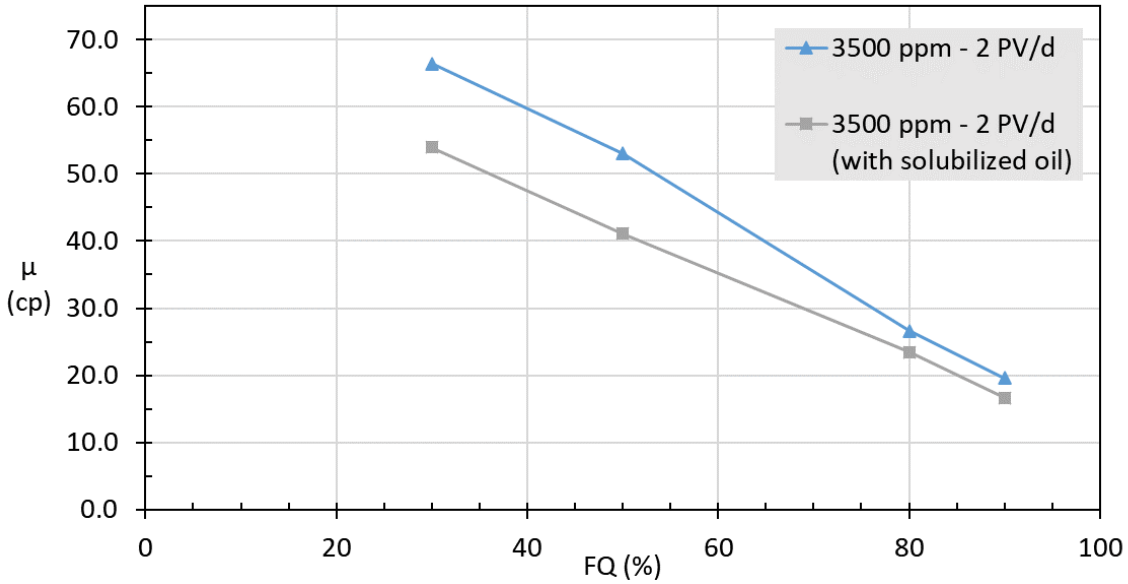

Figure 26: Foam apparent viscosity for 2 PV/d, 3500 ppm, with and without solubilized oil in solution

It can be observed from the results of Figure 26 that the presence of solubilized oil in solution does reduce the strength of the generated foam. However, the generated foam at the optimal FQ of 30-50% is still considerably strong at 40-50 cp apparent viscosity. The reduction in foam strength of around 20-25%, is due to the effective reduction in surfactant concentration in solution that is available for foaming as some of the surfactant binds to the microemulsions of oil in solution.

4.3 Impact of Residual Oil Saturation on Foam Performance

WW-C was carried out in water wet Estaillades limestone cores, the core was water flooded with formation brine, then injected with Brine and gas to simulate WAG flood, and reducing the oil saturation to the residual oil saturation. This closely resembles the conditions in reservoir layers of high permeability whereby most of the oil has been swept out.

The same process was repeated for OW-A whereby this core was aged in oil for over 8 weeks, establishing an oil/mixed wet state.

Figure 27 and Figure 28 show the results of the steady state foam strength at Sor for both mobile oil experiments, OW-B (oil wet) and WW-C (water wet) in terms of the apparent foam viscosity, and the effective mobility reduction factors.

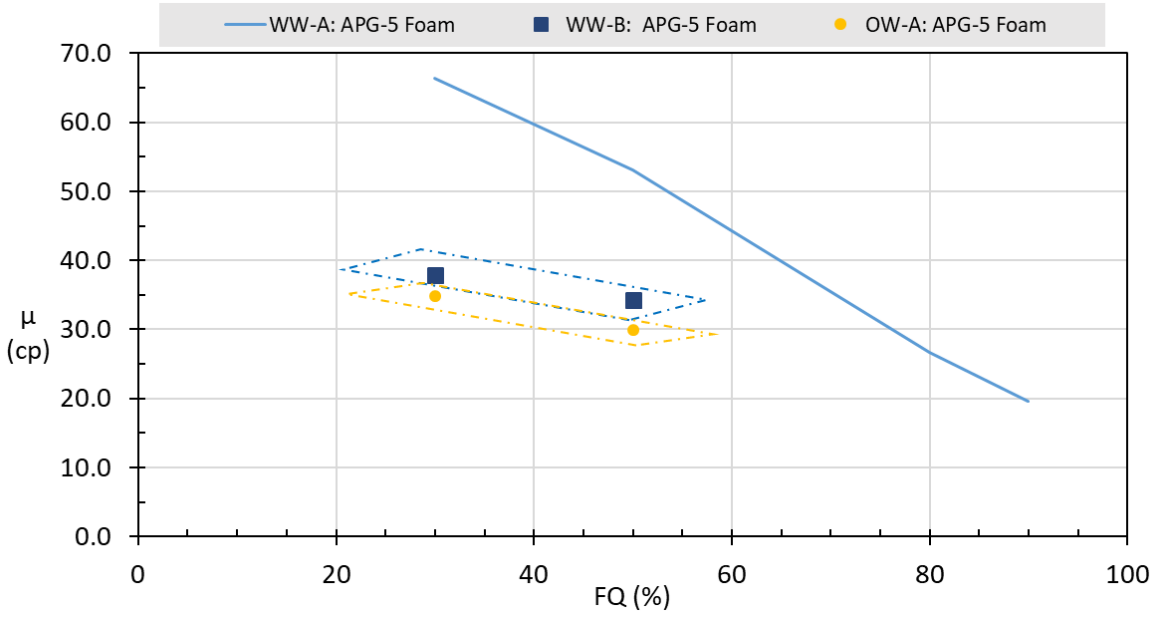

Figure 27: Apparent viscosity results for APG-5 foam at residual oil in oil wet and water wet conditions

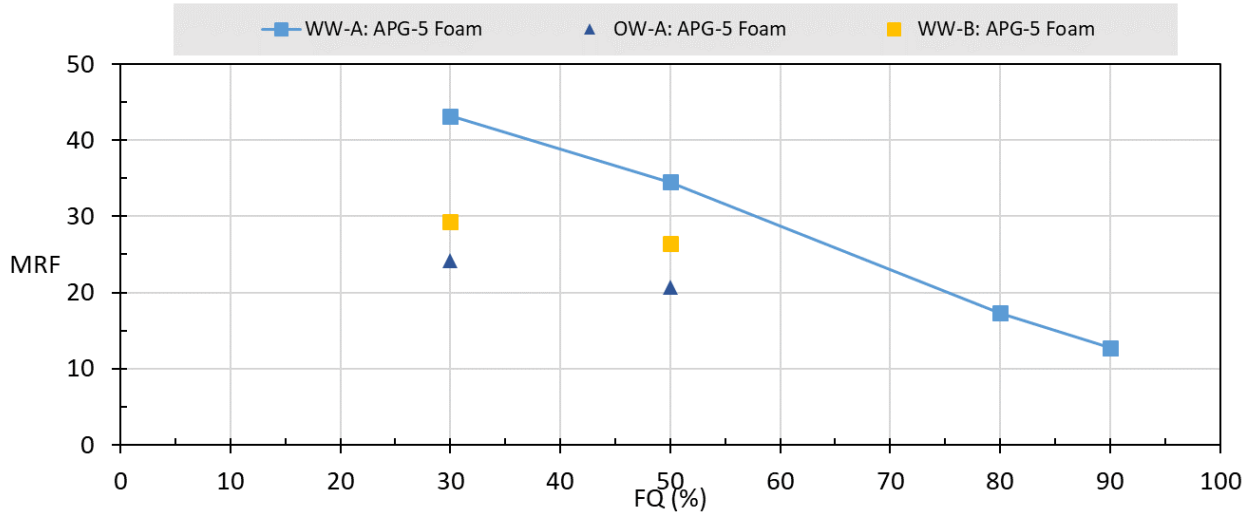

Figure 28: MRF Data for APG-5 (3500 ppm) foam at 2 PV/d for OW and WW cases at Sor

As we can see in Figure 27 and Figure 28, the presence of oil generally impacts the foam negatively compared to the no oil water wet case (solid lines) with a reduction of 25% for the water wet case, and about 44% for the oil wet case. In both wettability states, the APG foam can create an effective foam with MRF values ranging between 20-25 (2 PV/d 50, 30%) for the oil wet case, and 25-30 for the same rates in the water wet case. Foam strength and MRF are impacted due to the oil wet nature of OW-A, with a reduction of 35% of the foam strength.

The above results show that the APG-5/methane foam system is stable to the Al-Shaheen crude oil. This supports the results of the entering and spreading coefficients which indicated a non-entering system, whereby oil droplets do not protrude into the foam film. However, the significant drop in foam strength due to oil presence must be explained.

Foam films are thermodynamically unstable structures, that decay with time if no more lamellae are generated. Furthermore, contact with oil creates a pseudo emulsion film (PS-film) between the oil-gas-water phases. This film is asymmetric, and also

thermodynamically unstable. However, the disjoining pressure of these asymmetric films have two possible regions (local minima in the disjoining pressure of the film) where the film can exist in a metastable state, however if the film thins too much (below 5 nm), or is too thick (higher than 50 nm) (Garret, 2016) then the film is unstable.

(Nikolov et al., 1989) and (Lobo and Wasan, 1993) showed that a micellar structure of surfactant molecules exists in stable PS-film and helps prevent further thinning and maintains the metastable state. However, since the PS-film is asymmetric, and film drainage processes are dynamic in nature, the PS-film stability is also kinetic in nature. (Manlowe and Radke, 1990). All of the mentioned researchers show that the asymmetric nature of these films, and the complexity of the interfaces, makes them more unpredictable and unstable than normal foam films.

Considering the impact of oil saturation separately, shows that it plays a role in the foam stability in presence of oil. The oil saturations in OW-A and WW-B were 11.4 and 5.3% respectively, whereby the higher oil saturation in OW-A, led to foam strength that is 25% weaker than WW-B. In higher oil saturation, there is a higher probability of foam and oil contact, combined with the discussion of the PS-film above, this explains at face value the weaker foam in higher oil saturation. Furthermore, the mechanics of three phase flow show that having a higher oil saturation leads to higher interstitial velocities of the other two phases.

A key observation found during the above experiments was the delayed foam propagation to reach the steady state values listed above. This was also experimentally proven by (Mannhardt et al., 1999) where they showed a reduction in the rate of foam propagation (time to reach the maximum strength) at higher oil saturations. While they claim a critical oil saturation that limits foam strength if exceeded, we argue based on results in this study that this concept is flawed. Instead, it is the spatial distribution of oil

in the reservoir, as well as the pseudo-emulsion film stability that determine the level of destabilization at higher oil saturations. Whereby higher oil saturation that is isolated in high permeability pockets with minimal contact with propagating foam may not destabilize foam as much as lower oil saturation that is spread out evenly in the pore space with high contact with propagating foam.

While an effective foam is achieved with the APG surfactant in the presence of oil and various wettability states, further improvement to the MRF may be required for optimal field implementation for mobility control. There are two possible optimizations, one focusses on the APG-foam resistance to oil, and improving the pseudo emulsion film stability of the foam-oil system. The second possible improvement targets altering the wettability towards water wet, which enhances the foam generation sites, and also improves the foam stability. These are discussed in chapter 6.

4.4 Impact of Mobile Oil on Foam Performance

Mobile oil that is produced during EOR processes has a higher chance of contacting foam lamellae. For this reason, a detailed experimental procedure (outlined in Appendix B: Experimental) was designed in five key stages.

First establishing foam at a rate of 4.75 PV/d and 50% FQ, then during stage 2, the co-injection of foam and oil is done with oil at 0.25 PV/d until 0.5 PV of oil is in the core. The third stage is foam alone, followed by the fourth stage which is with oil co-injection to steady state, and finally the fifth stage has foam alone to steady state. Mobile oil is present in the core starting in the second stage, however due to the relative permeability effects in stage 4 and 5, the analysis focuses on the foam alone stages 3 and 5 whereby oil is being desaturated. To eliminate capillary entry effects at the core inlet, the middle and top sections only were used in the analysis of the mobile oil experiments.

Figure 29 shows the apparent viscosity estimation and the oil saturations for the oil-coinjection experiment in oil wet conditions of OW-B.

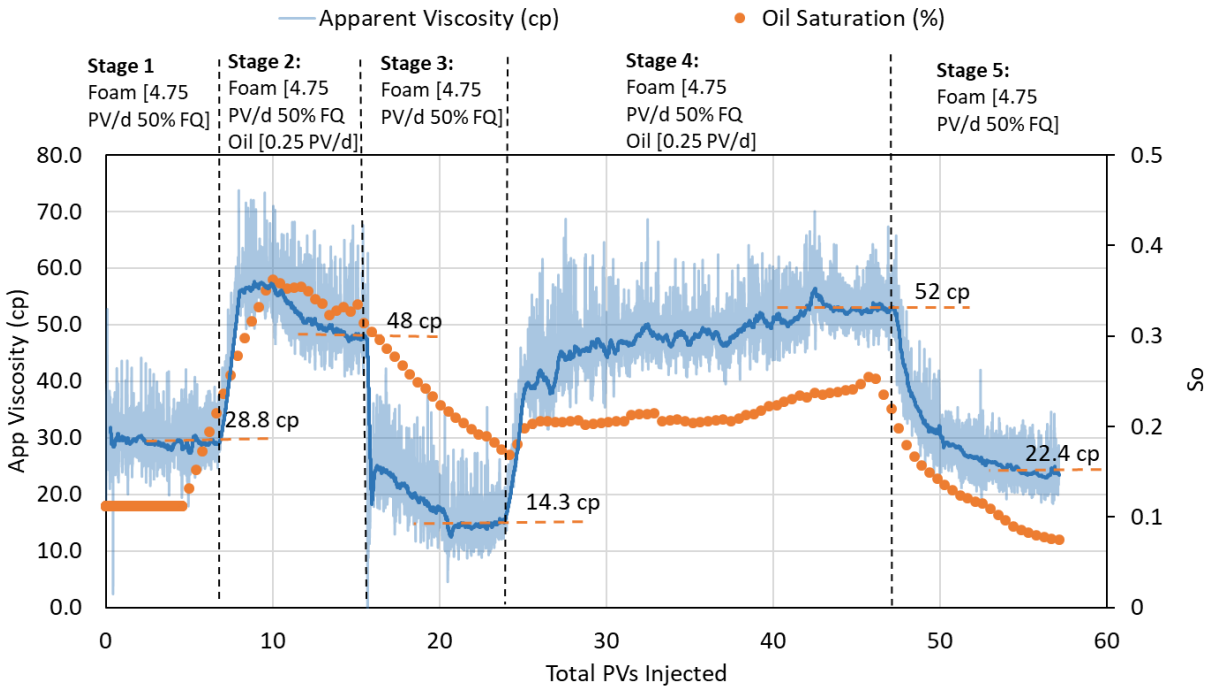

Figure 29: OW-B Mobile oil experiment transient apparent viscosity

As shown above in Figure 29, during co-injection the pressure drop and apparent viscosity rises considerably due to relative permeability changes associated with three phase flow. However, during stage 2 where 0.5 PV of oil is co-injected with foam, causes the apparent viscosity is stage 3 where its foam alone to drop down to 14.3 cp at the end of stage 3. This can be attributed to the higher oil saturation of 18. Wettability also plays a key role here, and this is discussed further in chapter 5.

During the long stage 4, higher pressure drops were encountered, this led to more of the oil that was previously immobile to be recovered, and the oil saturation dropped to bellow the Sor at 8% compared to 11% at start of the experiment. In order to better understand the effect of the mobile oil on foam, the same experiment above (OW-B) was conducted in water wet conditions (WW-C) starting from a strong foam state, and no oil in the core in this case. The results of the co-injection experiment are shown in Figure 30:

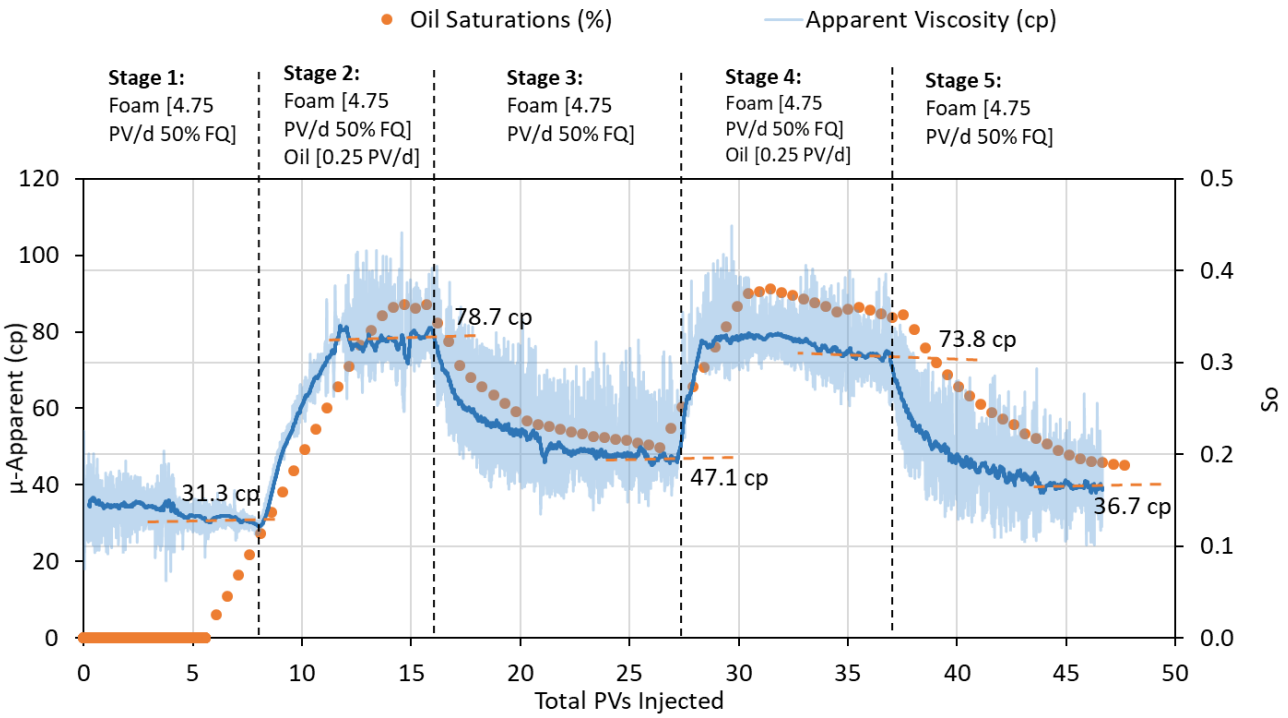

Figure 30: WW-C Mobile oil experiment transient apparent viscosity

In this experiment, the apparent foam viscosity in stage 3 is 1.5 times higher than before the co-injection case (47 cp vs 31 cp). And in stage 5 it is close to 1.2 times higher at 37 cp compared to 31.3 cp. This higher apparent viscosity can be attributed in part to the relative permeability effect due to the higher oil saturations in stages 3 and 5 (~20% oil saturation). However, it is likely that strong foam continued to be generated even in the presence of such a high oil saturation, as a high pressure drop, and apparent viscosity was still seen in stage 3 and 5.

This can be supported by the fact that very strong foam present in the core before co-injection was not completely destabilized, and only the points of contact between the foam and the injected oil may have been impacted. In their mobile oil experiments (Boeije, 2016, p119) show that effective foam can still exist even in presence of significant mobile oil, but in a severely reduced capacity (50% reduction). However, their study suffered from

a few issues. Firstly, timescale of the study was insufficient in observing the oil-foam interaction, and their surfactant/crude mixture seemed to create stable and microemulsions that may have impacted the results. Finally, no estimation of the oil saturation is given, thus no inference can be made about how the oil saturation impacted the foam.

In the results we presented, the oil saturation changes during the co-injection experiments, combined with the observed apparent viscosities in the foam alone stages, has important connotations that support that foam-oil interactions are governed mainly by oil saturation distribution within the pore space, and the contact probability between oil droplets and foam lamella, as well as the inherent foam film stability in presence of oil, and finally the wettability of the cores.

4.5 Summary

In this chapter we outlined the experiments focused on studying the impact of oil on foam in three main facets. Firstly, the impact of emulsified oil droplets in surfactant solution (solubilized oil) was studied. It was shown that it reduces foam stability by a factor of 20% approximately.

Secondly, the impact of residual oil saturation on foam was studied. Presence of oil was shown to reduce foam strength considerably, however effective foam can still be seen in both water wet cores and oil wet cores at residual oil having mobility reduction factors (MRFs) of around 28 for the former and 24 for the latter.

Finally, the impact of mobile oil was studied. The key takeaway from this experiment is that the presence of mobile oil does not preclude the formation of an effective foam, and that this foam is stronger in the water wet experiment. However, the relative permeability effects made the analysis more complicated and limited the quantification of these observations.

5 IMPACT OF WETTABILITY ON FOAM PERFORMANCE

One of the main aspects of foam oil interactions on the core scale that is not well studied is the effect of wettability. Researchers generally assume a negative impact on foam when the rock is in an oil wet or even mixed wet state. This was confirmed by Shramm and Mannhardt (1995) who showed that the foam effectiveness was reduced in oleophilic rock more than hydrophilic rocks at residual oil saturations.

In the series of core flood experiments carried out in this work the effect of wettability on foam was explored more closely, in an attempt to quantify and clearly show its effect on foam propagation and strength.

5.1 Foam Performance at Residual Oil Conditions

Results presented in section 4.3 , Figure 27 show that the foam strength in water wet cores at residual oil saturation is 25-30% higher than that in an oil wet core at residual oil saturation.

This result includes a combination of factors. Firstly, the residual oil saturation in OW-A is higher at 11.4% vs 5.3% for the water wet conditions of WW-B. This higher oil saturation may play a big role in the above noted reduction. Secondly, relative permeability effects in the oil wet conditions play a role in the pressure drops seen and used to calculate the apparent viscosity and MRF for the foam which complicates the analysis.

Thirdly is the impact of wettability. Here, an oil wet/mixed wet state implies that that the rock grains are wetted with oil, thus the sites for foam generation are reduced. As mentioned in chapter 2, lamella division and snap off are key foam formation mechanisms, and these are impacted when the rock is not wetted with water.

Thus, one cannot conclude with absolute certainty, that the weaker foam in OW-A is solely due to one of these parameters, but is likely due to a combination of all three, whereby wettability plays a big role.

5.2 Wettability impact in Mobile Oil Experiments

The mobile oil experiments discussed in section 4.4 also sheds light on the impact of wettability on the foam strength and propagation. Figure 31 shows the apparent viscosity of the mobile oil experiments OW-B and WW-C. While Figure 32 below, shows the steady mobility reduction factors (MRFs) of the foam in the foam alone stages 1,3 and 5.

In the OW-B experiment, the initial 0.5 PV oil co-injected with foam reduces the foam apparent viscosity below 20 cp (stage 3). While in the water wet case WW-C, the apparent viscosity of the injected fluids increases to ~ 50 cp after co-injecting 0.5 PV of oil (stage 3). This indicates that the relative permeability changes due to oil injection into the water wet core is more impactful on the overall pressure drop than in the oil wet case. As discussed previously, in WW-C, the oil saturation rise in the core contributes to the apparent viscosity seen at the end of stage 3 and 5, however a big part of that apparent viscosity seen is due to foam. In this case the oil in the core is distributed within the pore space, and not at the grain surfaces.

Comparatively, in the oil wet case of experiment OW-B, relative permeability effects are evident during co-injection, but are less prevalent when the oil injection is stopped. This is likely due to the additional oil collecting at the pore surfaces mainly, with most of the original mobile oil being swept out during the waterflood, and gas and brine injection stages which preceded the experiment. This distribution of oil on the pore surfaces

is the likely behind the lower foam strength (apparent viscosity) and MRF in the foam alone stages 3 and 5, where it leads to more foam destabilization in the oil wet case.

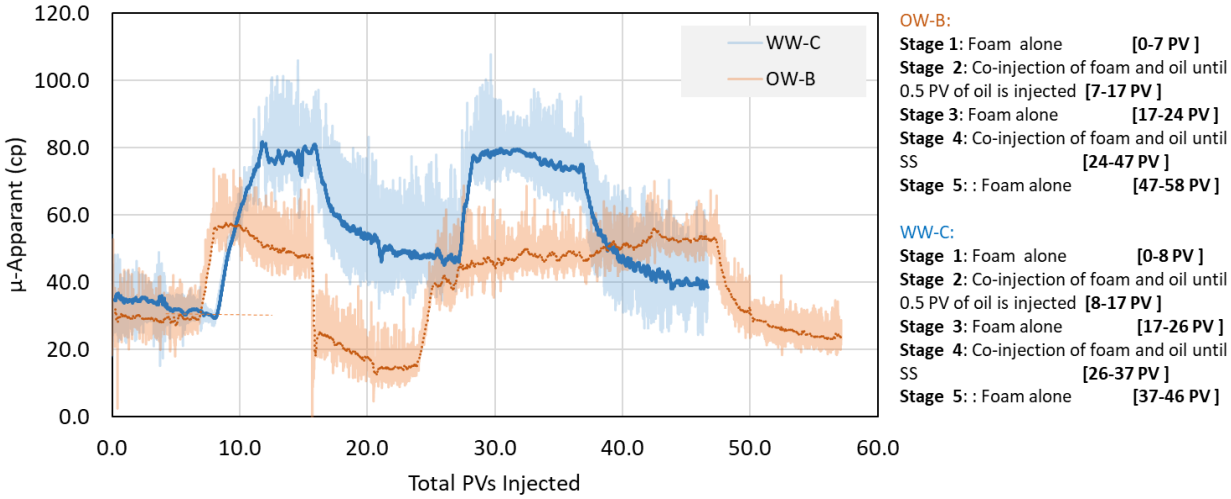

Figure 31: Mobile Oil Experiments, comparing water wet to oil wet conditions

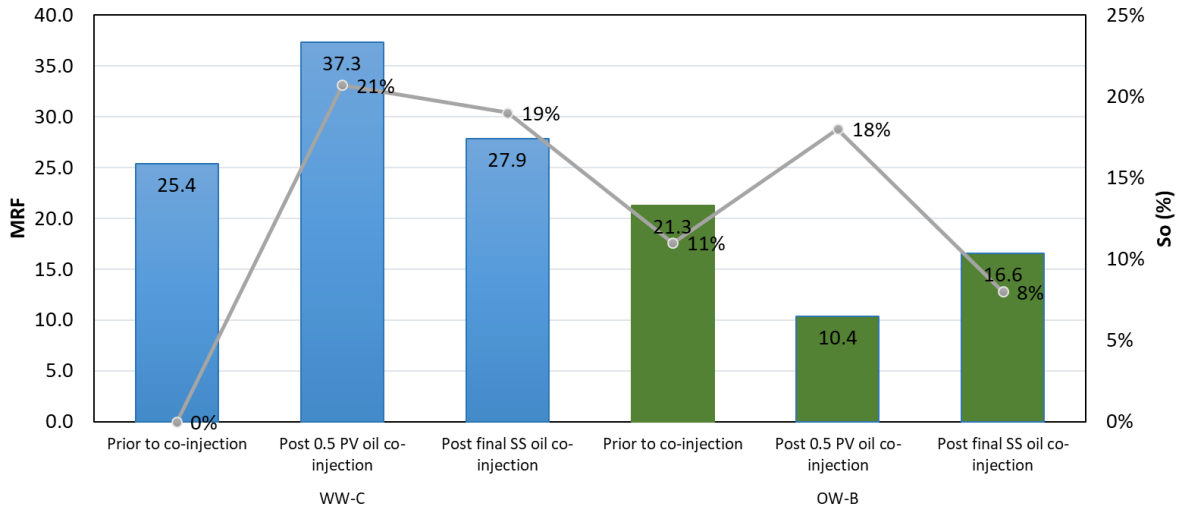

Figure 32: Mobile oil experiments - MRF data for foam alone stages for water wet and oil wet conditions

It can be clearly seen that having higher oil saturations increases the MRF for the water wet case, this is due in part to the relative permeability effects, as discussed above. In the oil wet case (OW-B) the higher oil saturation seems to impact the apparent viscosity

and MRF negatively, whereby we postulate that foam is more severely impacted by the introduction of mobile oil.

Specifically, looking at the first foam alone stage post co-injection in OW-B and WW-C shows a similar oil saturation 18% in OW-B and 21% in WW-C, but the foam is far weaker in the oil wet case. Thus, the above experiments further show that while strong foam can still form in oil wet conditions, the impact of oil on foam under these circumstances is more detrimental than in water wet conditions.

As established above, the presence of oil, as well as the wettability state of the reservoir have an impact on foam performance. In the following chapter 6 we explore enhancing foam strength by foam boosting as well as wettability alteration.

5.3 Summary

This section focused on the analysis of the impact of wettability (water wet or oil/mixed wet conditions) on foam performance. Two main findings were verified that align with the research in literature. Firstly, oil wet conditions severely impact the foam strength. These experiments showed an additional reduction of around 25% in foam strength over the water wet case at residual oil saturation. Mobile oil experiments show that mobile oil in oil wet rock impacts foam viability more than in a water wet rock.

Chapter 6 will discuss enhancements to the foam system that focus on improving foam resistance to oil, and altering wettability to enhance foam performance.

6 FOAM FORMULATION ENHANCEMENTS

Previous chapters outlined the process and evaluation of the APG-5/Methane Foam system. It was shown that the presence of oil, or oil wet state, both reduce the foam strength, but an effective foam can still be seen even in those conditions. Based on these results, two areas for enhancement of the foam system were identified. First, enhancing the foam's resistance to oil, and secondly, chemically altering the wettability of the rock to more water wet conditions to improve the conditions for foam generation and stability. These enhancements are tested in core flood experiments, and outlined in the following sections.

6.1 Foam Enhancement – Wettability Alteration

In this section, we explore wettability alteration to enhances the performance of the APG-5 Methane foam. Theoretically, altering the wettability state towards water wet conditions will improve foam propagation, and stability, however, relative permeability effects involved in three phase flow can complicate the observed behavior. First, we explore the characterization experiments carried out to arrive at a successful formulation.

6.1.1 WETTABILITY ALTERATION AGENT SELECTION

A detailed literature review has shown that multiple families of surfactants can change the rock wettability through different mechanisms. The first possible mechanism where the surfactant head group adsorb to the organic components of the crude oil on the rock surface through ion-pair formation, and having a hydrophilic tail, alters the wettability to water wet.

If the surfactant head groups are not charged, hydrophobic interaction between surfactant tail groups and adsorbed oil components forces surfactants to adsorb to the surface and change wettability. (Salehi et al., 2008) Based on the above, our main foaming

surfactant (APG-5), a nonionic surfactant (head group is not charged), was tested against another anionic surfactant TGT-1 and a cationic surfactant C25.

While contact angle tests showed the C25 to be very effective at altering wettability, it was excluded from further consideration due to its limited application in offshore environments. While the APG-5 and TGT-1 surfactants are both biodegradable and environmentally friendly alternatives. Contact angle tests were then carried out to verify the wettability alteration capability of TGT-1 and APG-5 and a blend of both, details of the experimental procedure are summarized in Appendix B: Experimental .

TGT-1 was successful in changing the contact angle of an oil droplet aged on calcite to less than 90 degrees at various concentrations (500, 1500, 2000 and 3000 ppm). Figure 33shows an example of the final contact angle of an oil droplet after being in contact with TGT-1, APG-5 and a blend of the two surfactants for a few hours.

TGT-1 Alone

Test (1500 ppm)	Final contact angle
	77.45
	80.4
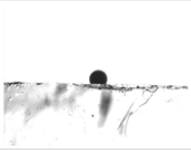	56.35
	77.15

APG-5 Alone

Test (2000 ppm)	Final contact angle
	136.35
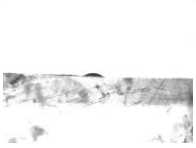	150.2
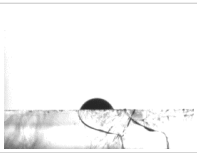	118.3
	121.85

APG-5 & TGT-1 Blend

Test (2000/1000)	Final contact angle
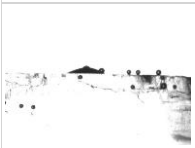	139.1
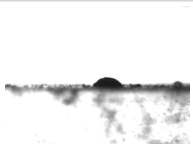	120.3
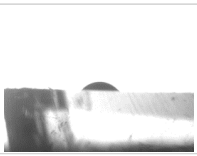	131.2
	134.7

Figure 33: Example Contact Angle Measurements for TGT-1 and APG-5 and their blends

A summary of the results is shown in Figure 34.

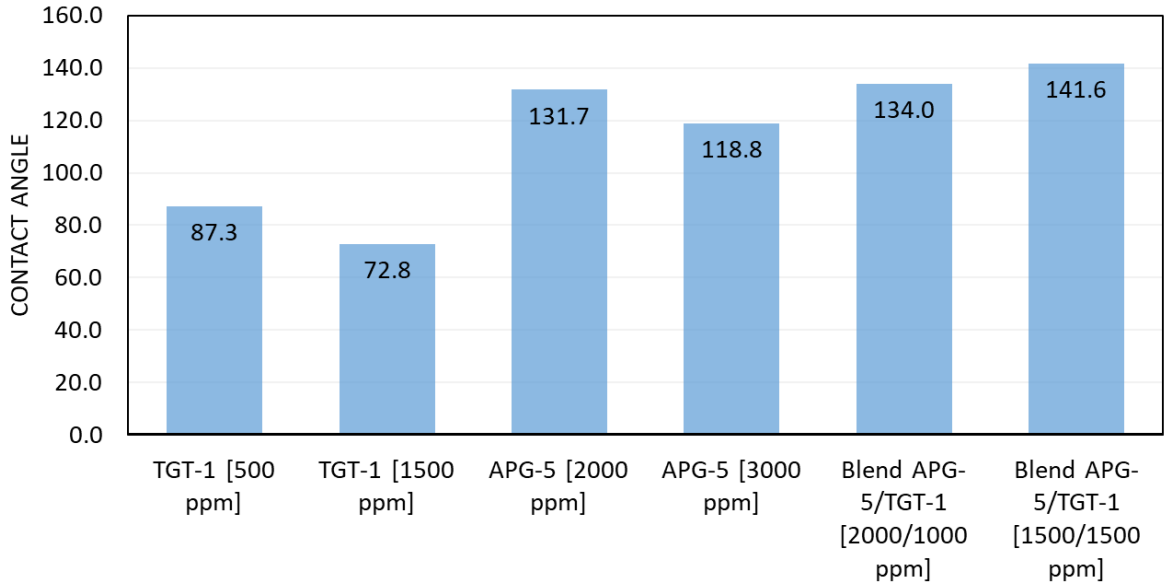

Figure 34: Average finalized contact angles for oil TGT-1, APG-5 and their blends

Based on the above results, it is clear that mixing APG-5 and TGT-1 blunts the wettability altering capability of TGT-1, thus it was concluded that a potential injection strategy would include a slug of TGT-1 followed by the APG-Methane foam whereby the optimized formulation is a 0.5 PV of 0.5% of TGT-1 chased with ~ 5 PV of brine and finally APG-5 and methane foam is injected.

In order to verify that the combination of APG-5 and TGT-1 does not form any viscous emulsions when in contact with the crude oil, a series of phase behavior tests were conducted, where 0.35% APG-5 with 0.15% TGT-1 was used. Figure 35 shows the results.

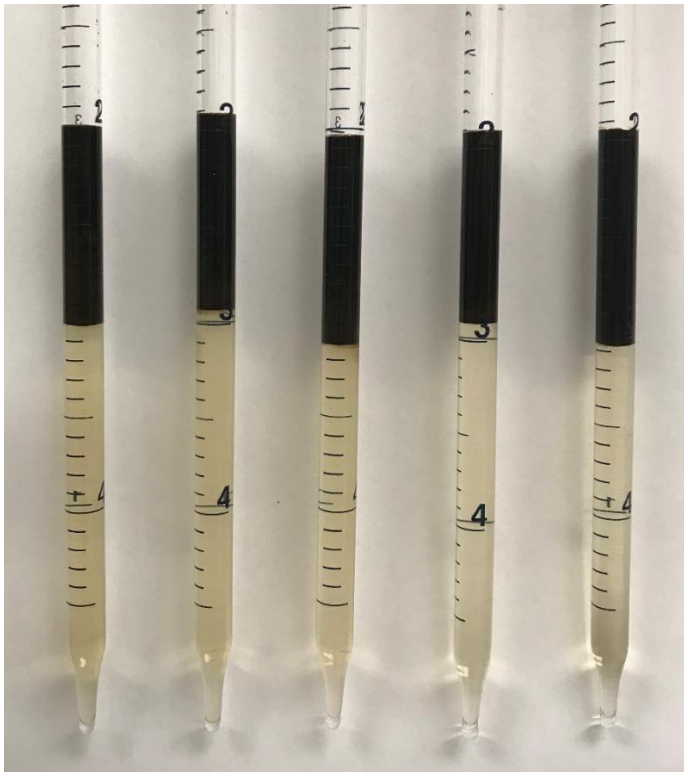

Figure 35: Phase behavior tests of APG-5 [0.35%] mixed with TGT-1 [0.15%] Salinity Right to Left (ppm): [48,000, 69.000, 96.000, 144.000, 173.000]

As seen, type-1 microemulsions form, like that with APG-5 alone. With an oil phase on top and an aqueous phase that includes microemulsions of oil on the bottom. No viscous phase forms, thus this is suitable for use for foam applications.

After the selection of the optimized formulation, it was then tested in oil wet cores, in core-flood experiments OW-D and OW-E. The results are discussed in the following section.

6.1.2 WETTABILITY ALTERATION – FOAM COREFLOODING

The optimized formulation was tested in OW-D, following the waterflood, and brine/gas co-injection, a slug of 0.5 PV of 5000 PPM TGT-1 surfactant was injected. Chased with 5 PVs of brine and followed by APG-5 and methane co-injection. Foam was first developed at 10 PV/d and 50% then foam was injected to steady state at 5 PV/d 50%, and 2 PV/d 50% and 30%.

Figure 36 shows a comparison of the foam propagation and strength for experiments OW-A (APG-5 foam without wettability alteration) and OW-D (APG-5 foam post wettability alteration. The transient pressure data for these experiments are included in Appendix C: Additional Core Flood Data.

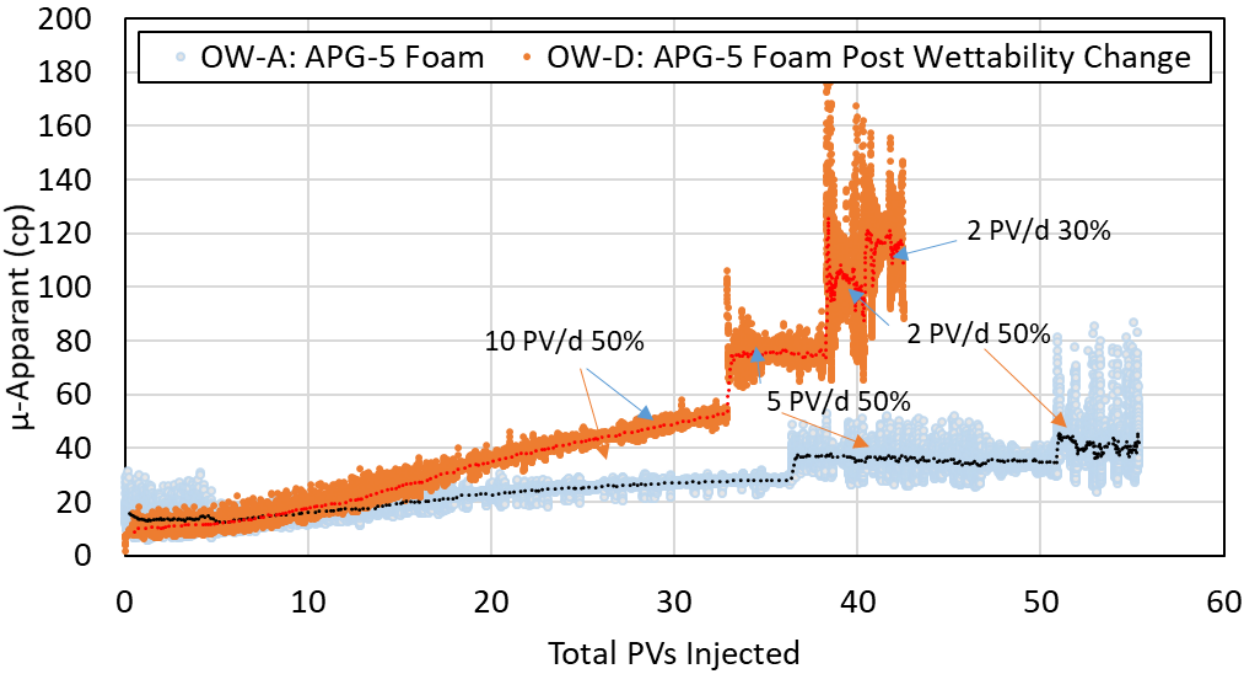

Figure 36: Transient foam data for OW-A and OW-D experiments - impact of wettability change

As shown above, the foam develops at a much more rapid pace in OW-D than OW-A, for the same rate of 10 PV/d 50% FQ. The steady state foam strength comparison for the chosen rates is listed in Table 6.

Experiment	Rate/FQ	Foam DP (psi)	μ-Apparent (cp)	MRF	MRF % Difference
OW-A	5 PV/d 50%	50.0	33.0	28.0	
	2 PV/d 50%	22.8	42.9	20.7	
	2 PV/d 30%	26.6	50.6	24.1	
OW-D	5 PV/d 50%	122.6	77.1	69.7	149%
	2 PV/d 50%	68.0	102.0	53.9	161%
	2 PV/d 30%	72.0	109.5	57.1	137%

Table 6: Comparison of MRF of APG-5 foam in OW-A versus OW-D with wettability alteration

As shown in Table 6, the wettability alteration causes a percentage increase of 150% to the MRF, or an increase by a factor of 2.5.

Appendix C: Additional Core Flood Data, lists the oil saturation changes throughout the different core flood experiments OW-A, OW-D which have residual oil saturations of 11.4 and 9.7 % successively.

This similarity in oil saturation highlights the importance of wettability to foam performance even further. In OW-D where the TGT-1 was injected, the foam propagates both faster and stronger at steady state.

Figure 37 shows the mobility reduction factors for the 2 PV/d rate for both OW-A and OW-D.

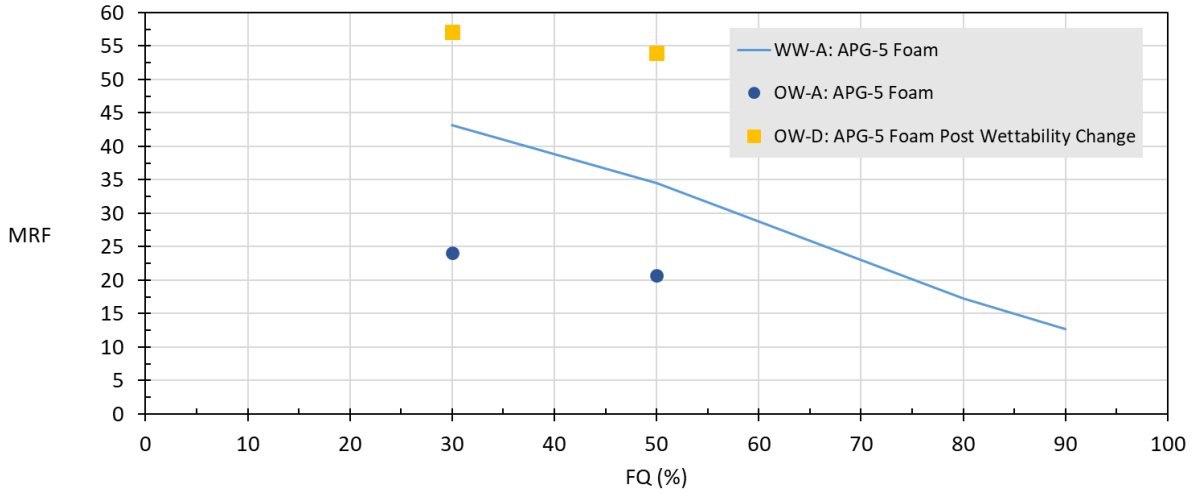

Figure 37: Comparing MRF values for OW-A and OW-D after wettability change

Such a considerable increase in foam strength is beyond the impact of foam hysteresis, and confirms that wettability alteration towards more water wet conditions improves foam stability and propagation.

Furthermore, the foam strength for OW-D is considerably higher than the water wet, without oil case (WW-A). This can be attributed to the difference in permeability, whereby OW-D had a permeability of 130.5 mD, and the water wet no oil core flood (WW-A) had a permeability of 103 mD, and as shown by (Farajzadeh et al., 2015), permeability correlates with foam strength, whereby the higher permeability cores are more favorable to strong foam propagation.

6.2 Enhancing Foam Resistance to Oil

In order to enhance the APG foam system's resistance to oil, a comprehensive literature review of foam boosters was conducted. Two families of surfactants used to enhance foam resistance to oil were considered, Betaines, and Fatty-acid N-Methylethanolamide surfactants.

The latter was shown by (Sakai and Kaneko, 2004) to only improve the foamability/ and foam generation, which is strong for APG foam. Thus, it was excluded. Betaines however were used for their influence on the foam-oil film stability, and thus their foam boosting relates to the foam's resistance to oil. (Chang et. al, 2018) postulate that it increases foam resistance to oil by enhancing the pseudo-emulsion film strength.

6.2.1 SURFACTANT FORMULATION FOR ENHANCING FOAM RESISTANCE TO OIL

In order to verify the improvement in foam strength of the APG-5 system by the addition of Lauryl betaine, a series of foam characterization experiments were carried out. The baseline concentration of APG-5 was maintained at 0.35%, with LB added on top (0.05 to 0.15%) was tested. Bulk foam tests were carried out with and without oil. Results of the experiments with oil are shown in Figure 38 and Figure 39.

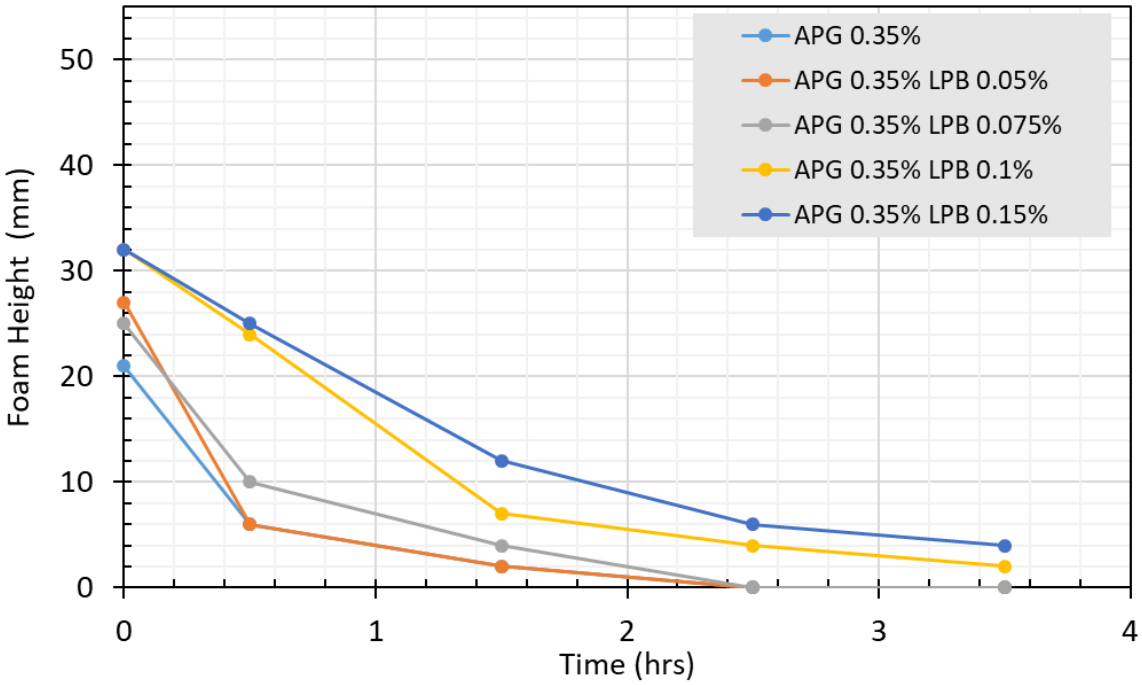

Figure 38: Foam Height results for bulk foam tests of APG-LB formulations

Figure 39: Bulk foam tests of APG-LB formulations

As shown, the addition of LB improves the foam stability to oil, with the vials containing LB maintaining a foam column far longer than the APG-5 alone did. Based on the above, the formulation chosen was APG-5 at 0.35% and 0.15% LB.

Phase behavior testing of the chosen formulation was carried out for a scan of different salinities. Results are shown in Figure 40.

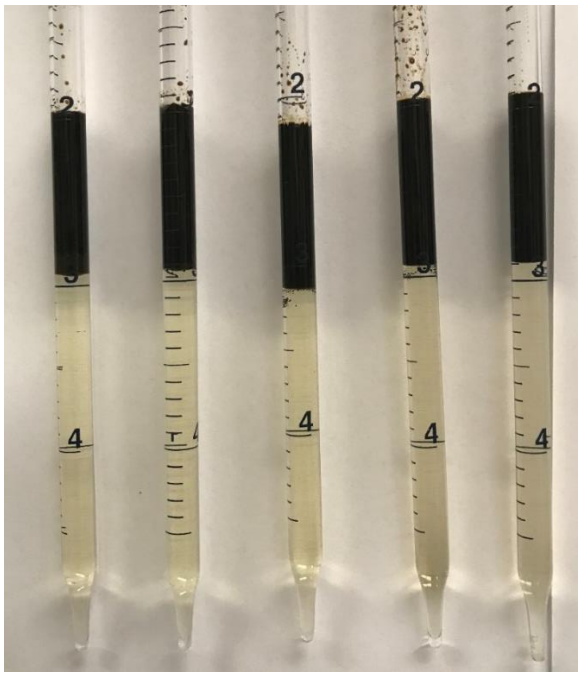

Figure 40: Phase behavior tests of APG-5 [0.35%] mixed with LB [0.15%] Salinity Right to Left (ppm): [48,000, 69.000, 96.000, 144.000, 173.000]

As shown above, type 1 microemulsion forms which is similar to the APG-5 case. This shows no unfavorable conditions for the formulation in the application of foam for mobility control. Interfacial tension measurements and subsequent classical entering and spreading coefficients as well as the lamella number for this formulation are shown in Table 7.

Sample	**ST [mN/m]**
APG-5 + LB (0.35%-0.15%] - Oil	0.339
Oil-Air	45.5
APG-5+LB (0.35%-0.15%] - Air	14.1
Entering Coefficient	-31
Spreading Coefficient	-32
Lamella Number	6.2

Table 7: APG-5/LB – Oil - Air IFT Measurements

Similar to the APG-5 formulation, a negative entering coefficient indicates an inherently stable foam-oil system. However, it is worth mentioning that the lamella number rises from 4 to 6.2 which indicates further emulsification of oil. In their work on foam boosters (Basheva et al., 2000) proposed that the role of betaine as a foam booster is in raising the barrier energy for emulsified oil droplets to enter the foam films and so it strengthens the pseudo-emulsion film. In a study of foam boosters (Zhang et al., 2005) proposed that combining a zwitterionic surfactant (Lauryl betaine) with an anionic surfactant (APG-5), may lead to closer packing in the surfactant monolayer due to a more balanced charge distribution. This causes the foam films to be more compact and leads to stronger foam films, and PS-films.

Thus, while a higher lamella number may point a more unstable foam system, we can only conclude with confidence that more emulsification occurs, and due to the PS-film strengthening, the foam stability is increased as a net effect.

6.2.2 FOAM ENHANCEMENT – FOAM COREFLOODING

The above formulation was tested in OW-C and OW-E, which provides a clear understanding of the improvement in foam propagation and stability. Figure 41 shows a plot of the initial foam development in OW-A for the APG-5 alone, and OW-C for the (APG-5 and LB) formulation. If we compare the slope of the foam overall pressure drop for the 10 PV/d rate, we notice a much steeper line for the (APG-5 and LB). This shows that the foam propagates much faster through the core.

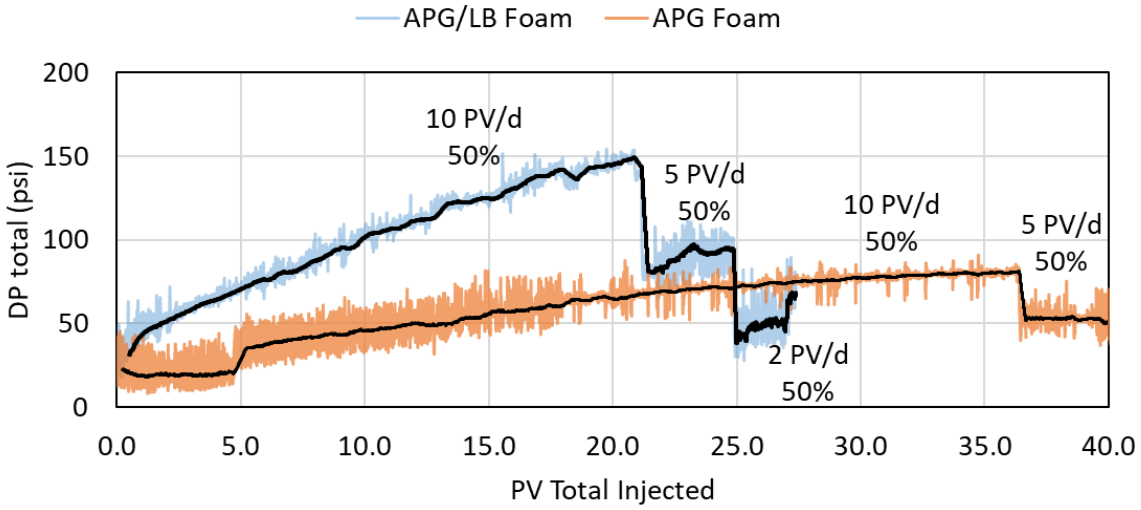

Figure 41: Comparing foam propagation for OW-A (APG Foam) and OW-C (APG/LB Foam)

The (APG-5 and LB) formulation requires 80% less injected surfactant and gas volume to arrive to the same foam strength developed by the APG-5 foam system. In terms of field optimization and economics, this additional enhancement can provide a considerable cost saving, despite the additional cost of the LB surfactant used.

Figure 42 shows the apparent viscosity results and MRF data for experiments WW-A, OW-A, OW-C, OW-D and OW-E. APG-5 foam at Sor is presented for OW-A, and OW-D (here after wettability alteration with TGT-1). While APG-5 and LB foam is presented

for OW-C and OW-E (here after wettability alteration with TGT-1). WW-A is presented as the reference case with no oil present, and in water wet conditions.

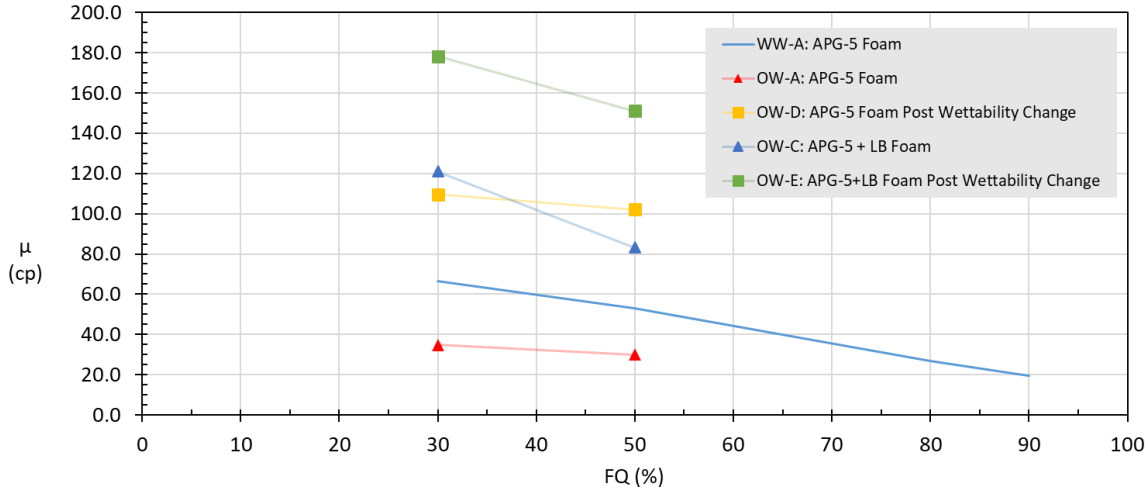

Figure 42: Effect of Wettability Alteration on Foam Strength for APG foam System at 2 PV/d rate

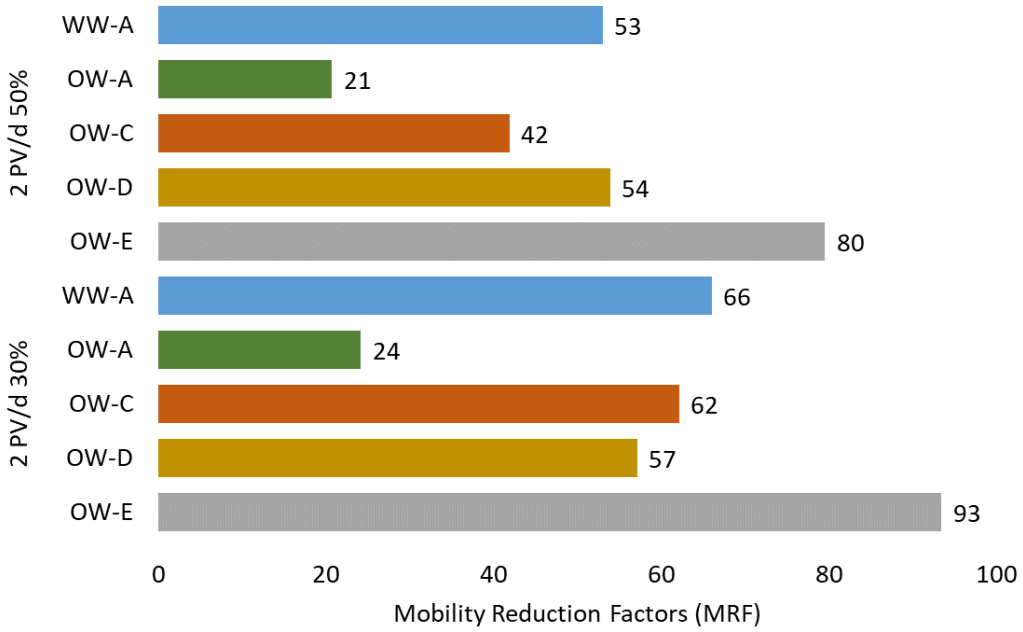

Figure 43: Effect of Wettability Alteration on MRF of APG foam System at 2 PV/d rate

As seen above the apparent viscosity of the foam in OW-C is enhanced by a factor of 1.77 compared to OW-A, while in OW-E its improved by a factor of 1.56 over OW-D.

The MRFs are reduced due to oil presence and oil wet state of the cores, however foam boosting creates a significant improvement in both OW-C where it is improved close to the reference foam strength of WW-A. Changing the wettability in experiment OW-D has a significant effect on the foam strength and improves to within 5% of the reference values with no oil present (WW-A). Finally, looking at OW-E whereby wettability alteration is done first, then APG-5 and LB foam is tested, shows the best improvement, with foam that is even stronger than the reference case at MRFs of 80, and 93 for the 2 PV/d 50% and 30% successively.

6.3 Summary

In this chapter two optimizations to the foam system were discussed. The first optimization focused on altering the wettability of the cores to more water wet conditions by the injection of a wettability altering surfactant pre-flush (TGT-1 at 0.5 wt. %) This was shown to also strongly improve foam propagation speed, as well as the steady state strength of the developed foam. Secondly. improving the APG-5/Methane foam system's resistance to oil using a foam booster. An addition of 0.15 wt.% Lauryl Betaine to the formulation was shown to enhance the foam propagation and steady state strength.

7 CONCLUSIONS

This research work was focused on design and validation of a foam system that can generate effective foam for Al-Shaheen reservoir conditions, in the presence of oil and in various wettability states. The main goal of foam in this application is to minimize gas loss into high permeability zones during WAG EOR. A suitable surfactant was selected, following a detailed screening process. The surfactant formulation was tested in water wet and oil wet core flood experiments, and enhancements to the formulation were tested and their improvement to the foam strength is quantified. The following conclusions can be drawn from the study:

1. A screening of five APG surfactants resulted in the selection of APG-5 for detailed study as it had the best foaming ability, with and without the presence of oil
2. Bulk foam stability tests of APG-5 show that the presence of solubilized oil in surfactant solution only marginally reduces the foam stability. While increasing bulk oil concentration in solution strongly diminishes the foam stability.
3. Static adsorption results of APG-5 on Estaillades limestone cores show adsorption of up to 2.5 mg/g, which is reduced by up to 40% when the test is done with oil wetted grains and in presence of oil
4. Core flood experiments revealed a suitable APG-5 concentration of 3000-5000 ppm is required. The foam rheology of APG-5 and CH4 gas foam is shear thinning, displaying higher foam viscosity at lower rates (far field conditions) compared to higher rates (near-wellbore region). The ideal foam

quality resulting in the strongest foam was found to be between 30 and 50 %.

5. APG-5 and methane foam system can produce effective foam in presence of residual oil in both water wet cores, as well as oil wet cores, with MRF values of ~ 28 for the former and ~ 24 for the latter.
6. Wettability has a considerable impact on foam strength, whereby an oil wet core negatively impacts foam propagation and steady state strength.
7. The use of a wettability altering agent TGT-1 improved the APG-5 methane foam performance in terms of propagation and steady state strength. MRF values of ~ 47 were achieved in OW-D, an increase of 150% over OW-A whereby no TGT-1 was injected.
8. Mobile oil presence does not negate the presence of foam. It was shown through mobile oil experiments, that foam does survive even in presence of mobile oil. Additionally, water wet conditions show stronger foam in presence of mobile oil. Relative permeability effects complicate the analysis of actual foam strength during mobile oil injection, and only general inferences can be made.
9. The use of Lauryl betaine as a foam booster was found to enhance the foam performance of APG-5 foam in terms of the propagation and steady state strength. Achieving MRF values of ~ 52 in OW-B, and ~ 85 in OW-E whereby the wettability was altered.

Based on the above conclusions, a practical injection strategy and formulation is suggested whereby TGT-1 is used as a pre-flush. A combination of APG-5 and Lauryl Betaine are then injected with reservoir waste gas (methane) to create foam for mobility

control. Further optimization to this formulation can focus on cost reduction by compromising on actual foam strength and MRF required for field implementation.

8 FUTURE WORK

The next stage in this project is to study the impact of rock morphology and pore structure on foam performance in conjunction with the effects of oil, wettability, and permeability. A detailed experimental program is planned for tests on several rock outcrops, as well as actual reservoir cores from two different reservoirs in the Al-Shaheen offshore field. Following that a detailed simulation and modelling stage is planned to model a field implementation program.

Innovative dual injection experiments where low and high permeability reservoir plugs are tested simultaneously are planned as well. The second area of interest will be to look deeper into the impact of oil on foam on a fundamental level. This is to try and answer the question, what specific parameters about a crude oil and a surfactant formulation, or a combination of both, can be used to predict a stable foam in the presence of oil.

Appendix A: Summary of Experiments

ID	Description	Experimental Steps	Permeability (mD)	Porosity (%)	Sor (%)
WW-A	APG-5 foam characterization at water wet conditions with no oil.	Core is saturated in brine Baseline water flood dp is measured at various rates Baseline brine and gas co-injection DP is measured at various rates APG-5 at different concentrations injected with methane	118	23.2	N/A
		APG-5 at 3500 ppm and methane gas are co-injected to steady state (SS) at different rates and foam qualities	103	23.2	N/A
		After Foam rheology tests, a scan of surfactant at 3500 ppm with solubilized oil is done.	103	23.2	N/A
WW-B	Test of APG-5 Foam at Sor.	Core is saturated in brine Core is flooded with crude oil Core is then water flooded until 99% water-cut Core is subjected to Gas + Brine co-injection until oil is at Sor APG-5 at 3500 ppm and methane gas are co-injected to steady state (SS)	134.7	25.3	5.3
WW-C	Test of APG-5 and oil co-injection to verify impact of mobile oil on foam viability in water wet conditions starting from a strong foam state.	Core is saturated in brine, and baseline water flood DPs are measured Baseline brine and gas co-injection DP is measured at various rates Foam at 4.75 PV/d 50% is Injected until fully developed and at SS Foam and Oil are co-injected until 0.5 PV of oil is injected (oil rate: 0.25 PV/d) Foam at 4.75 PV/d 50% is Injected alone to SS Co-injection of oil and foam is resumed to SS Foam at 4.75 PV/d 50% is Injected again until SS Foam viability is evaluated based on the foam alone steps with higher oil saturation (mobile oil)	134.7	23.6	start: 0 Co-inj: 20-38

Table 8: Summary of Core flood experiments in water wet cores

ID	Description	Experimental Steps	Permeability (mD)	Porosity (%)	Sor (%)
OW-A	Test of APG-5 Foam at Sor.	Core is saturated in brine Core is flooded with crude oil Core is aged in crude oil for 8 weeks Core is then water flooded until 99% water-cut Core is subjected to Gas + Brine co-injection until oil is at Sor APG-5 at 3500 ppm and methane gas are co-injected to steady state (SS)	100.8	25.7	11.4
OW-B	Test of APG-5 and oil co-injection to verify impact of mobile oil on foam viability.	APG-5 foam at 4.75 PV/d 50% Is injected until SS (at OW-01-A Sor) Foam and Oil are co-injected until 0.5 PV of oil is injected (oil rate: 0.25 PV/d) Foam at 4.75 PV/d 50% is Injected alone to SS Co-injection of oil and foam is resumed to SS Foam at 4.75 PV/d 50% is Injected again until SS Foam viability is evaluated based on the foam alone steps with higher oil saturation (mobile oil)	100.8	25.7	7.5-36.2
OW-C	Test of optimized formulation to enhance resistance to oil.	Core is restored to initial conditions of OW-A by injection of 15-20 PV of brine APG + Foam Booster is co-injected with methane at various rates to SS Foam strength is evaluated for propagation and steady state strength (apparent viscosity and MRF)	100.8	25.7	7.5
OW-D	Test of APG-5 Foam at Sor post wettability alteration.	Core is saturated in brine Core is flooded with crude oil Core is aged in crude oil for 8 weeks Core is then water flooded until 99% water-cut Core is subjected to Gas + Brine co-injection until oil is at Sor A 0.5 PV of wettability altering agent is injected followed by 5 PV of brine APG-5 at 3500 ppm and methane gas are co-injected to steady state (SS)	130.5	29.1	9.4

Table 9: continued next page.

OW-E	Test of optimized formulation to enhance resistance to oil post wettability alteration.	Core is restored to initial conditions at end of OW-D by injection of 15-20 PV of formation brine Optimized formulation (APG + Foam Booster) is co-injected with methane at various rates to SS Foam strength is evaluated for propagation and steady state strength (apparent viscosity and MRF)	130.5	29.1	9.4

Table 9: Summary of Core flood experiments in oil wet cores

Appendix B: Experimental Procedures

Bulk Foam Tests

In order to screen surfactants for the best bulk foaming performance, bulk foam stability experiments were carried out as follows:

- First 10 ml of surfactant solution were placed in 50 ml glass vials and placed in a 55 °C oven.
- The vials are then systematically shaken for 10 seconds to introduce air into the surfactant solution and create foam.
- The height of foam generated is measured and recorded at regular intervals.
- The foam stability of surfactant solutions with and without oil was evaluated. The oil tests were done using the same procedure but with the addition of a set volume of oil.

These tests were also used to evaluate the surfactant concentration ranges for use in the porous media experiments.

1. **Phase behavior Tests**

In order to test the behavior of the best APG surfactant solutions when interacting with the Al-Shaheen's Shuaiba reservoir crude oil, microemulsion phase behavior tests were carried out. The experiment is carried out as follows:

- First, 0.5% by wt. surfactant solutions in 144,000 formation brine were prepared.
- The aqueous stability at the FB salinity, and reservoir temperature (55°C) was tested by monitoring the solutions over time.
- For microemulsion testing, 2 ml of surfactant solution was mixed with 1 ml of crude oil in glass pipettes.

- The pipettes are then sealed and mixed thoroughly for a few days.
- They were then placed in a temperature-controlled oven at 55°C for monitoring.
- The same test was repeated for a salinity scan from 48k to 144,000 ppm salinity.

The goal of the above tests is to monitor for the formation of any type II or II microemulsions. Type 1 microemulsions whereby a bottom aqueous phase with oil droplets and a top oleic phase exist is desired for foam propagation.

2. Static Adsorption Tests

This experiment was designed in order to quantify the amount of surfactant that adsorbs to the rock. The procedure followed is as follows:

- Estaillades limestone rock was crushed, and then sieved through 600-300 Mesh size. The grains remaining on the 300 Mesh Sieves were used in the experiment.
- 10 grams of crushed rock was then weighed in plastic vials, 20 ml of surfactant solution prepared in 144,000 ppm FB was then added.
- The mixture was thoroughly mixed (every 2 hours), for 4 days while placed in a 55 °C oven.
- The solution was then gravity segregated, and the surfactant was then filtered through 0.45μm filters and was analyzed using Liquid Chromatography Mass spectrographic testing (LCMS).
- The analysis method focused on four unique mass spectroscopy peaks that are unique to the surfactant tested.
- A correlation curve was created and then used to estimate the concentration in (ppm) of the surfactant in the tested solution.

The adsorption per g of rock is then estimated as per equation 6 in Appendix D: List of Equations.

This was repeated for various concentrations. It was also done with oil wetted grains to evaluate the effect of oil and oil wet grains on adsorption.

3. Contact Angle Experiments:

Contact angle measurements are carried out to quickly screen for surfactants which are more successful at altering the wettability of a calcite plate. The procedure carried out using a rami-hart set up is as follows:

- An oil droplet is placed on a polished calcite plate and aged at 55 °C for 1 week
- The plate is then placed in the optical cell of the rami-hart set up
- Surfactant solution is carefully added to the cell
- The contact angle of the oil droplet is then monitored until the change reaches steady state
- The final contact angle is recorded and averaged over a period of time
- For each reading, the test is repeated 3 times to minimize error and the results are averaged

4. Interfacial Tension Measurements

Interfacial tension measurements between oil, surfactant solutions, and air was conducted using the pendant drop method. The measurements were carried out at room temperature and atmospheric pressure.

The measurements were carried out using a high precision tensiometer.

Air was used instead of methane to represent the gas phase. The following is the general procedure followed:

Surfactant solution was placed in an optical cell

An oil droplet was injected slowly using a micro-needle

The measurement is carried out until the surface tension reached steady state, and averaged over 2 minutes

Using the interfacial tension measurements, the entering, spreading, and lamella numbers are calculated as per equations 1, 2, and 3 in Appendix D: List of Equations.

5. Porous media flow experiments (core floods):

In order to characterize the foam behavior for the Al-Shaheen field application, porous media flow experiments were designed. The design of the experimental set-up is included in Figure 44.

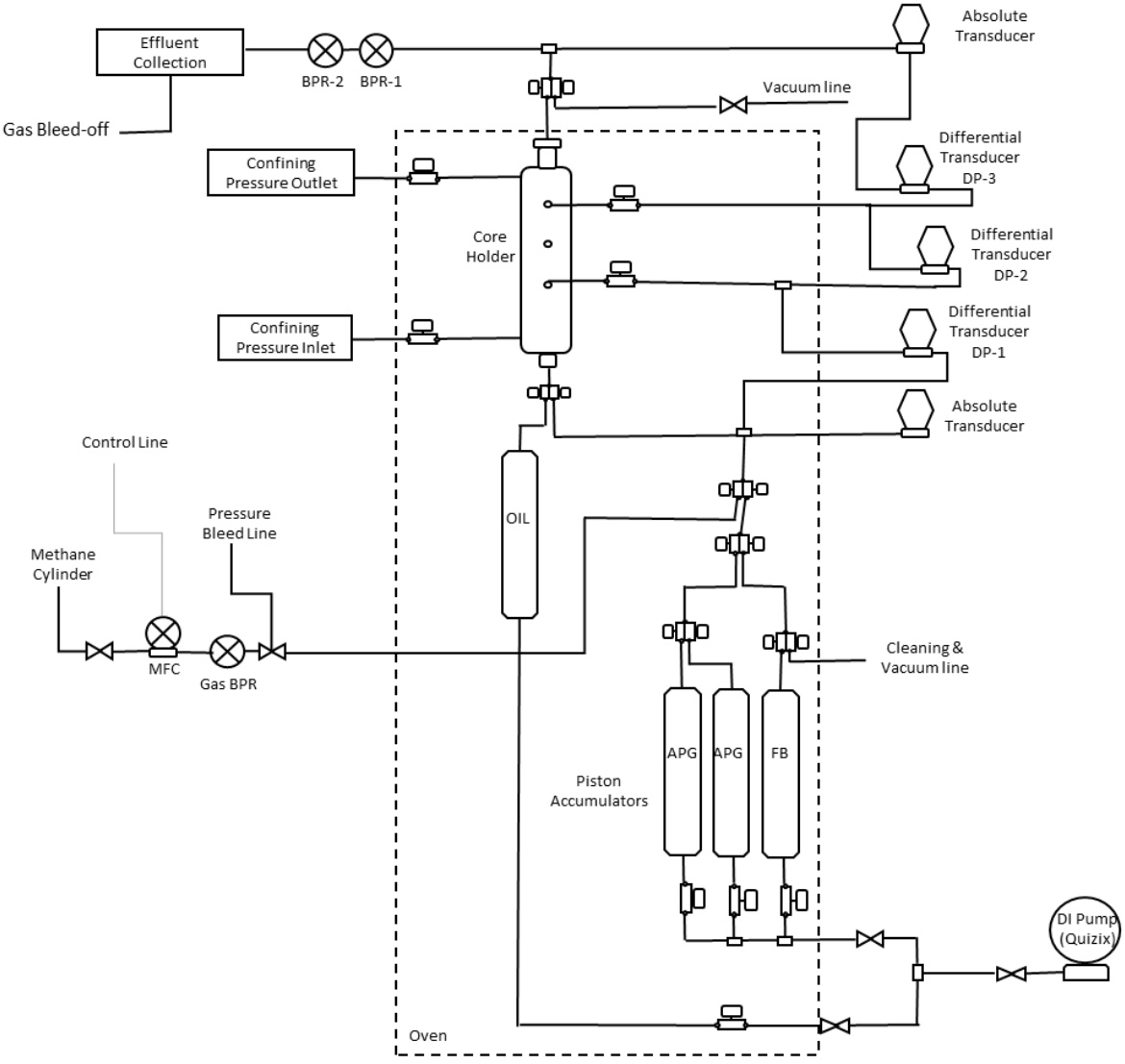

Figure 44: Core flood experimental setup

- The core is loaded into a Hassler type core holder and is then connected to the set up.

- Pressure testing with lab air and then nitrogen at the reservoir pressure of 1450 psi is done.
- The core is then vacuumed, for 3-5 hours before being saturated with formation brine (144,000 ppm). Injection is done by a De-ionized water Quizix pump, which displaces a piston accumulator at a controlled rate.
- The porosity and permeability are then measured.
- Gas injection is controlled by a Matheson mass flow controller (MFC), where the gas pressure downstream of the MFC is controlled with a Back-pressure valve (BPR) to be always higher than the liquid pressure.
- In experiments containing oil, the next step is to flood the core with oil for close to two times the pore volume, and until 99% of the effluent is oil.
    - For oil wet cores, the cores are stored in oil for over 4 weeks at the reservoir pressure and temperature before continuing the next steps.
- The core is then water flooded and brine and gas co-injection is done to mimic reservoir production history
- Foam testing is then done by co-injection of surfactant and gas at various rates

Foam experiments are done by surfactant solution and methane gas co-injection; the effluent goes through a set of two BPRs that ensure the outlet pressure is maintained close to (1400-1450) psi. Steady state pressure drops across the core are recorded every 30 seconds, by the differential transducers DP1, DP2, and DP3.

These pressure drops are averaged over the length of the core at steady state and are then used to estimate the apparent foam viscosity using equation (4): While the mobility reduction factors (MRF) is estimated using equation (5).

Appendix C: Additional Core Flood Data

Bulk Foam Tests

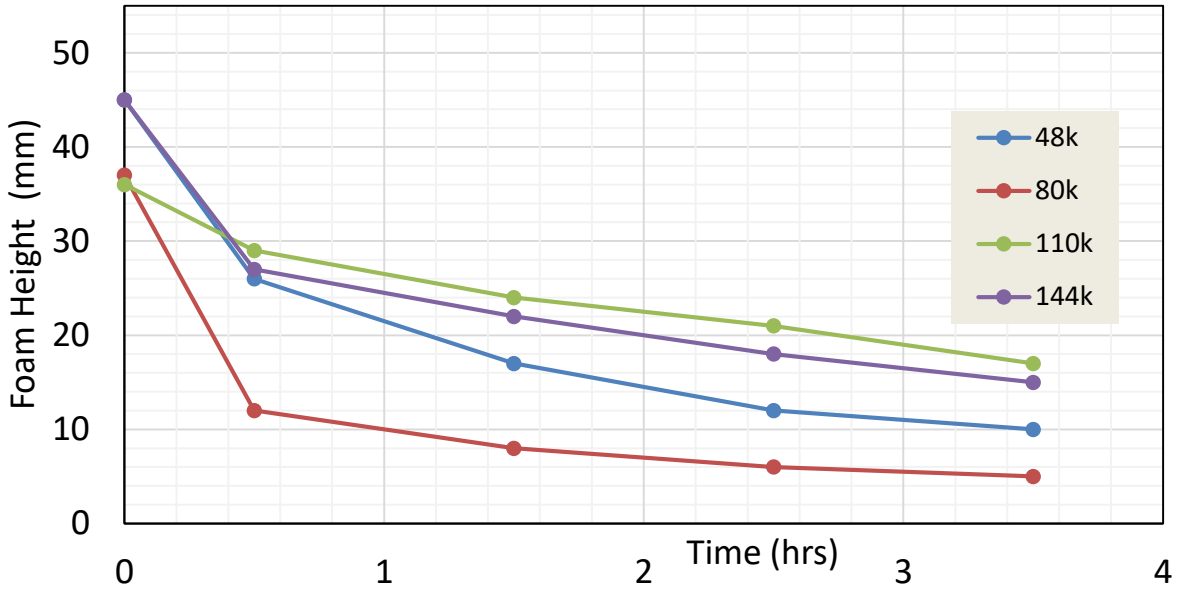

Figure 45: Bulk foam tests for APG-5 with a change in salinity in 1000 ppm

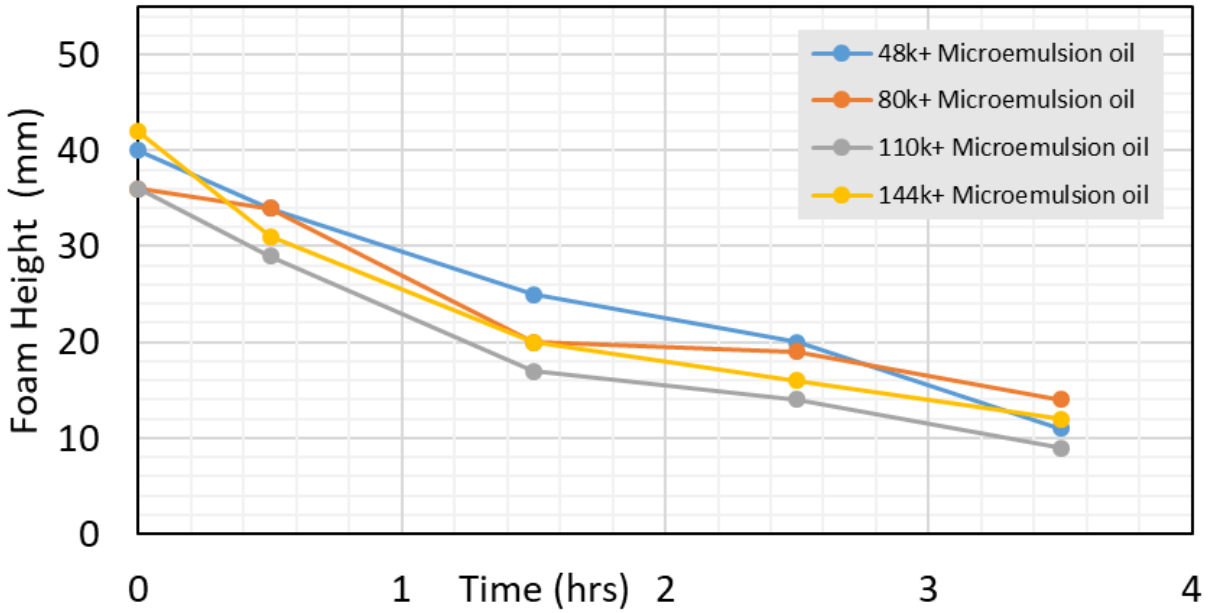

Figure 46: Bulk foam tests for APG-5: Salinity and microemulsions effect

WW-A

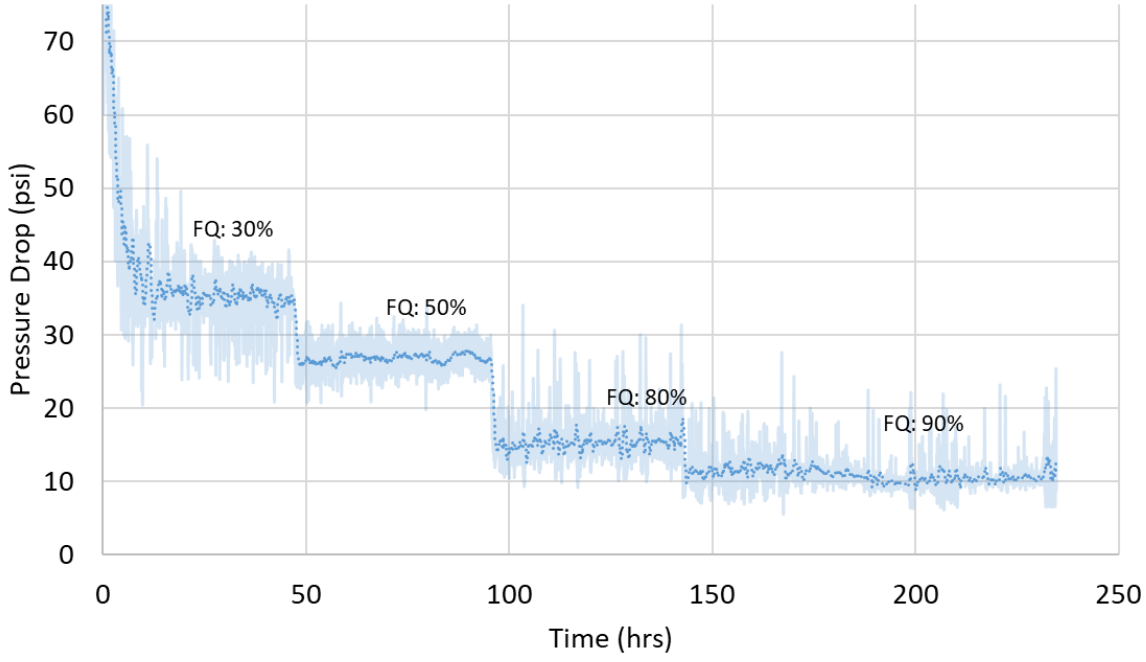

Figure 47: WW-A: APG-5 at 3500 ppm, 2 PV/d Foam Scan

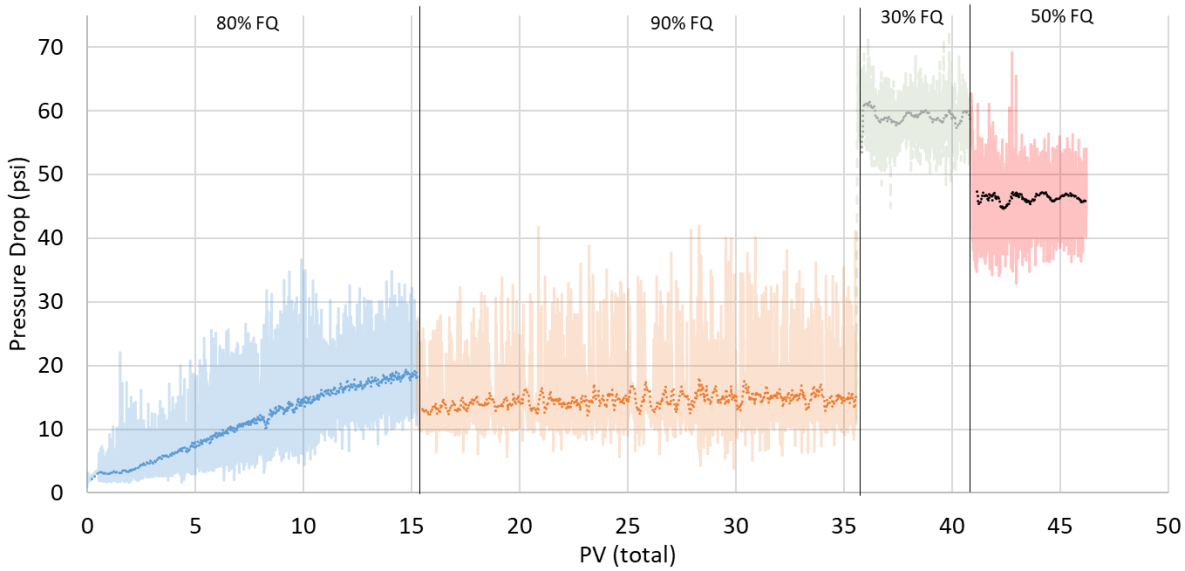

Figure 48: WW-A: APG-5 at 3500 ppm, 5 PV/d Foam Scan

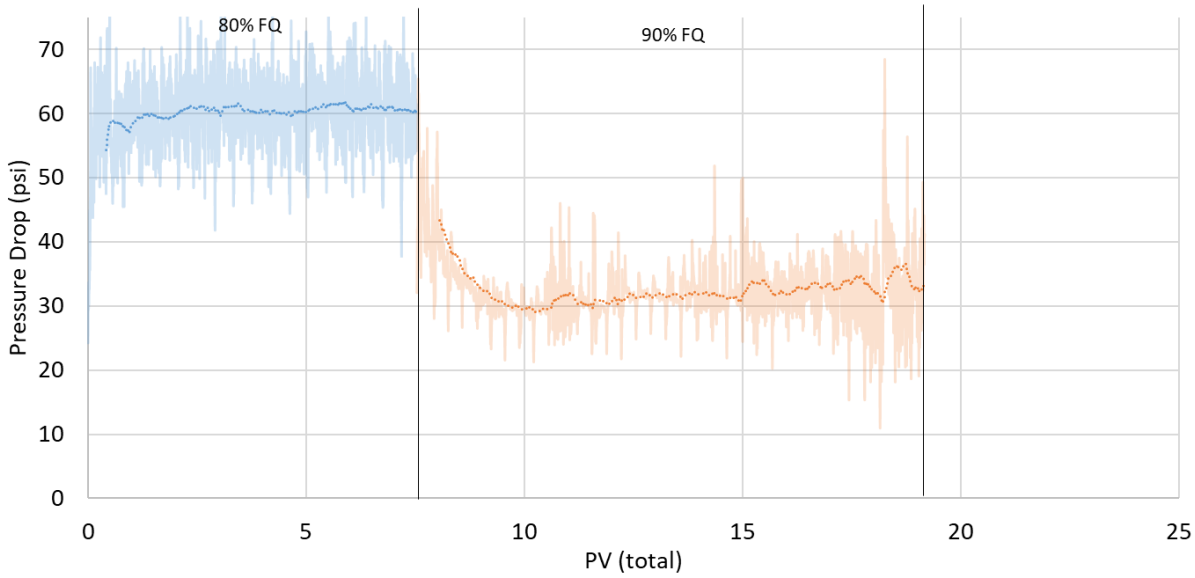

Figure 49: WW-A: APG-5 at 3500 ppm, 10 PV/d Foam Scan (80, and 90% FQ)

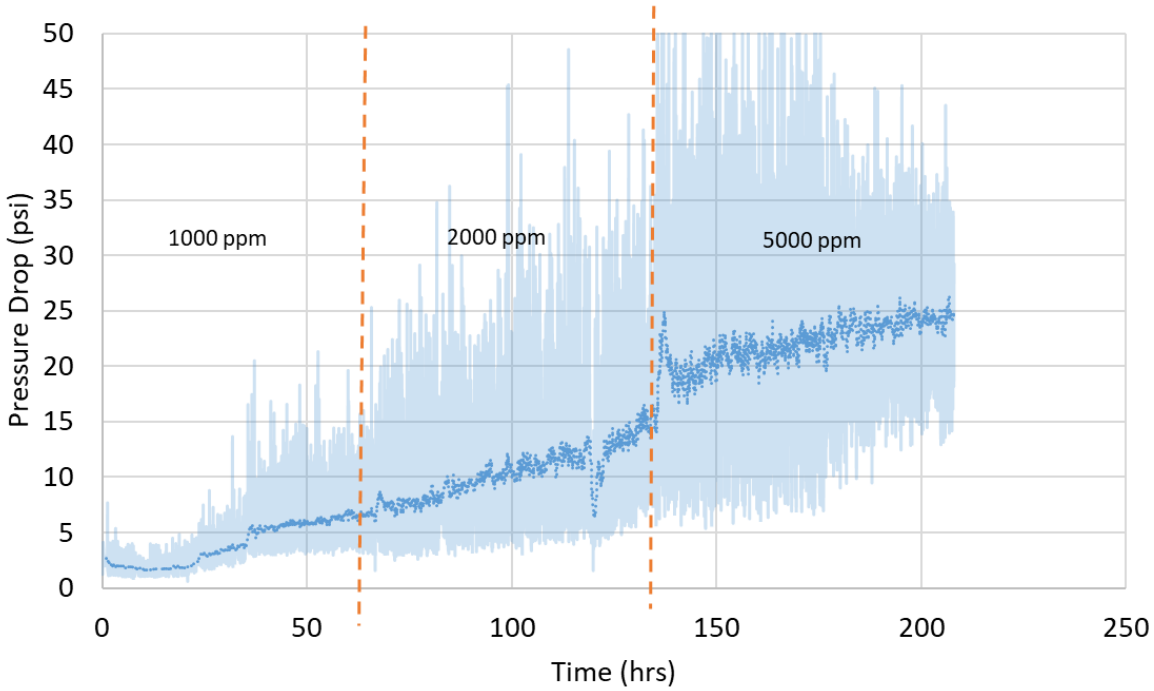

Figure 50: Foam Concentration scan at 5 PV/d and 80% FQ

WW-B:

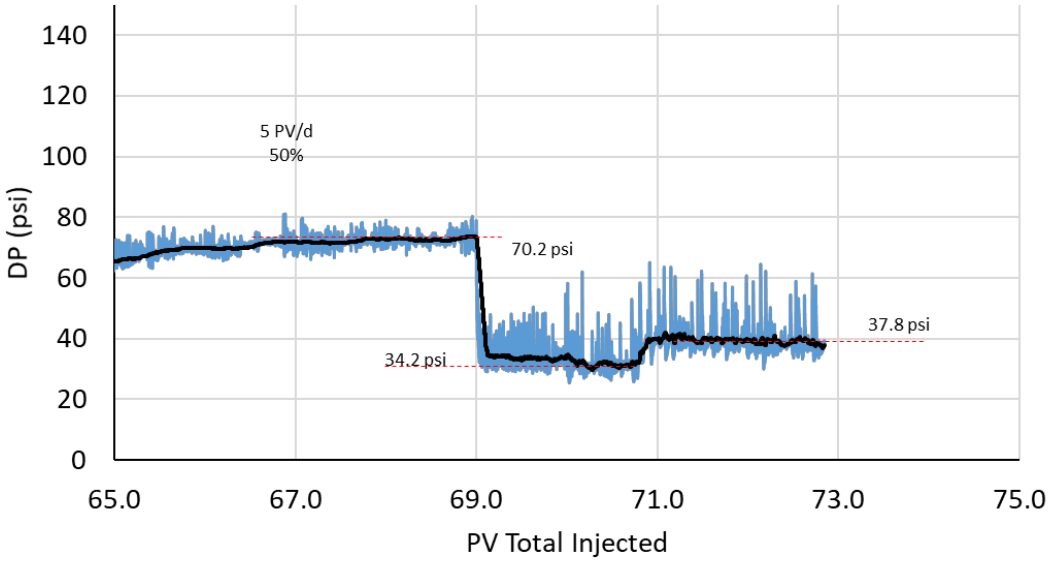

Figure 51: WW-B Foam scan in WW rock at Sor = 5.3%

Stage	Description
1	Oil Flood
2	Water Flood
3	Brine + Gas Injection [5 PV/d 50% Gas]
4	Foam [Multiple rates]

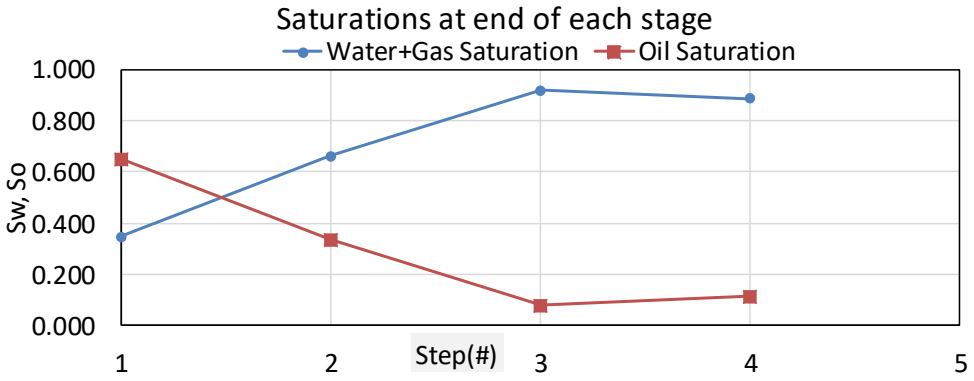

Figure 52: Oil Saturation Changes in WW-B experiment

WW-C:

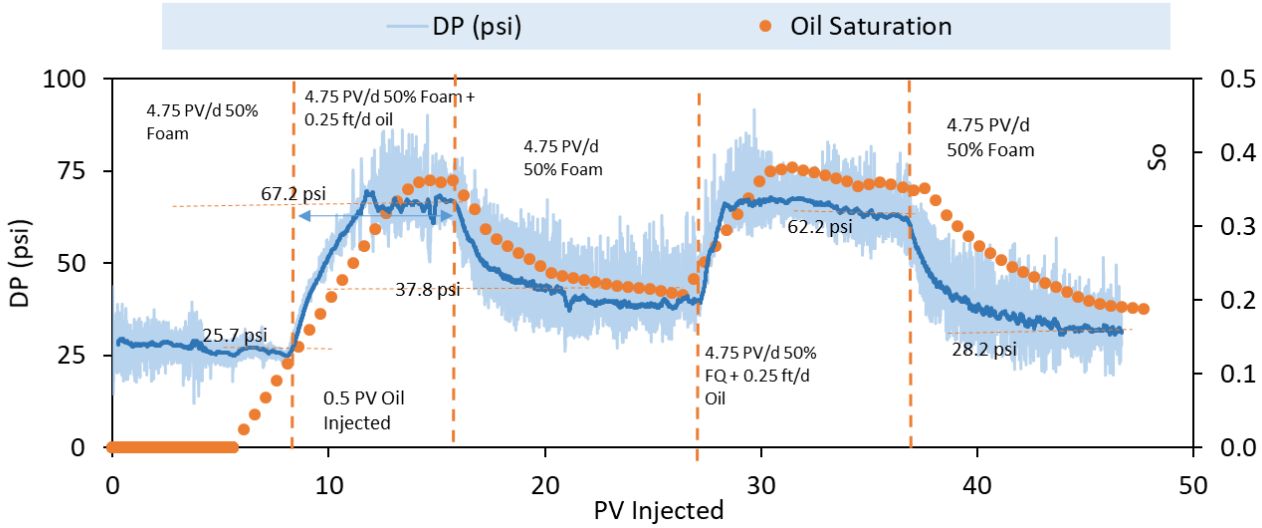

Figure 53: WW-C Mobile oil experiment transient pressure drop and oil saturation

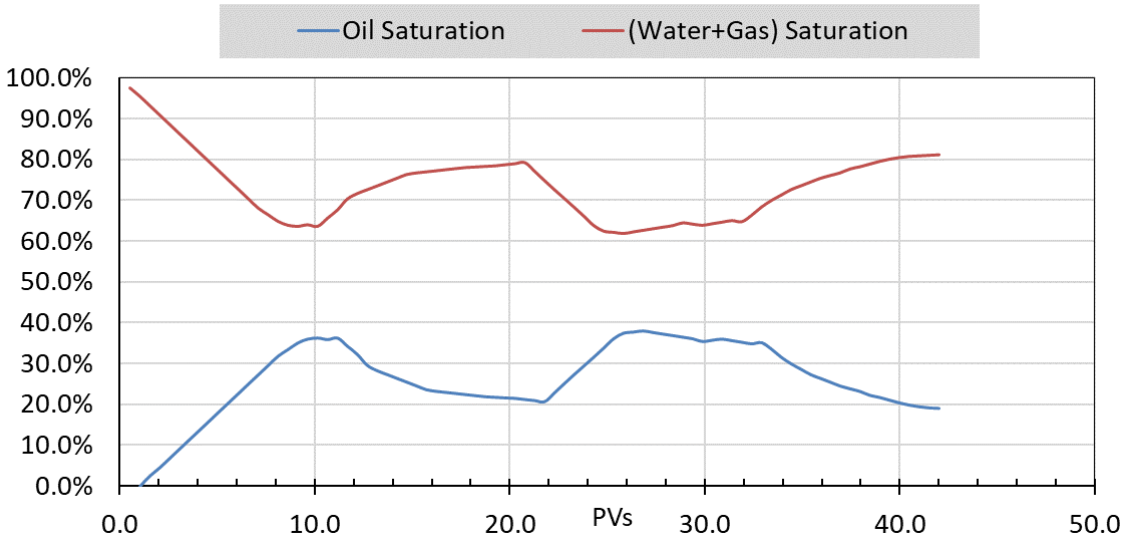

Figure 54: WW-C Mobile oil experiment Oil Saturation changes

OW-A:

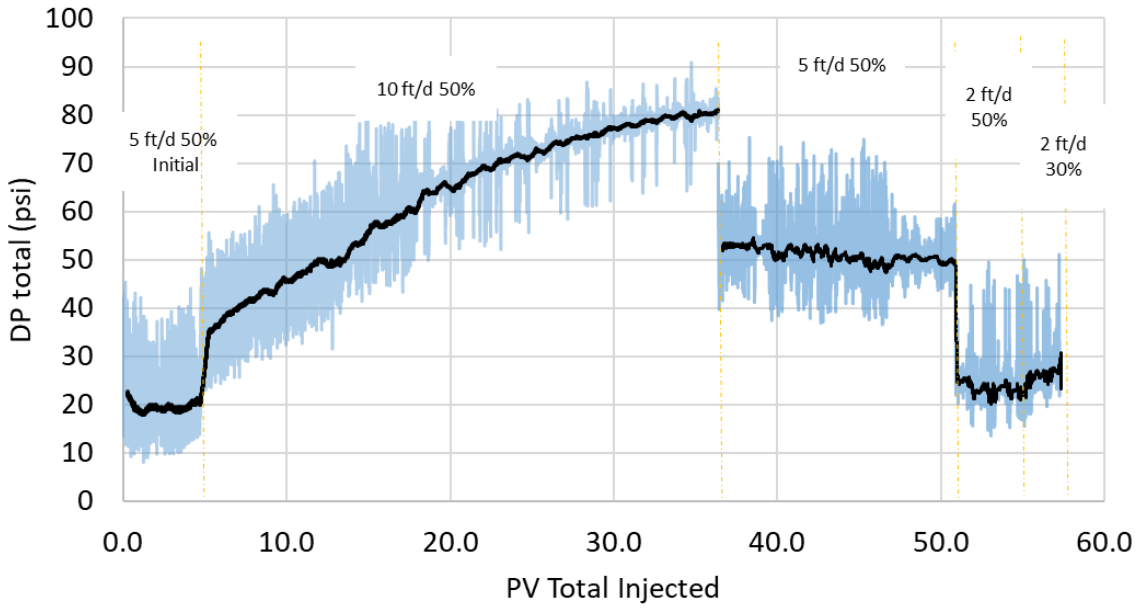

Figure 55: OW-A APG-5 at 3500 ppm foam scan at Sor = 11.4%

Stage	Description
1	Oil Flood
2	Aging of Core
3	Water Flood 2 ft/d
4	WAG [2 ft/d 30%, 2 ft/d 50%, 5 ft/d 50%]
5	Foam [SF650 0.35%, multiple rates]

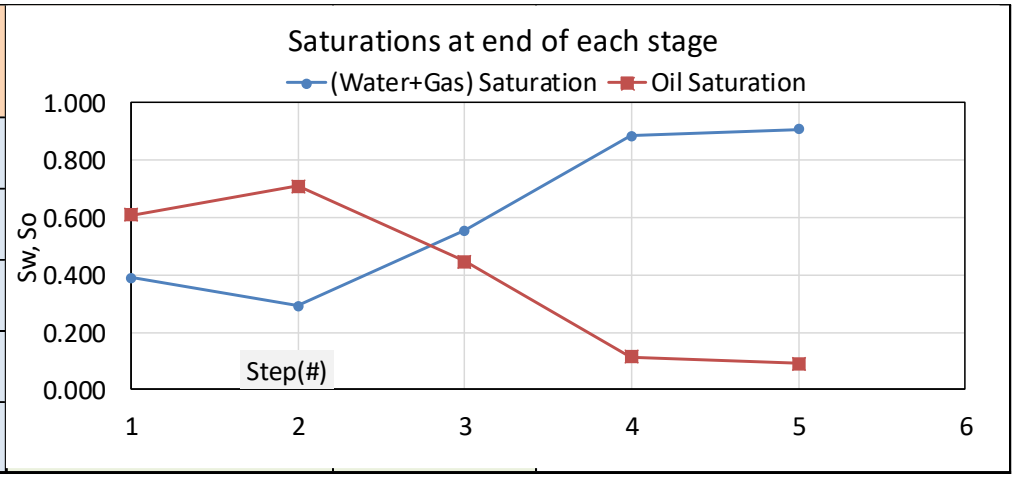

Figure 56: OW-A oil saturation changes

OW-B:

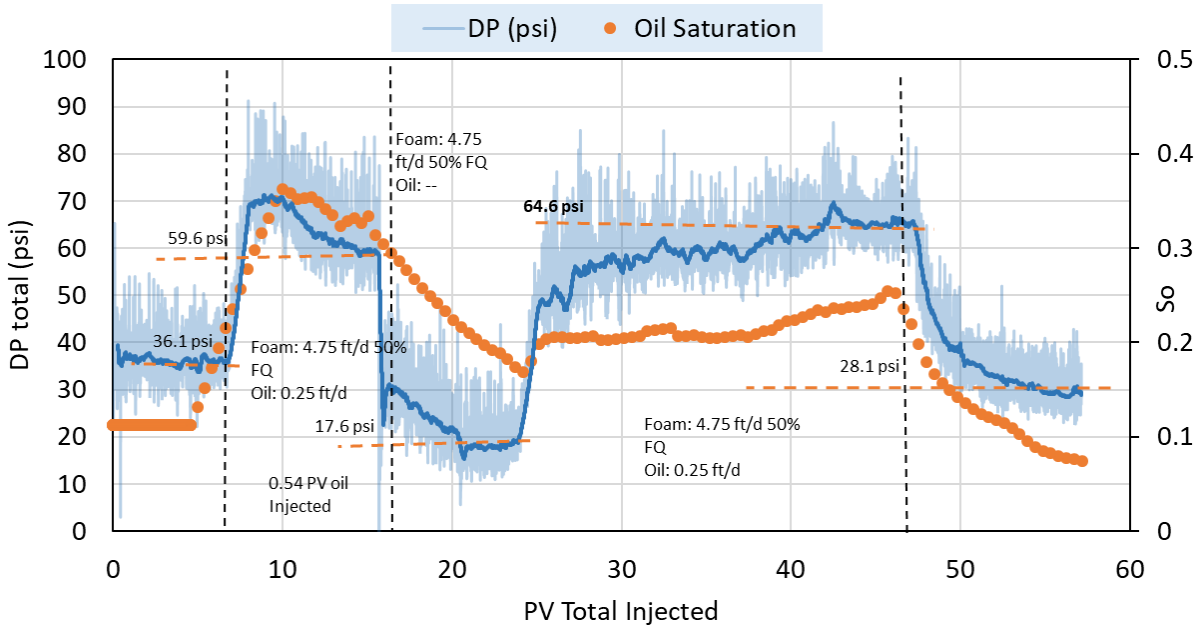

Figure 57: OW-B mobile oil experiment transient pressure and oil saturation changes

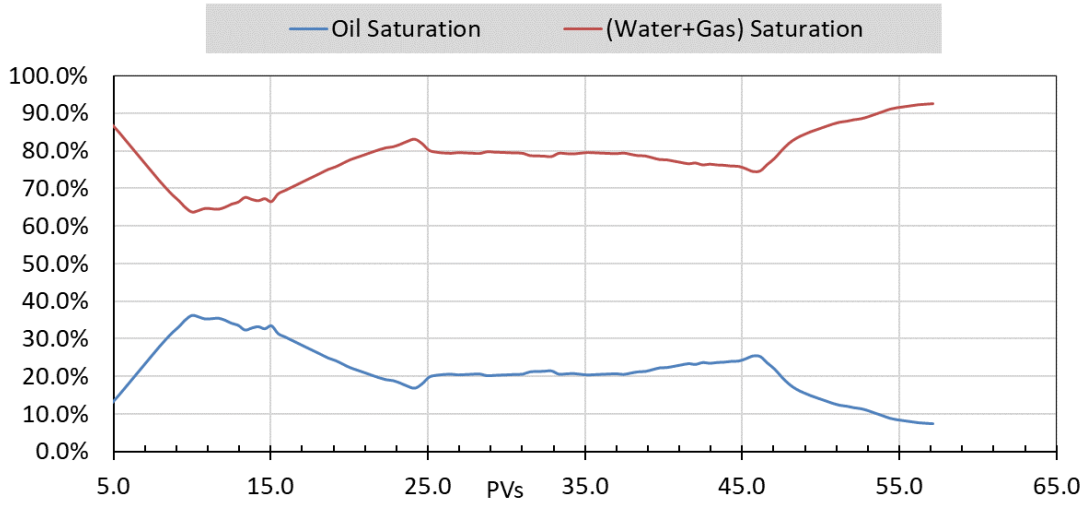

Figure 58: OW-B Oil saturation changes

OW-C:

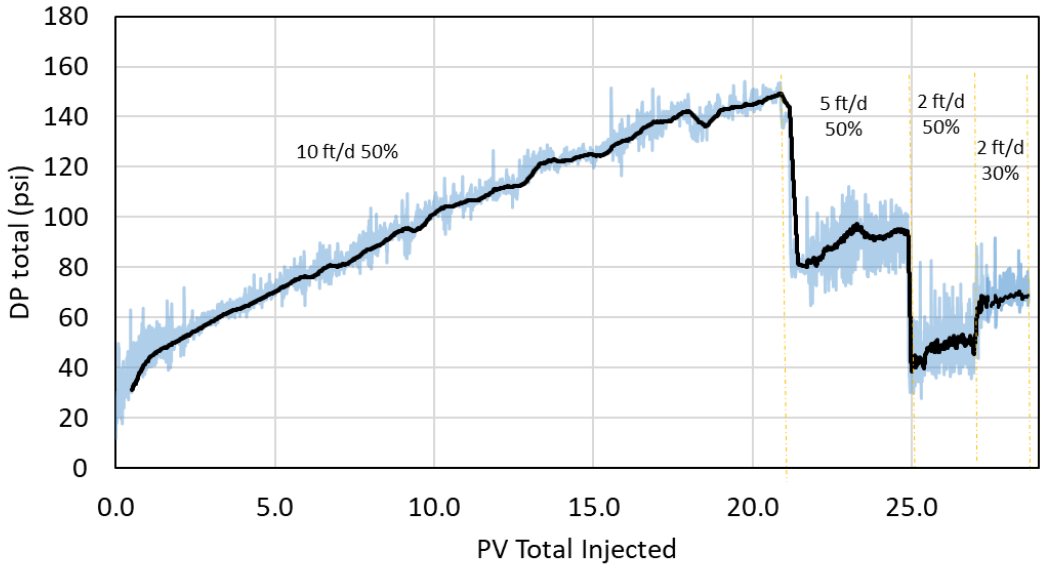

Figure 59: OW-C Foam transient pressure drop (APG + LB at 0.35/0.15 wt.%) at Sor = 7.5%

OW-D:

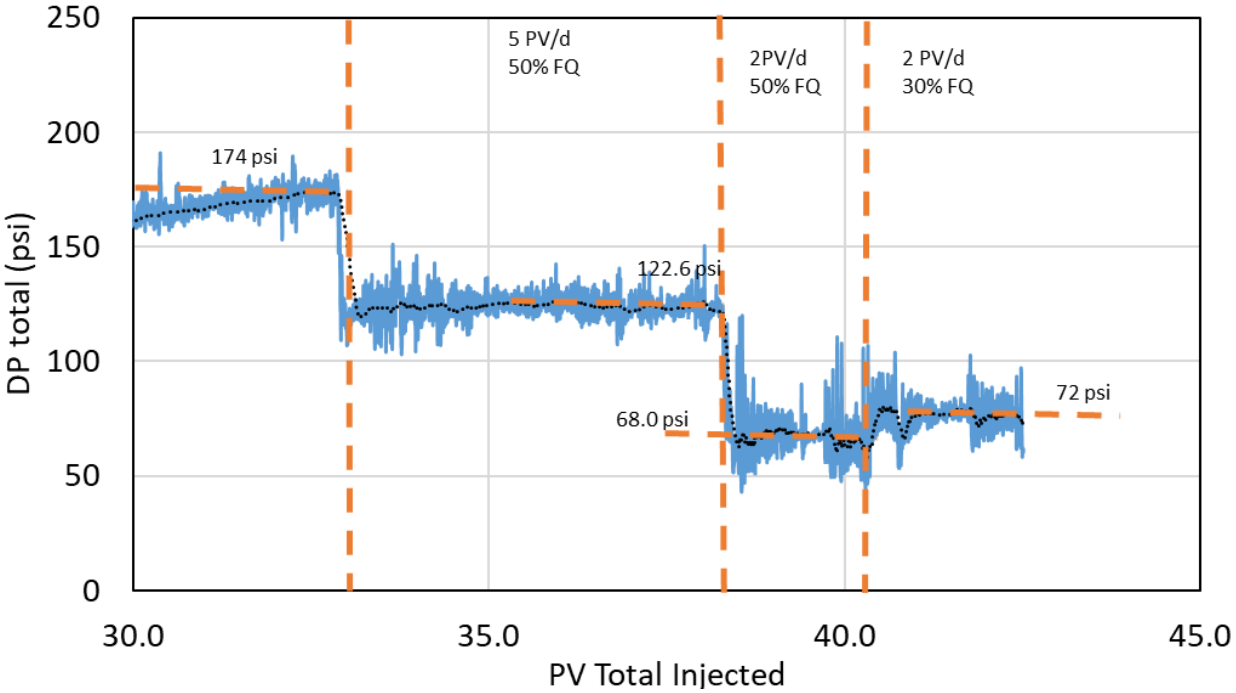

Figure 60: OW-D transient pressure data for APG-5 foam post wettability alteration at Sor=9.4%

Stage	Description
1	Brine Saturation & Permeability test
2	Oil Flood
3	Core Aging
4	Waterflood at 2 PV/d
5	Brine+Gas Co-injection
6	Wettability Alteration + Chase Waterflood
7	APG-5 Foam Injection [Multiple Rates

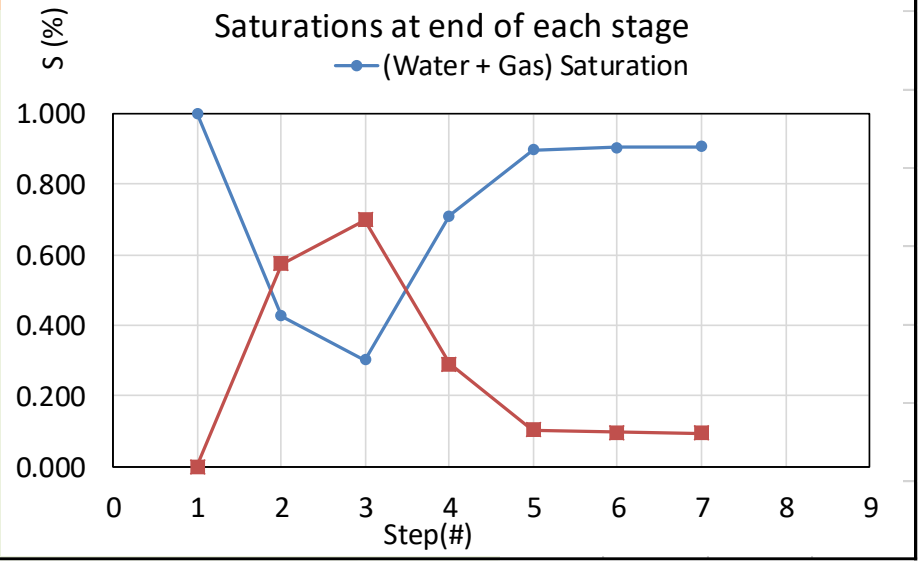

Figure 61: OW-D Oil Saturation changes

OW-E:

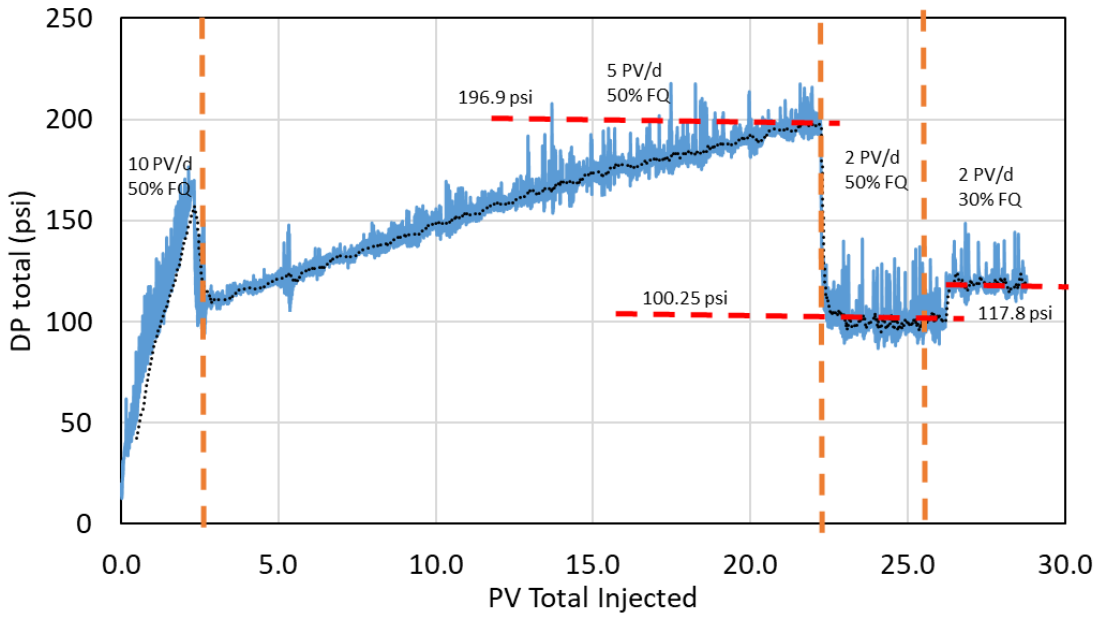

Figure 62: OW-D transient pressure changes for APG+LB foam post wettability alteration at Sor=9.4%

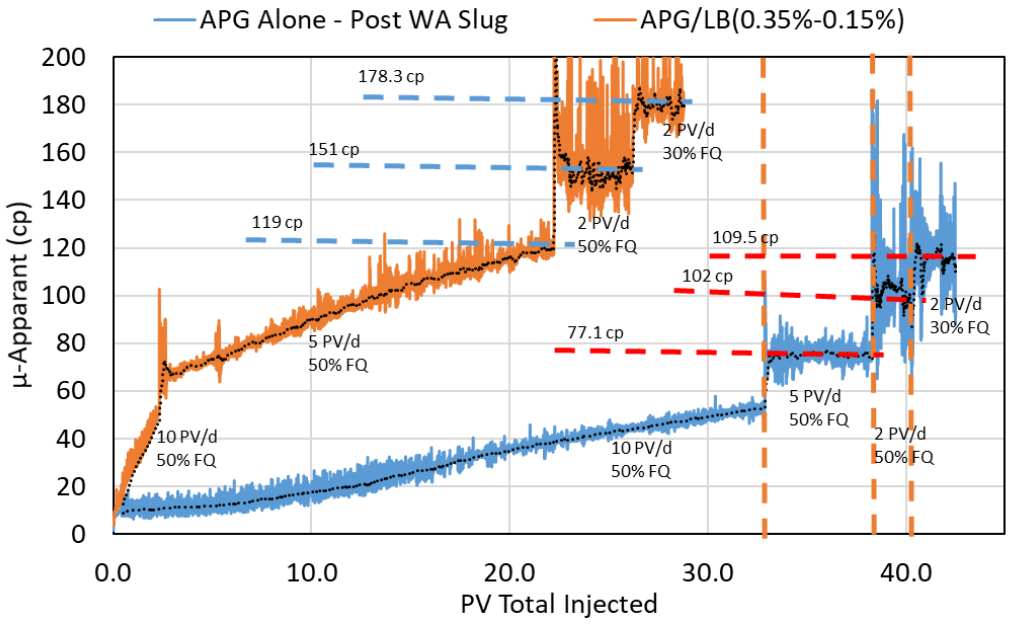

Figure 63: OW-D (APG-5 alone) compared to OW-E (APG-5/LB) post wettability alteration

Appendix D: List of Equations

Entering Coefficient

$$E_{\frac{oil}{water}} = \sigma_{\frac{water}{gas}} + \sigma_{\frac{oil}{water}} - \sigma_{\frac{oil}{gas}} \quad (1)$$

σ: Interfacial tension between two phases

Spreading Coefficient

$$S_{\frac{oil}{water}} = \sigma_{\frac{water}{gas}} - \sigma_{\frac{oil}{water}} - \sigma_{\frac{oil}{gas}} \quad (2)$$

Lamella Number

$$L = \left(\frac{r_o}{r_p}\right)\left(\frac{\sigma_{\frac{water}{gas}}}{\sigma_{\frac{oil}{water}}}\right) \approx (0.15)\left(\frac{\sigma_{\frac{water}{gas}}}{\sigma_{\frac{oil}{water}}}\right) \quad (3)$$

r_o: oil drop/surface radius
r_p: foam plateau border radius

Apparent Viscosity

$$\mu_{apparent} = \frac{\Delta p * A}{L * u} \quad (4)$$

Δp: pressure drop, A: Cross section to flow, L: Length

u: velocity of flow

Mobility Reduction Factors (MRF)

$$MRF = \frac{\Delta P_{Foam}}{\Delta P_{Brine}} \quad (5)$$

Surfactant Adsorption

$$\left(\frac{m_{surfactant}(mg)}{\mathrm{m_{rock}}(g)}\right) = \left(\frac{\mathrm{m\ after\ adsorption} - \mathrm{m_{initial}}}{\mathrm{m_{rock\ (g)}}}\right) \quad (6)$$

m: mass in mg or g

Pseudo-emulsion film interfacial tension

$$\sigma_{(PS-Film)} = \sigma_{wg} + \sigma_{ow} + \int_{\boldsymbol{\Pi(h_\infty)=0}}^{\boldsymbol{\Pi=\Pi(h_0)}} \boldsymbol{h\ d\Pi} \quad (7)$$

h: film thickness

π: disjoining pressure

Generalized Entering Coefficient -

$$E_{o/w}^{g} = -\int_{\boldsymbol{\Pi(h_\infty)=0}}^{\boldsymbol{\Pi=\Pi(h_0)}} \boldsymbol{h\ d\Pi} \quad (8)$$

Laplace Capillary Pressure

$$\Delta p = -\sigma\left(\frac{1}{R_1} + \frac{1}{R_2}\right) \quad (9)$$

References

[1] Aarra, M.G., A. Skauge, and H.A. Martinsen. 2002. “FAWAG: A Breakthrough for EOR in the North Sea.” In *SPE-77695-MS*, 12. SPE: Society of Petroleum Engineers. https://doi.org/10.2118/77695-MS.

[2] Almajid, Muhammead, and Anothony Kovscek R. 2015. “Microvisual Observation of Foam Generation and Coalescence Using Micromodels in the Presence and Absence of Oil.” Stanford University. https://pangea.stanford.edu/ERE/pdf/pereports/MS/Almajid2015.pdf?

[3] Araktingi, U.G., and F.M. Orr Jr. 1993. “Viscous Fingering in Heterogeneous Porous Media.” *SPE-18095-PA* 1 (01): 71–80. https://doi.org/10.2118/18095-PA.

[4] Ashour, Ibrahim, Nabeel Al-Rawahi, Amin Fatemi, and Gholamreza Vakili-Nezhaad. 2011. “Applications of Equations of State in the Oil and Gas Industry.” In . https://doi.org/10.5772/23668.

[5] Aveyard, R. 1994. “Defoaming. Theory and Industrial Applications. Edited by P. R. Garrett, Marcel Dekker Inc., New York, 1993, Viii + 327 Pp., Price: UK 135.00. ISBN 0 8247 8770 6.” *Journal of Chemical Technology & Biotechnology* 59: 114–15.

[6] Awan, Anwar R., Rune Teigland, and Jon Kleppe. 2008. “A Survey of North Sea Enhanced-Oil-Recovery Projects Initiated During the Years 1975 to 2005.” *SPE-99546-PA* 11 (03): 497–512. https://doi.org/10.2118/99546-PA.

[7] Balan, Huseyin Onur, Matthew Thomas Balhoff, and Quoc Phuc Nguyen. 2012. “Modeling of Foamed Gas Mobility in Permeable Porous Media.” In *SPE-154233-MS*, 13. SPE: Society of Petroleum Engineers. https://doi.org/10.2118/154233-MS.

[8] Basheva, Elka S., Dragomir Ganchev, Nikolai D. Denkov, Kenichi Kasuga, Naoki Satoh, and Kaoru Tsujii. 2000. “Role of Betaine as Foam Booster in the Presence of Silicone Oil Drops.” *Langmuir* 16 (3): 1000–1013. https://doi.org/10.1021/la990777+.

[9] Bergeron, V., M. E. Fagan, and C. J. Radke. 1993. “Generalized Entering Coefficients: A Criterion for Foam Stability against Oil in Porous Media.” *Langmuir* 9 (7): 1704–13. https://doi.org/10.1021/la00031a017.

[10] Blackwell, R.J., J.R. Rayne, and W.M. Terry. 1959. “Factors Influencing the Efficiency of Miscible Displacement.” *SPE-1131-G*, January, 8.

[11] Blaker, T., H.K. Celius, T. Lie, H.A. Martinsen, L. Rasmussen, and F. Vassenden. 1999. “Foam for Gas Mobility Control in the Snorre Field: The FAWAG Project.” In *SPE-56478-MS*, 10. SPE: Society of Petroleum Engineers. https://doi.org/10.2118/56478-MS.

[12] Blaker, Tore, Morten G. Aarra, Arne Skauge, Lars Rasmussen, Harald K. Celius, Helge Andre Martinsen, and Frode Vassenden. 2002. “Foam for Gas Mobility Control in the Snorre Field: The FAWAG Project.” *SPE Reservoir Evaluation & Engineering* 5 (04): 317–23. https://doi.org/10.2118/78824-PA.

[13] Boeije, C.S. 2016. “Experimental and Modelling Studies of Foam Enhanced Oil Recovery.” TU Delft Petroleum Engineering. https://doi.org/10.4233/uuid:ddef69d2-a31a-4c92-9d93-4a0152c23583.

[14] Chambers, K. T., and C. J. Radke. 1991. “Capillary Phenomena in Foam Flow through Porous Media.” In *Interfacial Phenomena in Petroleum Recovery*, by Marcel Dekker, 191–225.

[15] Christensen, J.R., E.H. Stenby, and A. Skauge. 1998. “Review of WAG Field Experience.” In *SPE-39883-MS*, 14. SPE: Society of Petroleum Engineers. https://doi.org/10.2118/39883-MS.

[16] Claridge, E.L. 1972. “Prediction of Recovery in Unstable Miscible Flooding.” *SPE-2930-PA* 12 (02): 143–55. https://doi.org/10.2118/2930-PA.

[17] Da, Chang, Armo Elhag, Guoqing Jian, Leilei Zhang, Shehab Alzobaidi, Xuan Zhang, Ali Al Sumaiti, Sibani Biswal, George Hirasaki, and Keith Johnston. 2018. “CO2/Water Foams Stabilized with Cationic or Zwitterionic Surfactants at Temperatures up to 120 °C in High Salinity Brine.” In *SPE-191479-MS*, 14. SPE: Society of Petroleum Engineers. https://doi.org/10.2118/191479-MS.

[18] Dalland, Mariann, Jan Erik Hanssen, and Tove Strøm Kristiansen. 1994. “Oil Interaction with Foams under Static and Flowing Conditions in Porous Media.” *Colloids and Surfaces A: Physicochemical and Engineering Aspects* 82 (2): 129–40. https://doi.org/10.1016/0927-7757(93)02628-R.

[19] Dawe, Robert D., Thomas Oswald, and Ian A. Robson. 1992. Oil recovery process using mobility control fluid comprising alkylated diphenyloxide sulfonates and foam forming amphoteric surfactants. 5203411, filed March 11, 1992, and issued March 11, 1992.

[20] Denkov, Nikolai D. 2004. “Mechanisms of Foam Destruction by Oil-Based Antifoams.” *Langmuir* 20 (22): 9463–9505. https://doi.org/10.1021/la049676o.

[21] Farajzadeh, R., Alexey Andrianov, Rumen Krastev, G. Hirasaki, and William Rossen. 2012. “Foam-Oil Interaction in Porous Media: Implications for Foam Assisted Enhanced Oil Recovery.” *Advances in Colloid and Interface Science* 183–184 (July): 1–13. https://doi.org/10.1016/j.cis.2012.07.002.

[22] Farajzadeh, R., M. Lotfollahi, A. A. Eftekhari, W. R. Rossen, and G. J. H. Hirasaki. 2015. “Effect of Permeability on Implicit-Texture Foam Model Parameters and the Limiting Capillary Pressure.” *Energy & Fuels* 29 (5): 3011–18. https://doi.org/10.1021/acs.energyfuels.5b00248.

[23] Fayers, F. John, and Ann H. Muggeridge. 1990. “Extensions to Dietz Theory and Behavior of Gravity Tongues in Slightly Tilted Reservoirs.” *SPE-18438-PA* 5 (04): 487–94. https://doi.org/10.2118/18438-PA.

[24] Finlay, S., X. Marquez, T. Solling, N. Bounoua, and T. Gagigi. 2014. “Multi-Scale Carbonate Reservoir Characterisation and Artificial Neural Networks Reveals Complexity in the Shuaiba Reservoir, Al Shaheen Field.” In *IPTC-17639-MS*, 16. IPTC: International Petroleum Technology Conference. https://doi.org/10.2523/IPTC-17639-MS.

[25] Garrett, P. 2013. “The Science of Defoaming: Theory, Experiment and Applications.” In.

[26] Healy, Robert N., and Ronald L. Reed. 1974. “Physicochemical Aspects of Microemulsion Flooding.” *SPE-4583-PA* 14 (05): 491–501. https://doi.org/10.2118/4583-PA.

[27] Heller, J.P., D.K. Dandge, R.J. Card, and L.G. Donaruma. 1985. “Direct Thickeners for Mobility Control of CO2 Floods.” *Society of Petroleum Engineers Journal* 25 (05): 679–86. https://doi.org/10.2118/11789-PA.

[28] Homsy, G. 2003. “Viscous Fingering In Porous Media.” *Annual Review of Fluid Mechanics* 19 (November): 271–311. https://doi.org/10.1146/annurev.fl.19.010187.001415.

[29] Jensen, J.A., and F. Friedmann. 1987. “Physical and Chemical Effects of an Oil Phase on the Propagation of Foam in Porous Media.” In *SPE-16375-MS*, 14. SPE: Society of Petroleum Engineers. https://doi.org/10.2118/16375-MS.

[30] Jong, Stephen, Nhut M. Nguyen, Calvin M. Eberle, Long X. Nghiem, and Quoc P. Nguyen. 2016. “Low Tension Gas Flooding as a Novel EOR Method: An Experimental and Theoretical Investigation.” In *SPE-179559-MS*, 25. SPE: Society of Petroleum Engineers. https://doi.org/10.2118/179559-MS.

[31] Kapetas, L., S. Vincent Bonnieu, R. Farajzadeh, A.A. Eftekhari, S.R. Mohd Shafian, R.Z. Kamarul Bahrim, and W.R. Rossen. 2017. “Effect of Permeability on Foam-Model Parameters: An Integrated Approach from Core-Flood Experiments through to Foam Diversion Calculations.” *Colloids and Surfaces A: Physicochemical and Engineering Aspects* 530 (October): 172–80. https://doi.org/10.1016/j.colsurfa.2017.06.060.

[32] Koczo, K, L.A Lobo, and D. Wasan. 1992. “Effect of Oil on Foam Stability: Aqueous Foams Stabilized by Emulsions.” *Journal of Colloid and Interface Science* 150 (May): 492–506. https://doi.org/10.1016/0021-9797(92)90218-B.

[33] Koottungal, Leena. 2014. “2014 Worldwide EOR Survey.” *Oil & Gas Journal*, April.

[34] Kovscek, Anthony R., W. Patzek Tadeusz, and Clayton J. Radke. 1997. “Mechanistic Foam Flow Simulation in Heterogeneous and Multidimensional Porous Media.” *SPE-39102-PA* 2 (04): 511–26. https://doi.org/10.2118/39102-PA.

[35] Kovscek, A.R., and H.J. Bertin. 2002. “Estimation of Foam Mobility in Heterogeneous Porous Media.” In *SPE-75181-MS*, 14. SPE: Society of Petroleum Engineers. https://doi.org/10.2118/75181-MS.

[36] Li, Robert Feng, Wei Yan, Shunhua Liu, George Hirasaki, and Clarence A. Miller. 2010. “Foam Mobility Control for Surfactant Enhanced Oil Recovery.” *SPE-113910-PA* 15 (04): 928–42. https://doi.org/10.2118/113910-PA.

[37] Lindeloff, Niels, Kristian Mogensen, Paul Peter van Lingen, Son Huu Do, Soren Frank, and Rashed Noman. 2008. “Fluid-Phase Behaviour for a Miscible-Gas-Injection EOR Project in a Giant Offshore Oil Field With Large Compositional Variations.” In *SPE-115970-MS*, 21. SPE: Society of Petroleum Engineers. https://doi.org/10.2118/115970-MS.

[38] Liu, Yi, R.B. Grigg, and Baojun Bai. 2005a. “Salinity, PH , and Surfactant Concentration Effects on CO2-Foam.” In *SPE-93095-MS*, 11. SPE: Society of Petroleum Engineers. https://doi.org/10.2118/93095-MS.

[39] ———. 2005b. “Salinity, PH , and Surfactant Concentration Effects on CO2-Foam.” In *SPE-93095-MS*, 11. SPE: Society of Petroleum Engineers. https://doi.org/10.2118/93095-MS.

[40] Lobo, L.A., A.D. Nikolov, and D.T. Wasan. 1989. “FOAM STABILITY IN THE PRESENCE OF OIL: ON THE IMPORTANCE OF THE SECOND VIRIAL COEFFICIENT.” *Journal of Dispersion Science and Technology* 10 (2): 143–61. https://doi.org/10.1080/01932698908943167.

[41] Ma, Kun, Khalid Mateen, Guangwei Ren, Gilles Bourdarot, and Danielle Morel. 2018. “Modeling Foam Flow at Achievable Flow Rates in the Subterranean Formation Using the Population-Balance Approach and Implications for Experimental Design.” *Journal of Non-Newtonian Fluid Mechanics* 254 (April): 36–50. https://doi.org/10.1016/j.jnnfm.2018.02.007.

[42] Manlowe, David J., and Clayton J. Radke. 1990. “A Pore-Level Investigation of Foam/Oil Interactions in Porous Media.” *SPE Reservoir Engineering* 5 (04): 495–502. https://doi.org/10.2118/18069-PA.

[43] Mannhardt, Karin, and Idar Svorstøl. 1999. “Effect of Oil Saturation on Foam Propagation in Snorre Reservoir Core.” *Journal of Petroleum Science and Engineering - J PET SCI ENGINEERING* 23 (October): 189–200. https://doi.org/10.1016/S0920-4105(99)00016-9.

[44] Marquis, David M., and Donald L. Kuehne. 1992. Oil recovery technique employing non-ionic surfactants. Canada CA2044843A1, issued January 3, 1992.

[45] Masalmeh, Shehadeh K., Lingli Wei, and Carl P.A. Blom. 2011. “Mobility Control for Gas Injection in Heterogeneous Carbonate Reservoirs: Comparison of Foams versus Polymers.” In *SPE-142542-MS*, 21. SPE: Society of Petroleum Engineers. https://doi.org/10.2118/142542-MS.

[46] Nguyen, Quoc P., Alexander V. Alexandrov, Pacelli L. Zitha, and Peter K. Currie. 2000. “Experimental and Modeling Studies on Foam in Porous Media: A Review.” In *SPE-58799-MS*, 22. SPE: Society of Petroleum Engineers. https://doi.org/10.2118/58799-MS.

[47] Nikolov, A.D., D.T. Wasan, D.W. Huang, and D.A. Edwards. 1986. “The Effect of Oil on Foam Stability: Mechanisms and Implications for Oil Displacement by Foam in Porous Media.” In *SPE-15443-MS*, 16. SPE: Society of Petroleum Engineers. https://doi.org/10.2118/15443-MS.

[48] Ocampo, A., A. Restrepo, H. Cifuentes, J. Hester, N. Orozco, C. Gil, E. Castro, S. Lopera, and C. Gonzalez. 2013. “Successful Foam EOR Pilot in a Mature Volatile Oil Reservoir Under Miscible Gas Injection.” In *IPTC-16984-MS*, 8. IPTC: International Petroleum Technology Conference. https://doi.org/10.2523/IPTC-16984-MS.

[49] Ransohoff, T.C, and C.J Radke. 1988. “Laminar Flow of a Wetting Liquid along the Corners of a Predominantly Gas-Occupied Noncircular Pore.” *Journal of Colloid and Interface Science* 121 (2): 392–401. https://doi.org/10.1016/0021-9797(88)90442-0.

[50] Sakai, Takaya, and Youhei Kaneko. 2004. “The Effect of Some Foam Boosters on the Foamability and Foam Stability of Anionic Systems.” *Journal of Surfactants and Detergents* 7 (July): 291–95. https://doi.org/10.1007/s11743-004-0314-x.

[51] Salehi, Mehdi, Stephen J. Johnson, and Jenn-Tai Liang. 2008. “Mechanistic Study of Wettability Alteration Using Surfactants with Applications in Naturally Fractured Reservoirs.” *Langmuir* 24 (24): 14099–107. https://doi.org/10.1021/la802464u.

[52] Scherubel, Gary A., and Michael A. Thorne. 1981. Method using hydrocarbon foams as well stimulants. 4301868, filed October 15, 1979, and issued November 24, 1981.

[53] Schramm, Laurier L. 1994. "Foam Sensitivity to Crude Oil in Porous Media." In *Foams: Fundamentals and Applications in the Petroleum Industry*, 242:165–97. Advances in Chemistry 242. American Chemical Society. https://doi.org/10.1021/ba-1994-0242.ch004.

[54] Schramm, Laurier L., and Karin Mannhardt. 1996. "The Effect of Wettability on Foam Sensitivity to Crude Oil in Porous Media." *Journal of Petroleum Science and Engineering* 15 (1): 101–13. https://doi.org/10.1016/0920-4105(95)00068-2.

[55] Schramm, Laurier L., and Jerry J. Novosad. 1990. "Micro-Visualization of Foam Interactions with a Crude Oil." *Colloids and Surfaces* 46 (1): 21–43. https://doi.org/10.1016/0166-6622(90)80046-7.

[56] ———. 1992. "The Destabilization of Foams for Improved Oil Recovery by Crude Oils: Effect of the Nature of the Oil." *Enhanced Oil Recovery* 7 (1): 77–90. https://doi.org/10.1016/0920-4105(92)90010-X.

[57] Shan, D., and W.R. Rossen. 2004. "Optimal Injection Strategies for Foam IOR." *SPE-88811-PA* 9 (02): 132–50. https://doi.org/10.2118/88811-PA.

[58] Sheng, James J. 2013. "Chapter 11 - Foams and Their Applications in Enhancing Oil Recovery." In *Enhanced Oil Recovery Field Case Studies*, edited by James J. Sheng, 251–80. Boston: Gulf Professional Publishing. https://doi.org/10.1016/B978-0-12-386545-8.00011-7.

[59] Shi, J-X., and W.R. Rossen. 1998. "Improved Surfactant-Alternating-Gas Foam Process to Control Gravity Override." In *SPE-39653-MS*, 8. SPE: Society of Petroleum Engineers. https://doi.org/10.2118/39653-MS.

[60] Simjoo, Mohammad, Yufei Dong, Alexey Andrianov, Mohand Talanana, and Pacelli L.J. Zitha. 2011. "Novel Insight into Foam Mobility Control." In *IPTC-15338-MS*, 15. IPTC: International Petroleum Technology Conference. https://doi.org/10.2523/IPTC-15338-MS.

[61] Skauge, A., M.G. Aarra, L. Surguchev, H.A. Martinsen, and L. Rasmussen. 2002a. "Foam-Assisted WAG: Experience from the Snorre Field." In *SPE-75157-MS*, 11. SPE: Society of Petroleum Engineers. https://doi.org/10.2118/75157-MS.

[62] ———. 2002b. "Foam-Assisted WAG: Experience from the Snorre Field." In *SPE-75157-MS*, 11. SPE: Society of Petroleum Engineers. https://doi.org/10.2118/75157-MS.

[63] ———. 2002c. "Foam-Assisted WAG: Experience from the Snorre Field." In *SPE-75157-MS*, 11. SPE: Society of Petroleum Engineers. https://doi.org/10.2118/75157-MS.

[64] Spirov, Pavel, Svetlana Rudyk, and Arif Khan. 2012. "Foam Assisted WAG, Snorre Revisit with New Foam Screening Model." In *SPE-150829-MS*, 18. SPE: Society of Petroleum Engineers. https://doi.org/10.2118/150829-MS.

[65] Srivastava, Mayank, Jieyuan Zhang, Quoc Phuc Nguyen, and Gary A. Pope. 2009a. "A Systematic Study of Alkali Surfactant Gas Injection as an Enhanced Oil Recovery

Technique." In *SPE-124752-MS*, 15. SPE: Society of Petroleum Engineers. https://doi.org/10.2118/124752-MS.

[66] ———. 2009b. "A Systematic Study of Alkali Surfactant Gas Injection as an Enhanced Oil Recovery Technique." In *SPE-124752-MS*, 15. SPE: Society of Petroleum Engineers. https://doi.org/10.2118/124752-MS.

[67] Stalkup, Fred I., Jr. 1983. "Status of Miscible Displacement." *SPE-9992-PA* 35 (04): 815–26. https://doi.org/10.2118/9992-PA.

[68] Svorstol, I., F. Vassenden, and K. Mannhardt. 1996. "Laboratory Studies for Design of a Foam Pilot in the Snorre Field." In *SPE-35400-MS*, 11. SPE: Society of Petroleum Engineers. https://doi.org/10.2118/35400-MS.

[69] Szlendak, Stefan M., Nhut M. Nguyen, and Quoc P. Nguyen. 2016. "Investigation of Localized Displacement Phenomenon for Low-Tension-Gas (LTG) Injection in Tight Formations." *Journal of Petroleum Science and Engineering* 142 (June): 36–45. https://doi.org/10.1016/j.petrol.2016.01.042.

[70] Talebian, Seyedeh H., Rahim Masoudi, Isa M. Tan, and Pacelli L.J. Zitha. 2013. "Foam Assisted CO2-EOR; Concepts, Challenges and Applications." In *SPE-165280-MS*, 14. SPE: Society of Petroleum Engineers. https://doi.org/10.2118/165280-MS.

[71] Teletzke, Gary F., Prateek Dinesh Patel, and Amy Chen. 2005. "Methodology for Miscible Gas Injection EOR Screening." In *SPE-97650-MS*, 11. SPE: Society of Petroleum Engineers. https://doi.org/10.2118/97650-MS.

[72] Waggoner, J.R., J.L. Castillo, and Larry W. Lake. 1992. "Simulation of EOR Processes in Stochastically Generated Permeable Media." *SPE-21237-PA* 7 (02): 173–80. https://doi.org/10.2118/21237-PA.

[73] Xu, Q., and W.R. Rossen. 2003. "Experimental Study of Gas Injection in Surfactant-Alternating-Gas Foam Process." In *SPE-84183-MS*, 13. SPE: Society of Petroleum Engineers. https://doi.org/10.2118/84183-MS.

[74] Zhang, Hui, Clarence A. Miller, Peter R. Garrett, and Kirk H. Raney. 2005. "Lauryl Alcohol and Amine Oxide as Foam Stabilizers in the Presence of Hardness and Oily Soil." *Journal of Surfactants and Detergents* 8 (1): 99–107. https://doi.org/10.1007/s11743-005-0337-3.